Improving Fuel Economy via Management of Auxiliary Loads in Fuel-Cell Electric Vehicles

by

Christopher P. Lawrence

A thesis
presented to the University of Waterloo
in fulfillment of the
thesis requirement for the degree of
Master of Applied Science
in
Electrical and Computer Engineering

Waterloo, Ontario, Canada, 2007

Author's Declaration

I hereby declare that I am the sole author of this thesis. This is a true copy of the thesis, including any required final revisions, as accepted by my examiners. I understand that my thesis may be made electronically available to the public.

Abstract

The automotive industry is in a state of flux at the moment. Traditional combustion engine technologies are becoming challenged by newer, more efficient and environmentally friendly propulsion methods. These include bio-fuel, hybrid, and hydrogen fuel-cell technologies. Propulsion alone, however, is not the only area where improvements can be made in vehicle efficiency. Current vehicle research and development focuses heavily on propulsion systems with relatively few resources dedicated to auxiliary systems. These auxiliary systems, however, can have a significant impact on overall vehicle efficiency and fuel economy. The objective of this work is to improve the efficiency of a Fuel Cell Electric Vehicle (FCEV) through intelligent auxiliary system control.

The analysis contained herein is applicable to all types of vehicles and may find applications in many vehicle architectures. A survey is made of the various types of alternative fuels and vehicle architectures from conventional gasoline vehicles to hybrids and fuel cells. Trends in auxiliary power systems and previous papers on control of these systems are discussed. The FCEV developed by the University of Waterloo Alternative Fuels Team (UWAFT) is outlined and the design process presented. Its powertrain control strategy is analyzed with a proposal for modifications as well as the addition of an auxiliary control module to meet the aforementioned objectives. Simulations are performed to predict the efficiency and fuel economy gains that can potentially be realized using these proposed techniques. These gains prove to be significant, with an almost 2% improvement realized through intelligent control of the air conditioning compressor, and further gains possible through other auxiliary power reduction techniques.

Acknowledgements

This work was made possible through my participation in University of Waterloo's Alternative Fuels Team. I'm very grateful to have had the opportunity to work with this terrific group of students. Thank you to both Prof. Roydon Fraser and Prof. Michael Fowler, the team's active faculty advisors. They work tirelessly to ensure that the team has all the resources it needs to thrive and produce world class engineers. Their excellent guidance was and is crucial for the team's past and future success.

I owe many thanks to all the students on the Alternative Fuels Team, especially Matt Stevens, Erik Wilhelm and Chris Mendes who have played an instrumental role in my understanding of the team vehicle's construction and simulation. Thanks for the opportunity to act as the team's Electrical Lead a role that was very hard to fill after my predecessor Jen Marshall.

Thanks especially to my supervisors, Prof's Magdy Salama and Ramadan El Shatshat who have been instrumental in guiding me throughout my degree and the writing of this work. Thank you for seeing in me, the potential to continue my education while adding to your already hectic schedules.

Also, I would like to thank my friends and family who have carried me through the last two years. To Ferdinand Dachs, a true friend and inspiration, to Arati Pai and Darrell Gaudette who always have time to chat despite their seemingly endless todo lists, to my parents and siblings for their neverending moral support and encouragement.

Finally, to the person who was most on my mind throughout the writing of this work, Chrisi, thanks for coming into my life and for making me a part of yours.

Contents

List of Figures

List of Tables

Chapter 1

Introduction

The automotive landscape has seen a dramatic shift over the past decade. Gone are the days of seemingly unlimited oil when the engineering focused on maximizing power output irrespective of fuel economy. This, combined with heightened public interest in the environment today means car manufacturers are putting large amounts of time and money into vehicle efficiency research [1]. Many different technologies are coming to the forefront as potential candidates to help acheive these goals. To remain viable, however, the industry must achieve these goals while maintaining vehicle performance, utility and overall cost.

1.1 Background and Literature Review

1.1.1 Transportation Energy Usage

Based on information from the world resources institute [2], Canada's total energy consumption in 2001 was 248 million metric tons of oil equivalent (MTOE). That works out to 7,999 kg of oil equivalent (KGOE) per capita. Table 1.1 displays the total energy usage of a number of countries to illustrate worldwide norms. The units represent energy usage as the equivalent amount of oil needed to produce the energy used. One metric ton of oil equivalent (TOE) is equal to 10 Exp. 7 kilocalories, 41.868 gigajoules, or 11,628 gigawatt-hours (GWh). This data places Canada and the US as the 3rd and 4th largest consumers of energy per capita. Fig. 1.1, shows the energy usage breakdown in these two countries.

Table 1.1: National Energy Usage Comparison - 2001 Statistics

Country	**Total Energy Usage (MTOE)** *MegaTons of Oil Equivalent*	**Energy Usage per Capita (KGOE)** *Kg of Oil Equivalent*
Iceland	3.4	11,800
U.A.E.	32.6	11,332
Canada	248	7,999
United States	2,281	7,921
Finland	34	6,518
The Netherlands	77	4,831
Germany	351	4,263
United Kingdom	235	3,994
China	1,139	887
Nigeria	95	810

[2]

Looking at Fig. 1.1, transportation is the largest energy consumption sector in the US and the second largest in Canada. It accounts for 29% of Canadian energy usage and an immense 42% of US energy usage. This sector can be subdivided into personal transportation, which, in North America, is synonymous with gasoline-powered vehicles, and non-personal transportation such as industrial/commercial trucks, commercial airplanes, public transit, etc [3]. Based on gasoline consumption numbers for both countries, personal transportation amounts to 16% of the Canadian energy consumption chart and 26% of the US energy consumption chart shown in Fig. 1.1 (See Appendix A). This is over half of the total transportation energy consumed in both countries and constitutes a significant component in our North American energy appetite [2, 4].

While, relatively speaking, North America's rate of gasoline consumption is high, this would not be a problem if it were without consequences. Combustion of gasoline to provide mechanical energy results in gaseous by-products, or exhaust. Global warming and poor air quality in cities are both phenomena that have been attributed, in part, to this exhaust [5, 6]. Further, the supply of gasoline has come into question for North America's future energy needs [7]. With this in mind, it becomes apparent that the energy consumption rate should be slowed, or alternative energy sources found.

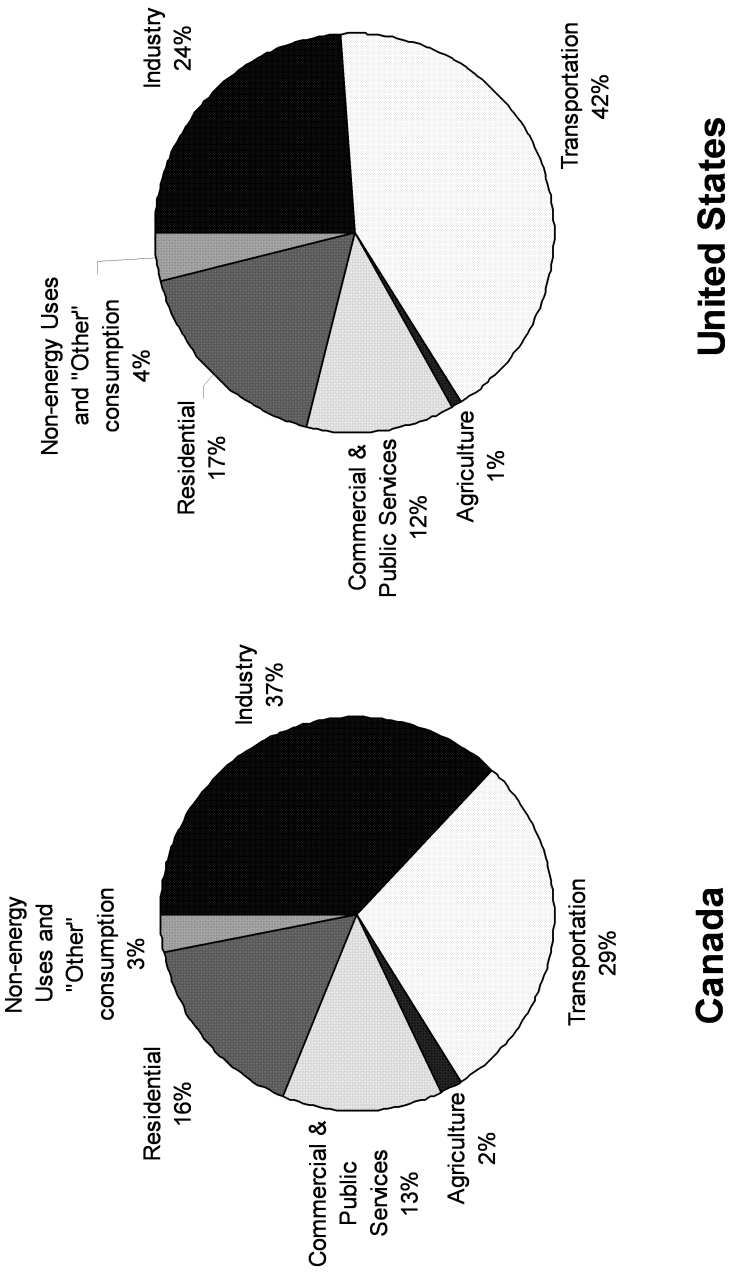

Figure 1.1: Canadian and U.S. Energy Usage Breakdown [2]

Coupling our voracious energy appetite with the recent awareness of environmental issues gives us three main goals for the automotive industry moving forward. These are (1) Reducing transportation energy consumption, (2) Finding alternative transportation energy sources, and (3) Reducing tranportation's environmental impact. There are a number of technologies currently being developed by automotive manufacturers and academia for propelling vehicles with less fuel, cleaner emissions and/or using alternative fuels such as bio-fuels and hydrogen. These include improvements in Internal Combustion Engine (ICE) technology, ICE-Electric Hybrid technologies and Fuel-Cell Electric vehicles. The following sections outline some key technological advancements while providing a basis for the research found in the latter chapters of this work.

1.1.2 ICE Improvements

Gasoline

Gasoline spark-ignition (SI) engines have come a long way in the last few decades with still further improvements on the horizon [8]. Fuel efficiency and emissions regulations have prompted a number of innovations since the days of carbureted engines. The advent of Electronic Fuel Injection (EFI) in the 1970's was the beginning of a continuing movement towards complex computerized engine control systems. EFI gave engine designers the ability to easily and precisely control the air/fuel mixture under any engine operating conditions. Previously, mechanical carburetors were used to control the air/fuel mixture and required complex mechanical/pneumatic systems to adjust this mixture under the most rudimentary engine operating parameters. With the newfound flexibility offered by EFI, air/fuel mixtures could be tuned to increase the burn efficiency, thus increasing engine power output and reducing emissions that are largely the result of an incomplete burn. As computers evolved and became more powerful throughout the 1980's and 1990's they have been able to take on more and more engine control tasks. These include Variable Valve Timing (VVT), Ignition Timing, and Transmission Control. All these technologies allow strict control and thus optimization of the combustion process. Table 1.2 summarizes some of the numerical emissions improvements required by federal U.S. regulations for the sale of new motor vehicles. Although certain manufacturers successfully lobbied to

postpone some of the proposed emissions restrictions, the majority of these regulations were met on time.

Table 1.2: U.S. Federal Emissions Regulations

Model Year(s)	**Hydrocarbons**	**Carbon Monoxide**	**Nitrogen Oxide**
1950-1967*	10.6-13	84-87	3.6-4.1
1950-1967*	10.6-13	84-87	3.6-4.1
1968-1971	4.1	34	3.1
1972-1974	3.0	28	3.1
1975-1976	1.5	15	3.1
1977-1979	1.5	15	2
1980	.41	7	2
1981-1995	.41	3.4	1
1996-2003 (Tier I)	.25	3.4	.4
2004-2009 (Tier II)**	.125	1.7	.2

*Pre-Regulation years - numbers represent average actual vehicle emissions.
**Tier II regulations follow a phase-in schedule for various classes of vehicles over the 5-year period.

[9, 10]

Future combustion engine improvements include Gasoline Direct Injection (GDI), which has the potential to dramatically improve engine efficiency and emissions results [11].

Diesel

Diesel combustion engines are consistently better from a fuel economy standpoint than gasonline engines, simply due to the higher energy content of diesel fuel and the higher compression ratio of diesel engines [6]. Emissions from a diesel engine have been improved alongside those of gasoline engines and there continues to be a debate as to which type of engine is cleaner. In the end it depends on which gaseous compounds are decidedly worse for the atmosphere. The main problems that have historically held Diesel sales down in North American cars are cost, winter performance and particulate matter in the exhaust.

These problems are currently being addressed and further efficiency improvements from diesel engines are in sight. Emissions can be treated with a combination of particulate filters and other exhaust gas aftertreatment systems [12]. Direct injection will see the performance and efficiency of diesel engines jump as it will with gasoline engines and emissions will improve as a result aswell [13].

Bio-Fuels

Bio-Fuels such as ethanol and bio-diesel are being looked at closely as possible replacements or at least partial replacements for gasoline and diesel fuel. General Motors, Ford and others are already producing vehicles that can run either normal gasoline or a blend of 85% ethanol and 15% gasoline [1, 6]. Although bio-fuels do not necessarily decrease engine emissions beyond what is already being achieved with gasoline and diesel, they do allow for a sustainable source of energy that can be grown on farms.

Combustion-Electric Hybrids

Combustion-Electric hybrids are a recent development in the automotive industry. They consist of a combination between an electric and an ICE drive train. Although purely electric vehicles do exist, they are not commonplace due to the lack of range and power that they generally exhibit. When combined with a high-efficiency ICE, the electric drive train augments the power output of the ICE and allows for an overall increase in drive train efficiency through complex power-split control strategies. To quantify the potential gains, simulations of a high efficiency diesel vehicle in conventional, parallel hybrid and series hybrid configurations show a 24% improvement in fuel econonmy for the parallel hybrid and an 18% improvement for the series hybrid over the conventional configuration. These results are for a combined city/highway drivecycle analysis, with peak fuel economy hitting 2.57 L/100km (Litres per 100km) [14]. Hybrid vehicles are already on the market today from Honda, Toyota, General Motors, Ford and others. Testing by the U.S. Environmental Protection Agency (EPA) of the Toyota Prius reveals fuel economies of 3.6-4.4 L/100km versus 6.5-7.5 L/100km of comparable compact models [15]. While these vehicles typically exhibit significantly better fuel economy than an ICE only vehicle, the initial purchase premium is hindering wide-spread acceptance [6].

1.1.3 Fuel-Cell Electric Technologies

As mentioned in the previous section, electric only vehicles suffer from a lack of range and power. Fuel-Cell's provide a way to remedy this by facilitating the storage of large amounts of electrical energy in chemical form. They can be thought of as batteries that run on fuel rather than internal stored chemicals [16]. There are different types of fuel-cells which use different fuels but the main element involved is hydrogen. The major advantages of hydrogen fuel-cell vehicles over vehicles utilizing combustion engines are:

1. Flexible energy source - As described in the following sections, hydrogen can be obtained through various means using other primary sources of energy.

2. Zero Local Emissions - At a vehicle level, no harmful emissions are produced through the conversion of hydrogen to electricity.

Often mis-represented in the media as an energy source, Hydrogen used to power fuel-cells is an energy carrier and does not occur on Earth in significant quantities in it's pure form. Gasoline and diesel fossil fuels on the other hand, were created over millons of years through natural processes and exist currently in a form that is immediately useful as a fuel. Therefore, when considering fuel-cell vehicles, one must consider not only the energy flow from hydrogen to wheel, but also the energy flow required to obtain the pure hydrogen initially.

Hydrogen Production Energy Flexibility

This brings us to the first major advantage of fuel-cells, energy source flexibility. There are two main sources of industrially produced pure hydrogen: Natural-gas reformation, and electrolysis.

Natural-gas is mainly composed of methane (CH_4) and is readily obtainable. A simple large scale technique exists for converting it into pure hydrogen (H_2) and carbon dioxide (CO_2). This process is self-sustaining, and therefore requires little or no energy input from external sources [17]. The conversion efficiency is around 90% but there is the unfortunate fact that the large amounts of carbon dioxide produced must either be released into the atmosphere or sequestered. Release results in the highest efficiency but leads to continued global warming problems as carbon dioxide is the main greenhouse gas. Sequestering involves storing the carbon dioxide by-product in deep rock formations or under-sea and has the potential to eliminate atmospheric carbon dioxide emissions at the cost of decreasing reformation efficiency. Hydrogen production via reformation produces relatively pure carbon dioxide making it ideal for sequestering techniques [18].

Electrolysis involves the use of electricity to split water (H_2O) into pure hydrogen (H_2) and oxygen (O). Large scale production using this technique can reach efficiencies around 80% or in the 56–73% range when including storage and other energy requirements [19]. As electricity is the source of energy required for this process, it is very flexible and can be driven via any source of electricity such as thermo-nuclear power, renewable hydro-electric and wind power. Depending on the source of electricity hydrogen production can still contribute to harmful atmospheric emissions (eg. coal-fired thermo-electric power), therefore the ideal solution is to use electricity from renewable resources.

Fuel Cell Types and Fuel Flexibility

On the usage end of the spectrum, there are different types of fuel cells. Although most require pure hydrogen as a fuel, some can use other fuels such as liquid methanol. Table 1.3 lists the common types of fuel cells, and the fuel requirements.

Table 1.3: Fuel Cell Types and Fuels

Fuel Cell Type	Fuel	Typical Efficiency
Alkaline	Ultra-Pure Hydrogen	60%
PEM	Hydrogen	30–50%
PEM	Liquid Methanol	10–20%
Phosphoric Acid	Impure Hydrogen	40%
Molten Carbonate	Multi-Fuel	60%
Solid Oxide	Multi-Fuel	55–60%

[20, 21]

Due to their size and low-temperature operation, PEM (Polymer Electrolyte Membrane) fuel-cells are often claimed as the type best suited to the automotive application [22, 23]. These cells require pure hydrogen, which presents a problem for public adoption: they require a hydrogen distribution infrastructure. There are systems for small scale reformation of fossil fuels and alcohols that can be placed on-board a vehicle to facilitate the usage of conventional gasoline or liquid methanol/ethanol. The added complexity of these systems, however, increases vehicle cost and decreases overall efficiency. The solution to this problem remains to be seen.

Fuel Cell Emissions

Depending on the fuel and initial energy sources chosen, fuel-cell power can result in siginificant emissions of greenhouse gases. Using natural-gas reformation for example can result in significant emissions as can the use fossil fuel based electrical power generation for electrolysis or on-board vehicle reformers. Despite this, it is possible to achieve zero emissions with fuel cells when using renewable electricitiy sources for electrolysis and pure hydrogen fuelled fuel cells. In this case the only exhaust is water vapour and a small amount of waste hydrogen. Vehicles operating with this energy source would remove the automobile from the environmental debate entirely, and the remaining problems of sustainable energy usage would be softened by the flexibility in possible power sources [22, 23].

1.1.4 Auxiliary and Parasitic Load Improvements

No matter which power train technology a vehicle utilizes, the ultimate goal of a vehicle is to transport people and cargo. Therefore, it is desired to use as much of a vehicle's stored fuel energy for propulsion as possible. Beyond propulsion, however, there are other auxiliary objectives that are either a necessary or desired aspects of vehicle operation. Some example auxiliary objectives include lighting of the road ahead for night driving, interior climate control, and power steering. Every vehicle has a number of energy consuming components, often called "auxiliary loads" designed to achieve these objectives.

In addition to the auxiliary objectives there are also other vehicle operation objectives that must be achieved in order for the vehicle propulsion system to operate correctly. Examples of these include engine cooling, fuel delivery, and engine control. Such tasks are performed by components that are generally considered "parasitic loads". Although these components are performing an essential vehicle function, none of the energy consumed by them is directly contributing to either propulsion or auxiliary objectives. To put this in the perspective of an electrical engineer, consider a segment of transmission line. It is useful for transferring energy between point A and point B, however that comes at the cost of the associated parasitic losses. The transmission line is a necessary component in a power system yet it does not contribute to the generation of electrical energy. Instead it consumes some of the generated energy before it reaches the customer. In much the same way, an engine cooling pump allows the engine to remain at the proper operating temperature while consuming some of the engine's output power. In this regard, the cooling pump is considered a parasite when considering the overall goal of propelling the vehicle.

Historical Load Development

At the turn of the century, in the days of the "Curved Dash Olds" and Model T Ford's, there were not any auxiliaries or parasitic loads to speak of [24]. Headlamps were initially oil fuelled and cooling was achieved by natural convection of water through the radiator. Even fuel delivery was often achieved using a gravity-fed system with no external pump required. As time progressed and people became more accustomed to the horseless carriage, people

began to demand luxuries above and beyond the simple utilitarian transport offered by these first vehicles [25]. Brighter headlamps which did not have to be lit, larger engines that required active cooling, and eventually interior climate control for the ultimate comfort and style on the road. By the 50's and 60's automobiles had become large and luxurious with power assisted steering, braking, and most of the other auxiliaries being powered mechanically via drive-belts from the engine crankshaft.

Since then, with the focus shifting from power and luxury back towards fuel economy and now environmental concerns, auxiliary loads may have decreased slightly, but the overall trend is still upward. Even the most basic model cars on the market today are furnished with a host of power hungry auxiliary systems from power steering and windows to heated seats [26].

In modern vehicles, automotive designers have chosen to use electric motors and devices instead of traditionally mechanically operated devices. In the past, radiator cooling fan(s) were typically directly driven by a belt or directly via the crankshaft. With the design flexibility and control that electric systems allow, most cars now have electric radiator fans. This is a trend that is growing to encompass more power hungry auxiliaries such as power steering. Not only are there control and design freedom advantages to electrical versus mechanical loads, there are also, in many cases, efficiency gains to be realized [27]. These efficiency gains come about because of the reduced mechanical load when the component is not being utilized. Mechanical power steering, for example, uses a belt-driven hydraulic pump that must run continuously to meet the response time requirements of the system. An electric power assist motor need only consume power when it is providing steering assistance with electrical controls that can respond very quickly to steering input. This efficiency advantage overcomes the efficiency loss caused in the conversion from mechanical to electrical energy [28].

With this shift from mechanical to electrical auxiliaries, new possibilities and new challenges arise, specifically in fuel-cell powered vehicles. The challenges include designing an electrical subsystem with the capacity to power all of these loads. The possibilities include the newfound ability to precisely control many of the loads that were previously either running continuously or with bang-bang control. With proper management, it should be possible to significantly reduce the average power of the auxiliary and parasitic loads.

Significance Relative to the Drive-Train

When talking about vehicles, components are usually classified in terms of peak and/or average power. When purchasing a car, the specifications consumers usually like to hear are: Peak propulsion power (engine horsepower) and fuel economy. Neither of these specifications give the cunsumer any insight into the auxiliary and parasitic power consumption. While it is understandable that consumers might not be interested directly in the power consumed by auxiliary and parasitic loads, they will surely be interested in the effects these have on fuel economy. According to the EPA (Environmental Protection Agency - U.S.A.) standardized fuel-economy testing regulations, vehicle tests are conducted with only the vehicle components required for operation. This means that manufacturers are free to test vehicles without power steering modules, without air conditioning, and with any other auxiliary systems shut off [29, 30]. Further, it has been found that the ratio of city to highway driving 55%–45% assumed by EPA testing procdures is unrealistic. Therefore in 1985 the EPA decided to reduce all reported fuel-economy numbers by approximately 15% rather than correct the testing procedures [6]. Thus, the majority of the public has no information about how using air-conditioning, for example, affects fuel economy.

The typical vehicle on the road today has a peak propulsion power of between 75 and 150 KW (100 to 200 Horsepower). Peak auxiliary and parasitic power combined is in the 3 to 5 KW range. This is a mere 2 to 6.6 percent of the peak propulsion output. This says nothing, however, about the average power outputs during normal driving conditions. Simulations of an electrically propelled Chevrolet Equinox using the UDDS (Urban Dynamometer Driving Schedule) industry standard drive cycle reveal an average propulsion power requirement of around 5KW (See Chapter 5). This represents the electrical power delivered to the motors before any mechanical drivetrain and vehicle losses, it also includes any energy recovered via regenerative braking and therefore might be somewhat lower than for a conventional vehicle. On a somewhat cold, rainy day, average combined auxiliary and parasitic power is 1-2KW [31]. With these numbers, we see how significant auxiliary loads really are at 20%–40% of the average vehicle propulsion power. Further simulations of a 1991 Ford Taurus in previous research [29] show a decrease in

fuel economy of 1.6 km/L or 3.8 mpg for an accessory load of 2kW. With air conditioning loads reaching as high as 4kW in hot weather, the EPA itself quotes fuel economy decreases of 21% when it is used.

1.1.5 Auxiliary Load Management Research

Load management is a field that has been explored in depth for large-scale power distribution systems. Electric utility operators are always interested in ways of reducing peak loads and therefore overall system requirements. This methodology carries over well to hybrid propulsion systems where battery operated electrical assistance allows for the reduction of gasoline engine requirements. For auxiliary and parasitic loads, although peak system capacity is also a large design consideration, the most important objective is the reduction of the average power. Average power is directly proportional to the amount of energy consumed in a given time period and thus directly corresponds to the fuel consumption attributed to these loads.

This section summarizes previous research efforts into managing the effect of auxiliary loads on fuel economy. Unfortunately, with the lack of public knowledge and interest in this aspect of vehicle design, most of the recent research focuses on the bigger items such as powertrain design and hybridization.

Heavy Vehicle Auxiliary Management

A study was done at the National Renewable Energy Laboratories (NREL) in the U.S. regarding management of auxiliary loads in class 7 and 8 tractor-trailers [32]. In this study the power consumed and the duty cycle were analyzed for each auxiliary load. Drive cycles were then developed that not only specified the vehicle propulsion factors such as speed and acceleration but also the auxiliary and parasitic load variations while driving. Simulating in NREL's ADVISOR using these drive cycles, the effect of individual auxiliary or parasitic loads was determined. Quantification of fuel-economy improvements with the removal of each individual component is argued to be useful as a basis for future research into auxiliary management. It provides the maximum improvement possible with the modification of a given component. It is proposed that the most likely methods for power consumption reduction are the conversion of mechanical auxiliaries to electrically operated

auxiliaries, alternative energy sources, and energy recovery (most likely electrical). Analysis of the simulated fuel-economy improvements identifies that a reduction in the auxiliary load has an effect on the powertrain efficiency throughout the drivecycle. This results in an erosion of the total gains and it is proposed that the powertrain be resized to account for changes in auxiliary loading.

Auxiliary Electrification in a Passenger Vehicle

Another study has presented the advantages of installing a 42V starter-alternator for boosting electrical system capacity [31]. The extra capacity and a novel mechanical belt system facilitates the operation of all the vehicle auxiliary and parasitic loads either directly via the ICE or seperately via the starter/alternator. This allows for engine idle elimination, however it does not remove the inherent inefficiencies of driving auxiliary loads over the wide rotational speed range of an ICE. When simulated, these modifications result in a 9% fuel-economy improvement with just the idle reduction. This however, is more of a power-train hybridization strategy than a true auxiliary management scheme.

The electrification of a number of vehicle auxiliaries and parasitics has been introduced by [33]. This paper has proposed the use of variable speed drives for cooling fan, water pump, air conditioning and power steering applications. The main benifits of which include reduction in mechanical parasitic losses and increase in controlability such that the device requirements can be met in a controlled manner rather then through engineered over-rating.

Overview of Future Automotive Electrical Loads

An overall look at the future of automotive electric systems has been presented by [30]. Existing auxiliary/parasitic loads are discussed and analyzed as is the topic of 42V electric systems. The authors correctly predict the auxiliary loading increases and re-iterate the significance of auxiliary power consumption on fuel economy. A new electrical system based on a higher voltage is suggested to support the larger electrical loads. Further, it is recognized that automotive electrical auxiliaries are designed to be over-rated so as to deal with extreme voltage variations on the poorly regulated 12V bus. A stable low voltage (6–12V) bus is suggested for lighting to avoid the

over-rating issues. Load control schemes are recommended to maintain peak loads below the maximum capabilities of a vehicles electric supply.

Reducing Passenger Vehicle Climate Control Loads

With climate control in passenger vehicles representing such a large proportion of the overall auxiliary power consumption, there are a number of papers suggesting possible improvements. Air conditioning loads can reach levels exceeding 4kW in passenger vehicles.

Climate control loads specifically in electric vehicles (EVs) have been examined in [29]. This paper identifies passenger comparment insulation and solar heat rejection as key areas for improvement. With better thermal isolation from the surrounding environment, the cooling and heating loads are reduced, thereby reducing the energy required and even the system size/weight. It is also noted that in EVs, powertrain waste heat is often insufficient for passenger compartment heating and heat pumps or resitive heaters are required. These heating loads would also benifit from improved thermal isolation.

Similar analysis regarding the reduction of cooling loads via different methods has been presented in [34]. It proposes the constant recirculation of the majority of the passenger compartment air to reduce the energy lost to the outside environment. It also proposes variable refrigeration strategies as opposed to the common automotive practice of varying air conditioning temperature by injecting engine waste heat into the passenger compartment.

Another group [35], has looked at the refrigeration energy losses incurred when the air conditioning compressor is forced to cycle on and off. This is the case for most automotive implementations and is compounded by the fact that wide engine rotational speed variations cause the compressor to operate in very inefficient modes. Variable capacity mechanical compressors or variable speed electrical compressors are suggested to combat these losses.

Management of Engine Cooling Loads

A recent study [36] looked at the fuel-economy benifits of controlling engine cooling components in both conventional and hybrid vehicles. This involved electrically driving all the cooling fans and pumps with microelectronic speed control system and thermal sensors. Control algorithms were implemented to match cooling power to the thermal loads and it was found that significant fuel-economy gains could result in both types of vehicles.

1.2 Objective and Contributions

The objective of this work is to show that through intelligent design and management of auxiliary systems alone, today's passenger vehicle energy efficiency can be significantly improved. This work focuses specifically on the systems and control of a Fuel Cell Electric Vehicle (FCEV) prototype developed at the University of Waterloo. The analysis in this work, however, is applicable to all types of vehicles and may find applications in many vehicle architectures. A survey is made of the various types of alternative fuels and vehicle architectures from conventional gasoline vehicles to hybrids and fuel cells. Trends in auxiliary power systems and previous research in control of these systems is discussed. The University of Waterloo Alternative Fuels Team (UWAFT) [37] FCEV is outlined and the design process discussed. Its powertrain control strategy is outlined and modifications to this as well as the addition of an auxiliary control module are proposed. Simulations are performed to predict the efficiency and fuel economy gains that can potentially be realized.

The research described in this thesis encompasses the following contributions made to the field of study:

1. Adaptation of a vehicle simulation environment for vehicle auxiliary loading characterization. This environment allows for auxiliary load fluctuations within a drive-cycle and provides the overseeing vehicle control strategy with the ability to modify auxiliary component operating parameters.

2. A simulation analysis on auxiliary loading in a FCEV (Fuel Cell Electric Vehicle) and its effect on vehicle fuel economy. These simulations show the merit of research in this field as the effect is quite significant.

3. Overview and classification of FCEV auxiliary components and the potential for energy savings in each. Two general methods of energy saving are introduced, the latter of which introduces the idea of transients in the auxiliary system demands benifiting vehicle powertrain efficiency.

4. Development of a simple vehicle air conditioning model for power usage analysis within a vehicle simulation environment. Two variations of this

model were made, one with a bang-bang control strategy and another with a PI control loop.

5. Adaptation of a cost based powertrain control algorithm for an FCEV. This algorithm considers and modifies auxiliary power demands in order to boost overall vehicle operating efficiency.

1.3 Thesis Outline

This thesis includes five chapters in addition to this introduction. These chapters are as follows:

Chapter 1 serves as an introduction to the field, providing background information on changes in the automotive industry and the overall trends influencing those changes. A number of new vehicle technologies are introduced and discussed while it is noted that research efforts now, as in the past, focus primarily on propulsion systems while auxiliary systems do not receive the attention they deserve. With this in mind, an outline of auxiliary system development over the past decades in automotive development is put forward, leading into the discussion of the following chapters.

Chapter 2 outlines the design and construction of University of Waterloo's own FCEV prototype vehicle. It covers the propulsion systems, the analysis and simulation that led to the vehicle's propulsion architecture and the vehicle control strategies.

Chapter 3 continues the discussion of UofW's FCEV, but specifically focusing on the auxiliary systems. Each system is discussed from the standpoint of power consumption, equipment ratings and purposer. For each, an evaluation is set forth for potential energy savings within the constraints of occupant safety and consumer acceptability.

Chapter 4 introduces a variety of auxiliary control strategies designed to reduce auxiliary energy usage and increase overall vehicle energy efficiency. These strategies are divided into two types, direct and indirect based on their primary control focus. An in-depth analysis of the FCEV's powertrain efficiency over a range of operating points is provided to support the theory of the indirect strategy.

Chapter 5 provides an overview of the vehicle simulations used to support the ideas outlined in the previous chapters. The simulation environment is described as are the individual experiments and their goals. The resulting data from each simulation experiment is tabulated and analyzed, quantifying

the gains that can theoretically be acheived using the methods and strategies described in chapter 4.

Chapter 6 summarizes the results and acheivements outlined in this work and makes reccomendations for future research in this area.

Following Chapter 6, a list of relevant references, publications and 3 appendices are given.

Chapter 2

Fuel Cell Electric Vehicle Prototype

With the motivation for this thesis outlined in the background information of Chapter 1, we can continue into the specifics of this work. The University of Waterloo has built a functioning Fuel-Cell Electric Vehicle (FCEV), based on a 2005 Chevrolet Equinox, with the goal of maintaining the original vehicle's performance characteristics. Much of the research and development effort has focused on sizing the powertrain components and developing powertrain control strategies. This chapter will outline the design choices and technical specifics of this FCEV prototype in order to lay the foundation for the analysis of it's auxiliary and parasitic loads.

2.1 ChallengeX Competition

The University of Waterloo Alternative Fuels Team (UWAFT) has been participating in a multi-year automotive design competition called "ChallengeX" since 2004 [38]. With main sponsors, General Motors and the U.S. Department of Energy (D.O.E.), the stated goals of the competition are to convert a factory original 2005 Chevrolet Equinox into a more fuel efficient, more environmentally friendly vehicle. These goals are to be achieved while maintaining the vehicle's original performance and customer acceptability. The competition has a total of 17 participating universities from the United States and Canada. The choice of powertrain technologies was left up to the par-

ticipants and UWAFT performed a great deal of analysis in choosing the powertrain that went into the current prototype vehicle.

2.2 Design Process

UWAFT's powertrain design was chosen with the help of PSAT (Powertrain System Analysis Toolkit) [39], a vehicle simulation tool built on Matlab^{TM} by Argonne National Laboratories (ANL). Using a methodology mirroring GM's own vehicle design process, UWAFT began running banks of simulations using the characteristics of the 2005 Chevrolet Equinox coupled with various fuel sources and powertrain architectures [40]. Table 2.1 summarizes the key performance metrics addressed in the competition, the performance of the stock factory vehicle and the competition Vehicle Technical Specifications (VTS) required for receipt of full performance points. Also note that the competition rules dictate that the use of the original engine is prohibited. Thus meeting the same emissions performance as the stock vehicle is not trivial and teams are forced to examine all powertrain options.

Table 2.1: ChallengeX VTS Targets

Metric	**Base Vehicle**	**ChX VTS**
Economy - combined EPA [L/100km]	≤ 10.10	≤ 7.35
Weight [kg]	≤ 1815	≤ 1996
Acceleration: 0-100 km/h [s]	≤ 8.9	≤ 9.0
Acceleration: 80-110 km/h [s]	≤ 6.8	≤ 6.8
Range - Highway [km]	≥ 515	≥ 320
Start Time [s]	< 2.0	≤ 5.0
Passenger Capacity	5	3,5
Emissions [Tier, Bin]	Tier 2, Bin 5	Tier 2, Bin 5
Trailering Grade-ability 7%gr. - 90 km/h - 0.4 km [kg]	1590	1135
Trailering Grade-ability 4%gr. - 90 km/h - 9.6 km [kg]	1590	1135

[40]

Analysis of fueling options for the vehicle resulted in a choice between two top contenders: Hydrogen (with fuel cell conversion) and Bio-Diesel. The key advantages that these fuels both have are the potential for sustainable energy, high efficiency powertrain operation, and low emissions. High powertrain efficiency translates into good fuel economy and low emissions make it easier to meet the EPA Tier 2, Bin 5 emissions requirements [41]. Sustainability was also a key factor in the decision despite the fact that it is not a competition requirement to use a sustainable fuel. Based on this alone, reformulated gasoline was ruled out as an option for fueling the vehicle. Ethanol was ruled out due to poor efficiency and poor emissions performance despite being a sustainable fuel. Electrical vehicles based solely on batteries were ruled out very early because of severe range limitations and therefore their inability to meet the competition VTS. Both bio-diesel and hydrogen fuel cell powertrains are complex and would present challenges to retrofit into the Chevrolet host vehicle. Hydrogen, however, being the more complex system of the two could only be chosen if it proved feasible to implement within the time scale of the competition. Fuel safety also played a key role in the analysis of different fuel types. Hydrogen, being a relatively uncommon automotive fuel, posed many unknowns and challenges for safe implementation.

2.2.1 Powertrain Architectures

Single Power-Source

The simplest vehicle powertrain architecture is the conventional single power-source as shown in Fig. 2.1. This power-source can be anything from fuel-cells to a bio-diesel ICE with some method of mechanically driving the wheels. The major advantage of this architecture is its simplicity that should result in a quick design and implementation cycle. Powertrain cost will also be relatively low with this architecture as there is no requirement for expensive batteries, complex mechanical power-splitting transmissions, or redundant sources of energy. This design quickly show's its disadvantages, however, when considering efficiency and fuel-economy performance. With a single power source, that source must be designed to handle the peak acceleration load of the vehicle and is therefore most likely not optimally sized for efficient operation at the average load [42, 43]. Further, using this architecture there can be no provision for the recapture of braking energy with the exception of a purely battery powered EV. With the development time available under the

competition schedule, there would easily be time to develop a more complex powertrain than this in order to realize the efficiency gains [42, 43, 40].

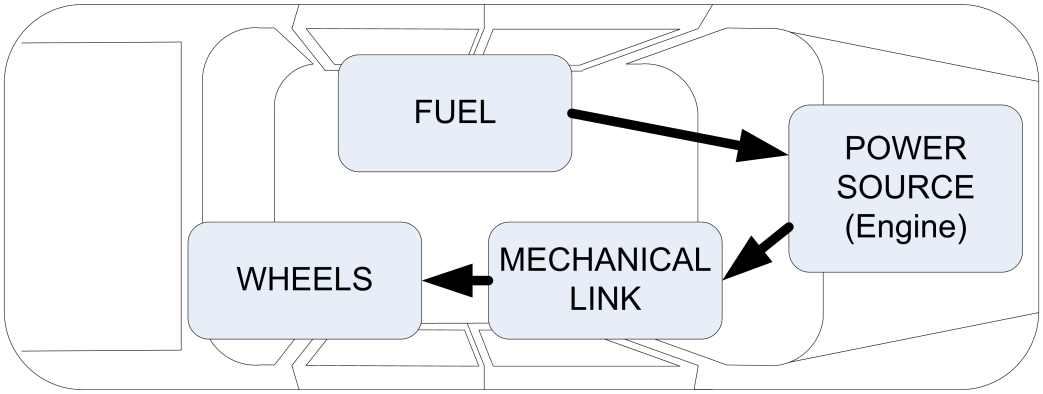

Figure 2.1: Single Source Powertrain Architecture

Parallel Hybrid

A parallel hybrid powertrain, shown in Fig. 2.2, employs multiple power sources that both have the capability to propel the vehicle simultaneously [42]. Typically a parallel hybrid employs only one fuel source which is consumed by the primary power source. The secondary power source is bi-directional, facilitating the temporary storage of energy in one form or another. Common primary power sources are ICE's fueled with various fuels and fuel cells fueled with either methanol or hydrogen. Common secondary power sources include hydraulic pump/motors coupled to an accumulator, electric motor/generators coupled to a battery and mechanical flywheel systems. The key advantage of this powertrain architecture is the increase in efficiency that can be gained by intelligently controlling the operating points of the primary and secondary power sources. With two power sources, neither has to meet the peak vehicle acceleration load independently and they can be sized more appropriately from an efficiency standpoint. Both can provide power when peak acceleration is required and the secondary power source can consume power to increase the operating efficiency of the primary power source at other times. The secondary source, being bi-directional, also allows the recapturing of braking energy by charging the energy storage in order to slow the vehicle.

With the linkage between the two power sources and the wheels being mechanical, it presents a complex problem to allow for any ratio of power split between the wheels and the sources. This places restrictions on the operating points that lead to some reduction in the efficiency gains. Overall this architecture allows for significant efficiency gains, in the order of 24% improvement over the single-source architecture, depending on the sizing and selection of components [14].

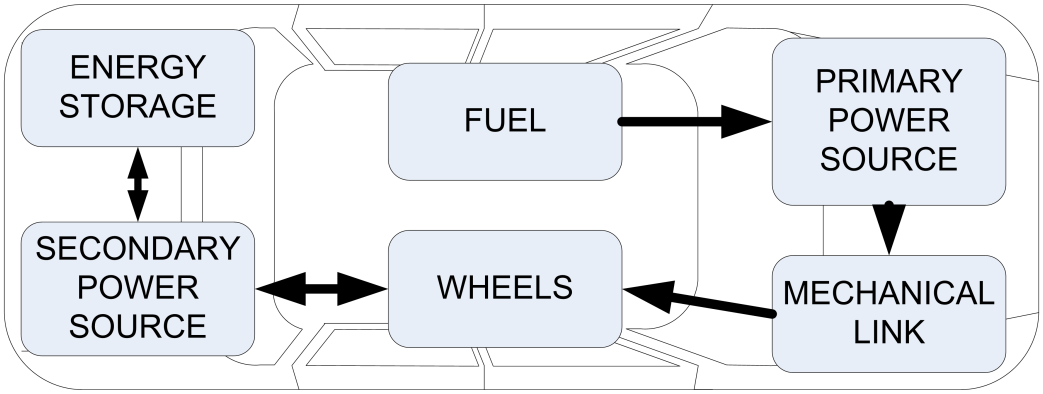

Figure 2.2: Parallel Hybrid Powertrain Architecture

Series Hybrid

Another architecture, the series hybrid outlined in Fig. 2.3 is arguably a simpler type of hybrid than the parallel hybrid. It is almost exclusively used with an electric generator, battery and motor for the energy storage and secondary power source components. The primary power source only provides power to the energy storage and the secondary power source, it cannot directly power the wheels. A primary power sourced sized to provide the average vehicle power requirements at optimal efficiency can thus constantly operate at its most efficient with the energy storage element absorbing the transients in the actual vehicle output power. An immediately obvious disadvantage of this architecture is the loss of energy caused by the multiple energy conversions. In a parallel hybrid vehicle, energy can flow directly from the primary power source to the wheels or from the primary power source through secondary power source to the wheels. In the series hybrid the later is the only possible route, incurring constant parasitic losses. Series hybrid vehicles implemented

with an ICE as the primary power source typically have slightly poorer efficiency than equivalent parallel hybrids [43]. Another disadvantage of this architecture is the need to have a large secondary power source that can supply the peak acceleration power demands of the vehicle alone, increasing costs and vehicle weight [42]. Fuel cell vehicles, as electricity is the output of the fuel cells, are typically implemented using this architecture, although they can also operate without the energy storage (battery) as in a single power source architecture.

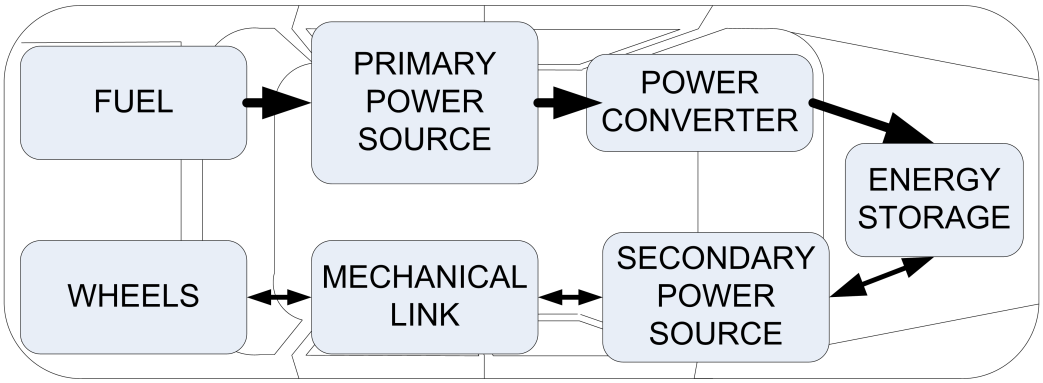

Figure 2.3: Series Hybrid Powertrain Architecture

Series-Parallel Hybrid

The most complex of the hybrid architectures is the Series-Parallel combined architecture as shown in Fig. 2.4. It contains all of the components of the series hybrid with an added mechanical link between the primary power source and the wheels as shown by the red arrow. With the potential to benefit from the advantages of both the parallel and series architectures, it also contains the most components and is generally the most costly to implement. Like the parallel hybrid, neither power source must provide for the peak vehicle acceleration power alone and like the series hybrid the primary power source can run almost constantly at it's maximum efficiency point [42].

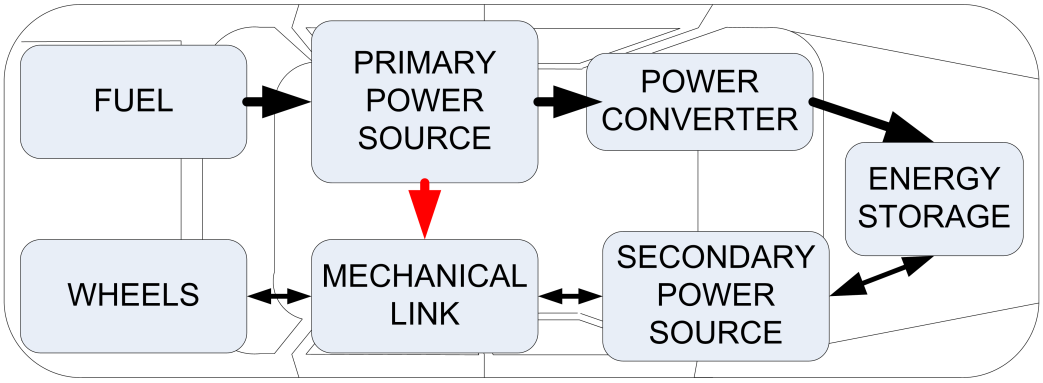

Figure 2.4: Series-Parallel Hybrid Powertrain Architecture

2.2.2 Selecting the Powertrain

Through the use of design of experiment (DOE) techniques, University of Waterloo's alternative fuels team was able to run enough vehicle simulations in PSAT to give a clear picture of the powertrain options. With hydrogen and bio-diesel chosen as the two main fuels of interest, the simulations were run with primary power sources based on both these fuels while varying the power capabilities of the individual vehicle components as well as the vehicle architecture. The result of this analysis was a hydrogen fuel cell series hybrid powertrain with components sized as shown in Table 2.2. Due to component availability and cost, the powertrain finally chosen was a compromise and is shown in the second column of Table 2.2 [40].

Table 2.2: Ideal and Final Powertrain Sizing

Component	**Ideal (kW)**	**Final Design (kW)**
Fuel Cell Power Module	46	65
Energy Storage System	60	70
Electric Traction Motors	87	103

[44]

Simulations of the final design selection predicted a VTS as outlined in Table 2.3. The areas where the design meets or exceeds the ChallengeX targets are left with a white bacground while the the trouble areas are shaded gray.

Table 2.3: UWAFT FCEV VTS Predictions

Metric	**ChX VTS**	**UWAFT FCEV**
Economy - combined EPA [L/100km]	≤ 7.35	≤ 6.96*
Weight [kg]	≤ 1996	≤ 2223
Acceleration: 0-100 km/h [s]	≤ 9.0	≤ 10.0
Acceleration: 80-110 km/h [s]	≤ 6.8	≤ 9.4
Range - Highway [km]	≥ 320	≥ 225
Start Time [s]	≤ 5.0	≤ 5.0
Passenger Capacity	3,5	2,5
Emissions [Tier, Bin]	Tier 2, Bin 5	Tier 2, Bin 1
Trailering Grade-ability 7%gr. - 90 km/h - 0.4 km [kg]	1135	1135
Trailering Grade-ability 4%gr. - 90 km/h - 9.6 km [kg]	1135	1135

*Calculated based on equivalent gasoline usage
White = FCEV meets Target, Gray = FCEV falls short of target

[40]

2.3 FCEV Powertrain Components

Based on the analysis and selections above, UWAFT was able to procure the powertrain hardware listed in Table 2.4. These components are linked via a high voltage bus as outlined in Fig. 2.5. Power flows from the FCPM as the primary power source via the DC/DC converter to all of the vehicle loads including the motors, battery (when charging), auxiliary and parasitic components.

Table 2.4: UWAFT FCEV Powertrain Component List

Device	**Make/Model**	**Specifications**	
Fuel Cell Power Module	Hydrogenics/ HYPM 65kW	Max Power: Voltage Range: Current Range: Mass:	65 kW 190-300V 0-300A 415kg
Hydrogen Storage	Dynetek/ZM180	Max Pressure: Tank Capacity: Tank Weight: Tank Volume:	5000 psi 4.31kg H2 92kg 178L
DC/DC Converter	UWAFT Custom	Input Voltage Range: Output Voltage Range: Converter Type: Mass:	190-300V 300-385V Boost 30kg
Traction Motors (x2)	Ballard/312V67	Peak Power: Continuous Power: Max Torque: Mass:	67 kW 32 kW 190 Nm 84kg
Motor Controllers (x2)	Ballard/312V67	Continuous Power: Input Voltage: Output Current:	67 kW 260-385V 280A RMS
Battery Pack	Cobasys/ NiMHax3 366-70	Voltage Range*: Capacity: Energy: Mass:	322-392V 8.5Ah 2.8kWh 85kg

*Open Circuit Voltage Range

[40]

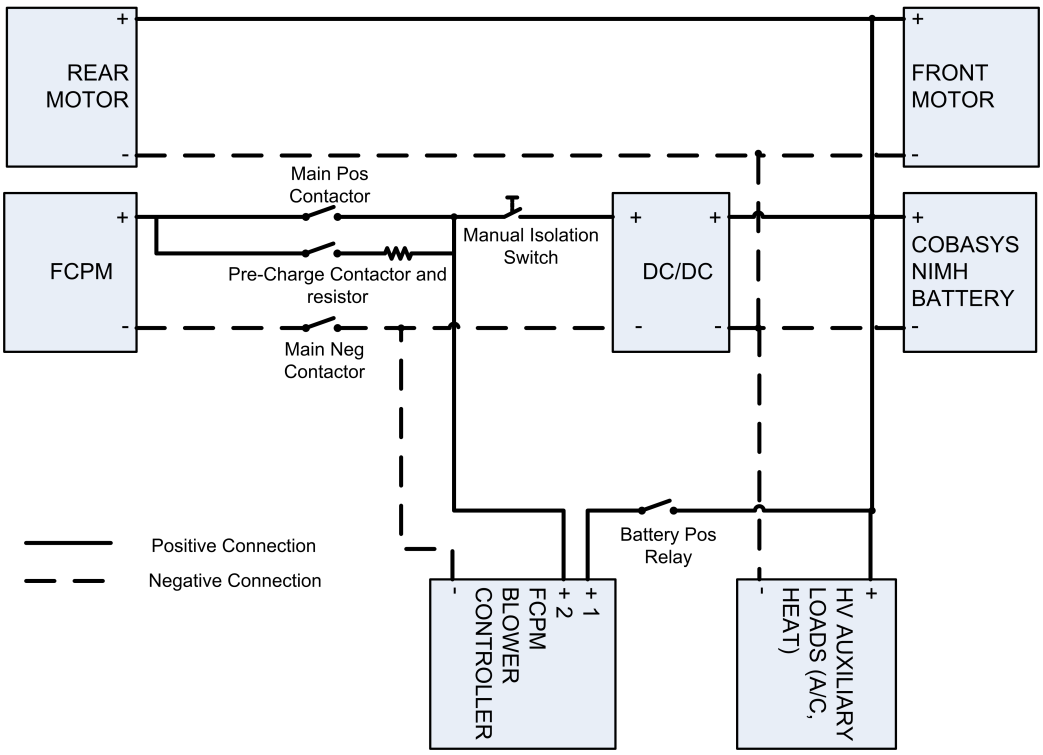

Figure 2.5: UWAFT FCEV High Voltage Bus Layout

2.3.1 Fuel Cell Power Module (FCPM)

The fuel cell power module (FCPM) is a Hydrogenics 65kW polymer electrolyte membrane (PEM) unit. It is a complete power delivery system with it's own on-board micro-controller and air delivery system. Communicating with the vehicle via a controller area network (CAN), the FCPM reports all of it's vital metrics to the vehicle and receives as input a power request. The power request command allows the vehicle control to, in effect, warn the FCPM controller when it is about to draw a specified amount of current. This allows the FCPM to spool up its air delivery blower and prepare itself for the requested power flow.

An FCPM such as this one, consists of individual fuel cells connected in series like the individual cells in a battery. Each cell consists of a an anode and a cathode separated by a polymer membrane where the electricity producing reaction occurs. The potential generated across each cell ranges from 0.6–1V depending on the concentration of reactants and the current being drawn [45]. Thus the voltage of the entire stack of cells in the FCPM varies significantly with the load or current draw. When operating with a battery connected to the FCPM's output, such as the nickel metal hydride (NiMH) battery pack used in this vehicle, this voltage fluctuation necessitates the use of a variable DC-DC converter to allow control of the FCPM current. Fig. 2.6 displays the typical voltage versus current curve for an PEM FCPM of this size.

Unlike a battery, the FCPM requires power in order to maintain the chemical reaction that produces the electricity. This power is consumed by the previously mentioned air delivery system, as well as the hydrogen recirculation pumps and other smaller devices. Including this parasitic power draw, the efficiency of a PEM FCPM looks like the curve shown in Fig. 2.7.

As can be seen, the efficiency of the FCPM varies greatly over the range of power output. To ensure that the operating point is consistently chosen to maximize this efficiency during vehicle operation, a control strategy must be employed. Section 2.4 outlines the control strategy designed and implemented for UWAFT's FCEV.

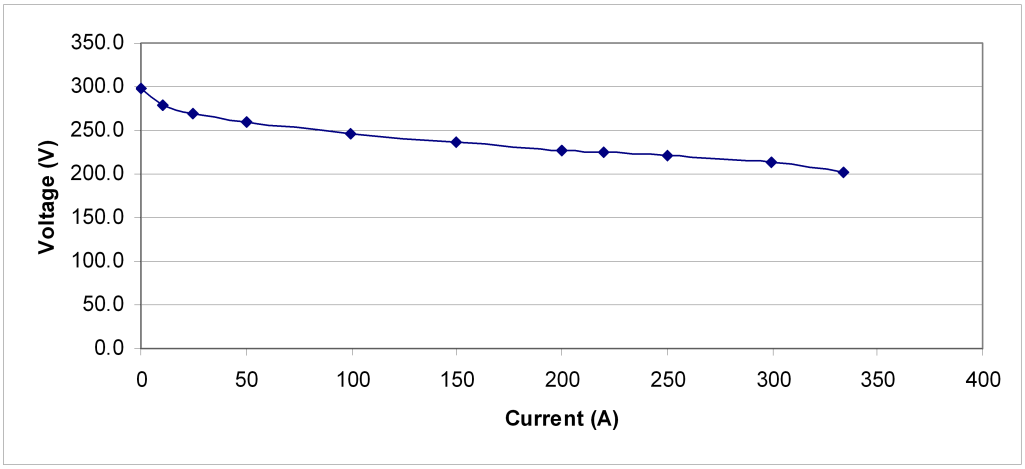

Figure 2.6: Voltage Fluctuation with FCPM Load

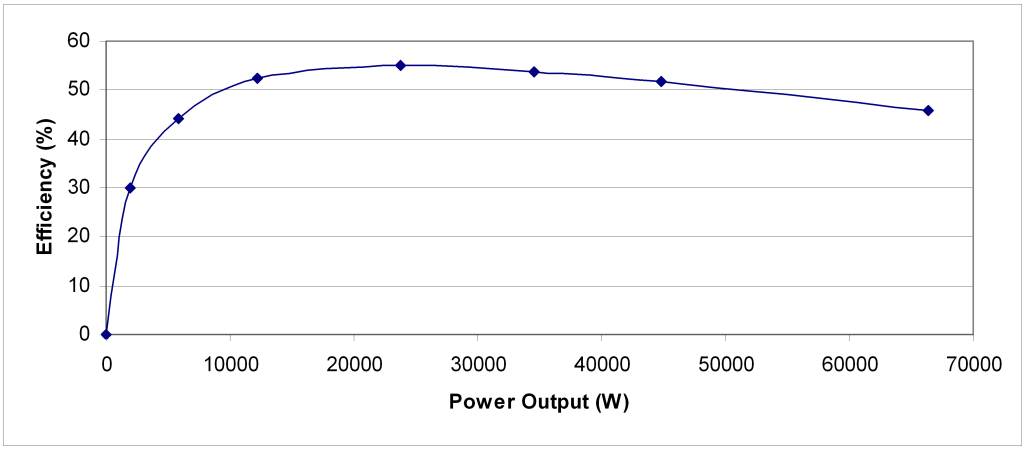

Figure 2.7: Efficiency Variation with FCPM Power Output

2.3.2 DC/DC Converter

As mentioned in the previous section, the DC/DC converter is required for facilitating and controlling the FCPM current flow. The converter installed in UWAFT's FCEV is a custom built boost converter developed at the university by Jen Marshall. It is capable of boosting a voltage as low as 190V at the input to 390V at the output with a maximum input current of 350A. It is a classic boost converter design whose circuit is shown in Fig. 2.8.

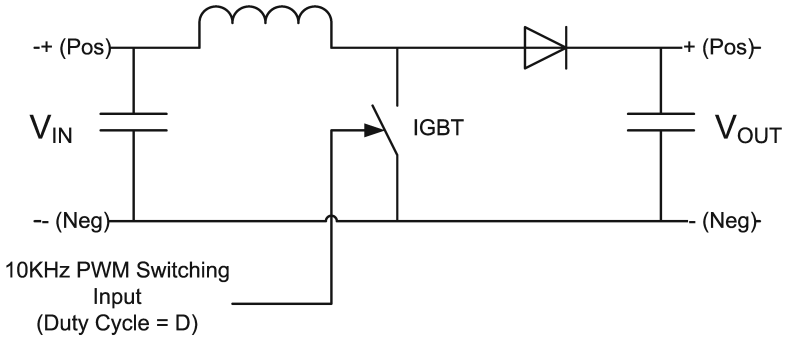

Figure 2.8: DC/DC Boost Converter - Main Components

The solid state switch used is an IGBT which receives a 10KHz pulse width modulated (PWM) signal from the main vehicle controller. The steady-state output voltage is determined by equation (2.1), and battery charging current is calculated with equation (2.3.2). With these two equations, the controller can determine the duty cycle to use for a desired battery current.

$$\frac{V_{IN}}{V_{OUT}} = \frac{1}{1-D} \tag{2.1}$$

where D = PWM Duty cyle in percent [0–1]

$$I_{Batt} = \frac{V_{OUT} - V_{Batt-OCV}}{R_{Batt-Series}} \tag{2.2}$$

where I_{Batt} = the charging current,
$V_{Batt-OCV}$ = the open circuit voltage, and
$R_{Batt-Series}$ = the series resistance of the HV battery

Upon calculating the required FCPM current, the vehicle controller calculates the necessary IGBT duty cycle and outputs the appropriate PWM signal. Transient variations in FCPM and battery voltage result in transient

variations in the current that flows, therefore a PI control loop is implemented in the vehicle controller to target the desired current flow.

2.3.3 Battery Pack

A Cobasys NiMHax^{TM} 336-70 NiMH battery pack [46] is connected to the output of the DC/DC converter and provides an energy buffer between the FCPM and the vehicle loads. As with any battery there is a cost associated with charging and discharging in terms of losses. These consist of series resistive losses which are proportional to the battery current squared (2.3) and inherent coulombic losses due to irreversibility's in the chemical reaction. Together these losses result in an energy turn-around efficiency of $\leq 80\%$ depending on the rate of charge/discharge. Fig.'s 2.9 and 2.10 show the efficiency curves of a typical NiMH battery pack for varying charge/discharge powers. Note: The discharge curve contains the coulombic efficiency factor and thus shows generally lower efficiency than charging.

$$P_{Resistive-Losses} = \frac{(V_{OUT} - V_{Batt-OCV})^2}{R_{Batt-Series}} \tag{2.3}$$

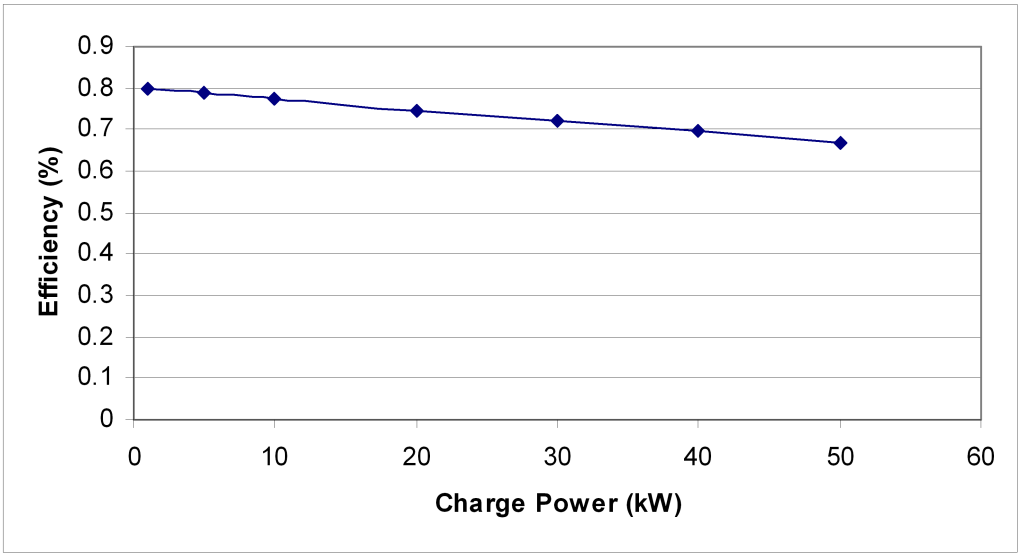

Figure 2.9: NiMH Battery Efficiency vs. Charge Power

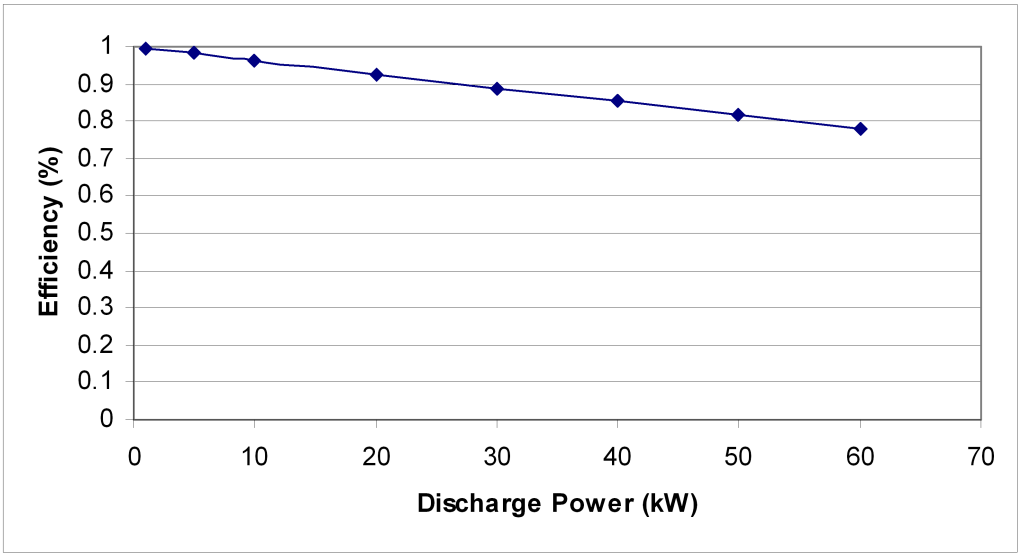

Figure 2.10: NiMH Battery Efficiency vs.Discharge Power

The Cobasys unit contains an integrated micro-controller which calculates the battery state of charge (SOC) via a proprietary algorithm and reports it as well as other battery metrics to the vehicle controller. It also contains a contactor to connect/disconnect itself from the FCEV's high voltage bus upon request from the vehicle controller or upon detection of a fault condition.

2.3.4 Traction Motors

The FCEV prototype is propelled by two Ballard 312V67 3-phase AC Machines. These traction motors come together with the motor controller/inverter which generates the 3-phase AC waveforms from a DC input. These include a micro-controller which also communicates with the vehicle controller via CAN like the battery and FCPM. To actuate them, a CAN message is sent from the main vehicle controller to the motor controller specifying a requested torque, which can be positive or negative (i.e. forward or reverse). The torque command is directly proportional to the drivers request via the throttle pedal. This command is relayed to the motor controllers which draw the required amount of power from the high voltage bus. The battery, motors, and FCPM all report their instantaneous voltages and currents to the

vehicle controller via CAN. With this information, the vehicle controller can calculate the optimal operating point for the FCPM such that the vehicle powertrain efficiency is maximized.

Had the vehicle utilized only one motor, and given that the motor torque directly mimics the driver's request, the motor efficiency curve would not be important to the control strategy but only to the vehicle designers in terms of choosing an efficient propulsion system. This is not the case, however, as the FCEV prototype utilizes two of these motors. One for the front two wheels, and one for the rear two wheels. With this configuration, there is the flexibility to optimize the torque request which is split between the front and rear motors. The goal of this optimization is to maximize the resulting propulsion power for a given torque request and is beyond the scope of this paper, but is analyzed in another thesis from the University of Waterloo [47].

2.3.5 Auxiliary Systems

The auxiliary systems are not necessarily directly related to the powertrain, however, they are significant in that they use power that the powertrain produces. There are two separate auxiliary subsystems, one operating at the automotive standard 12VDC and the other operating at 24VDC. To provide power to these subsystems, internally controlled DC/DC buck converters connected to the high voltage bus as in Fig. 2.5 convert from the approximately 300VDC to the required subsystem voltage. These converters have a nominal operating efficiency of 86%, varying slightly as the input and output currents and voltages fluctuate [48].

2.4 Vehicle Control

In the last section describing the components comprising the powertrain of UWAFT's FCEV, it can be seen that there are two main energy paths starting from the stored hydrogen fuel and ending at the vehicle loads: the auxiliaries and the wheels. These paths are outlined in Fig. 2.11 and each has it's own associated cost in terms of energy losses.

The power delivery efficiency of each path is the individual operating efficiency of each component in the path multiplied by the efficiency of the other components in the path. The first path in the figure has a power

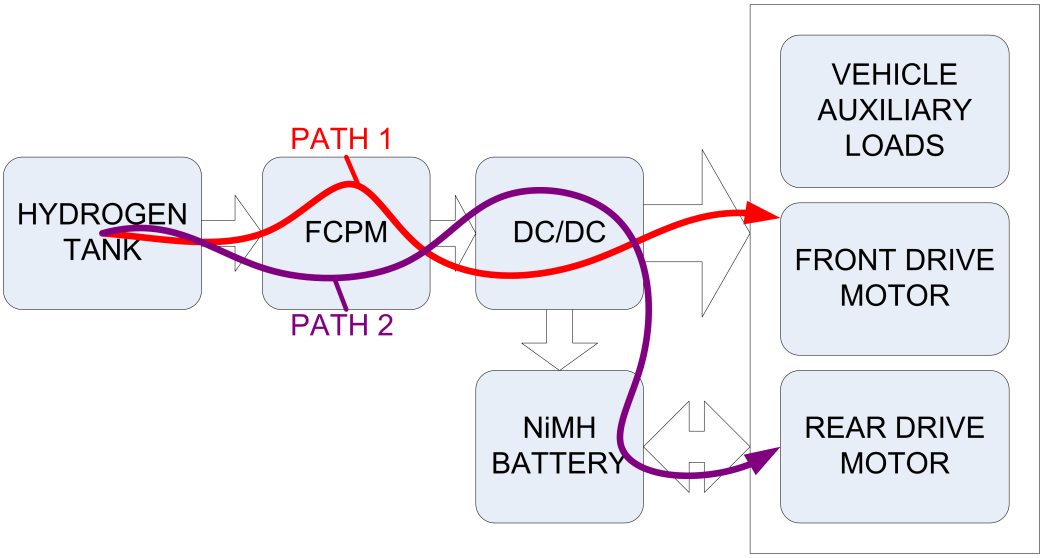

Figure 2.11: Two Power Paths in FCEV Hybrid System
Path 1: Energy travels directly to vehicle loads, uni-directional
Path 2: Energy travels through battery to vehicle loads, bi-directional

delivery efficiency computed by (2.4), while the efficiency of the second path is calculated as in (2.5).

$$\mathrm{Ef}_{Path1} = \mathrm{Ef}_{FCPM} \times Ef_{DCDC} \tag{2.4}$$

$$\mathrm{Ef}_{Path2} = \mathrm{Ef}_{FCPM} \times \mathrm{Ef}_{DCDC} \times \mathrm{Ef}_{BATT_{Chrg}} \times \overline{\mathrm{Ef}_{BATT_{Dschrg}}} \tag{2.5a}$$

or

$$\mathrm{Ef}_{Path2} = \overline{\mathrm{Ef}_{FCPM}} \times \overline{\mathrm{Ef}_{DCDC}} \times \overline{\mathrm{Ef}_{BATT_{Chrg}}} \times \mathrm{Ef}_{BATT_{Dschrg}} \tag{2.5b}$$

In these equations, $\overline{\mathrm{Ef}_X}$ represents the time averaged efficiency of component X. Path one's efficiency is simply the efficiency of the FCPM combined with the efficiency of the DC/DC at the instant of computation. Time must be included in the equation for the second path due to the nature of the battery. Energy must first accumulate in the battery before it can be used again at a later time. In order to calculate the instantaneous efficiency of this path then, the formula used is dependent on whether the battery is being charged or discharged. During battery discharge, as in (2.5a), the average efficiency of

the charging process, which includes the FCPM, DC/DC and battery charging efficiencies, must be combined with the current instantaneous discharge efficiency. During battery charge, as in (2.5b), the average discharge efficiency of the battery is combined with the instantaneous charging efficiency [49].

2.4.1 Powertrain Control Strategy

Average powertrain efficiency has a large effect on the vehicle's overall efficiency and in turn fuel economy. To ensure that the FCEV's powertrain is always operating at the best possible efficiency, a control strategy must be employed to vary the operating points on a continual basis. The currently implemented control strategy assumes one point of powertrain freedom α defined as:

$$\alpha = \frac{P_{BATT}}{P_{NET-LOAD}}, (1-\alpha) = \frac{P_{FCPM}}{P_{NET-LOAD}} \tag{2.6}$$

$P_{NET-LOAD}$ represents the total load on the electrical portion of the powertrain, including both the power requirements of the two traction motors and the power consumed by the auxiliary subsystems. α is a power split factor, or the percentage of power going through path two as defined above in Fig. 2.11. In this strategy, it is assumed that $P_{NET-LOAD}$ is fixed and the only way to vary the powertrain operating point is via changes in α. The reasoning behind this is that the driver's request is paramount in a production vehicle. In fact, it is the primary goal of any vehicle powertrain control system to match the driver's power or torque demand as closely as possible [50]. Variations in car behaviour for a given throttle position are to be avoided at all costs and extremely affect customer acceptability. Further, it is assumed that similar to the driver torque request, the power request from vehicle auxiliary systems is also paramount and must be met with the same degree of accuracy. Therefore a control strategy was designed to target the delivery of $P_{NET-LOAD}$ while maximizing the powertrain efficiency as much as possible. This is a common assumption that is made in many research papers and research efforts into hybrid vehicle control strategies [51, 50, 52].

There are a number of control techniques that can and have been employed for fuel cell hybrid and ICE hybrid vehicle powertrain control, in-

cluding fuzzy logic controllers [51], rules-based control [53] and continuous optimization methods of control [54]. Through simulations it was decided that optimization methods produced the overall fuel economy for UWAFT's FCEV and were able to be computed by the vehicle's on-board controller in real-time. The optimization strategy used is as follows [49]:

Cost Function

$$Cost(\alpha) = \frac{\beta_1}{\gamma_1}\mathrm{Ef}_{Elec}(\alpha) + \frac{\beta_2}{\gamma_2}\mathrm{SOC}(\alpha) + \frac{\beta_3}{\gamma_3}\mathrm{FC}_{sw}(\alpha) \tag{2.7}$$

With the objective to minimize the cost, (2.7) is repeatedly evaluated over a range of $\alpha's$ to determine the optimal value. Each term in this cost function is normalized by γ, and weighted appropriately by β. $\mathrm{Ef}_{Elec}(\alpha)$, defined in (2.8), is the total efficiency of the powertrain electrical sources at the instant of evaluation for the specified α. $\mathrm{SOC}(\alpha)$ is a battery state of charge (SOC) targeting factor that serves to ensure future powertrain efficiency by maintaining the battery at an efficient SOC point. SOC targeting also ensures that there is sufficient battery capacity available for absorbing braking energy. The last term, $\mathrm{FC}_{sw}(\alpha)$, adds cost of FCPM on/off cycling. When not delivering any power, it makes sense from an efficiency point of view to shut off the FCPM as it uses power when running even though it is not delivering any power. From an FCPM life expectancy point of view, however, it is beneficial to limit the number of on/off FCPM cycles. This term offsets the overall cost to prolong the FCPM lifetime at the expense of some vehicle efficiency [49].

Overall powertrain electric efficiency is defined in the following equations, and again depends on whether or not the battery is being charged or discharged. Assuming $P_{NET-LOAD}$ is positive, a positive value of α indicates discharging of the battery according to (2.6) and a negative value of α indicates charging of the battery. Thus we have the following formulas for calculating instantaneous powertrain electrical efficiency [49]:

$$\mathrm{Ef}_{Elec}(\alpha) =$$

Case 1: $\alpha > 0$

$$(\alpha)(\mathrm{Ef}_{FCPM} \times Ef_{DCDC})+ \quad (2.8a)$$
$$(1-\alpha)(\mathrm{Ef}_{FCPM} \times \mathrm{Ef}_{DCDC} \times \mathrm{Ef}_{BATT_{Chrg}} \times \overline{\mathrm{Ef}_{BATT_{Dschrg}}})$$

Case 2: $\alpha < 0$

$$(\alpha)(\mathrm{Ef}_{FCPM} \times Ef_{DCDC})+ \quad (2.8b)$$
$$(1-\alpha)(\overline{\mathrm{Ef}_{FCPM}} \times \overline{\mathrm{Ef}_{DCDC}} \times \overline{\mathrm{Ef}_{BATT_{Chrg}}} \times \mathrm{Ef}_{BATT_{Dschrg}})$$

Note: As before, $\overline{\mathrm{Ef}_X}$ represents the time averaged efficiency.

2.4.2 Controller Hardware

The FCEV is controlled by two supervisory controllers made by Mototron Inc. They are PowerPC processor based micro-controllers designed for automotive applications with a variety of analog and digital input and output channels. Table 2.5 lists the specifictions of the two contollers [55].

Table 2.5: UWAFT FCEV Controller Specifications

Specifications	**Front Controller ECU-565-128**	**Rear Controller ECU-555-80**
Processor (Clock)	32-bit MPC565 (56MHz)	32-bit MPC555 (40MHz)
Analog Inputs	30	19
Digital Inputs	4	3
Low Side Drivers	15	8
+/- 12V H-Bridges	3	2
TTL-Level Outputs	12	0
CAN Transceivers	2	2

Together the two controllers monitor all the vehicles important signals including operating temperatures, DC/DC current flow, throttle position, etc. They communicate with eachother and with the other vehicle microcontrollers via their integrated CAN transceivers. The CAN networks are set up as outlined in Fig. 2.12.

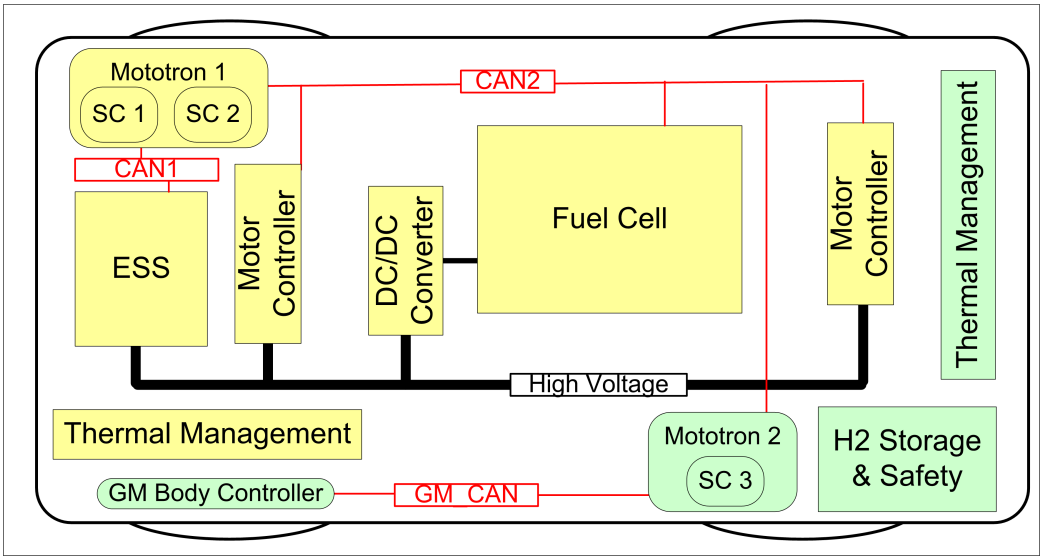

Figure 2.12: FCEV Controller Area Network Layout [56]

The front controller runs the overall vehicle control. This includes evaluating the cost function, powertrain operating point, sending the appropriate power requests to each component, controlling and monitoring the inputs and outputs of the rear controller via CAN, and running the PI current-control loop for the DC/DC converter. The rear controller is primarily idle except for the monitoring of it's inputs and the transmission of that data to the front controller, or the setting of the outputs based on commands from the front controller.

2.5 Chapter Summary

This chapter has provided a brief glimpse into the powertrain and inner workings of UWAFT's FCEV. The powertrain control strategy is outlined as it is implemented. With this vehicle as a test bed for examining auxiliary and parasitic loads, the following chapters will describe these vehicle loads and methods of altering their power consumption to improve overall fuel economy.

Chapter 3

FCEV Auxiliary and Parasitic Loads

This chapter outlines the auxiliary and parasitic systems present on-board UWAFT's FCEV. Each system will be discussed in terms of its purpose, power consumption, safety considerations, and consumer comfort or acceptability. The intent is to outline the key considerations for each component or system in order to analyze the overall optimization of their power consumption.

3.1 Climate Control

Climate control for the FCEV's interior encompasses the largest area of auxiliary power consumption. It consists of three main componenets: (1) Cabin Blower, (2) Refrigeration Unit, and (3) Heat Source. The first two of these are considered generally large auxiliary loads in conventional vehicles. The operating temperature for all of the FCEV's vehicle components is considerably cooler than a conventional vehicle at around 60–80°C. This is not sufficient to utilize the typical heat exchangers used for interior heating and a 3kW resistive heater provides the interior heating capacity instead.

3.1.1 Cabin Blower

The cabin blower is a 12VDC powered centrifugal multi-speed fan which drives air through the interior climate control system. At its highest speed,

this fan consumes 275W continuously. The air is ducted through the dashboard assembly to the location of the passenger's choice which may be the floor, the upper vents, or the windshield for defrost. The majority of the interior climate control system, with the exception of the air conditioning compressor and heater, consists of the original 2005 Chevrolet Equinox parts.

Requirements

This blower is critical for proper operation of all of the climate control systems as it pushes air through the heater coils and the cooling element of the air conditioning system. Thus in order to meet the heating and cooling requirements for these systems, this blower must be able to deliver sufficient air flow-rates. Being an original vehicle part, this blower is designed to meet the cooling and heating loads of this vehicle. It is also required to maintain a consistent air flow-rate as set by the passengers. If it were to be controlled, variations in speed would have to be gradual and small in order to avoid distracting the vehicle's driver. This is a very subjective requirement that would have to be tuned upon implementation.

3.1.2 Air Conditioning

Air-conditioning, although considered a luxury, was installed in over 80% of vehicles sold in 1990 and surely that number is larger today [57]. The air-conditioning system is the single largest auxiliary load in terms of energy consumption in the majority of vehicles. Its purpose is to provide passenger comfort by reducing the interior cabin temperature to comfortable levels. Beyond this, air-conditioning can also aid safety critical window de-fogging systems, and there are some studies suggesting cabin temperature regulation is an important objective for safe vehicle operation [29]. The main energy consuming component of the air-conditioning system is the compressor. In typical vehicles, this compressor is belt-driven by the ICE and must operate effectively at all ICE speeds. In UWAFT's FCEV, the absence of an ICE or any other consistently spinning mechanical power source precludes the use of such a compressor. In this vehicle, an electrically driven compressor with variable speed capability is employed. While bulky and expensive, this unit is very flexible in its operating parameters, allowing for efficiency optimization not typically afforded by commonplace belt-driven compressors [35, 58].

Performance standards and Regulations

As it is considered a luxury item and not officially safety critical, there are no North-American regulations directly requiring specific air-conditioning performance. In fact, as late as 2003, there were not even any standards for rating vehicle interior climate control system performance. As a result, the main system objective is customer comfort and in turn customer acceptability. This means that each automotive manufacturer has its own internal and proprietary performance metrics. The typical rule of thumb is that the vehicle should cool to room temperature (22°C) within 30 minutes after sitting for an extended period in the sun on a hot day. At the same time, air outlet temperature should not be cold enough to cause passenger discomfort, and should not fluctuate by more than a couple of degrees after a specific setting has been chosen [29].

Equipment Ratings

The air-conditioning system currently installed in UWAFT's FCEV consists of a compressor driven by a controlled 320V DC machine, the condenser, evaporator and interior blower from a stock 2005 Chevrolet Equinox, and a custom controller for the condenser fans. The complete refrigeration circuit is outlined in Fig. 3.1 and it operates to move heat from the inside of a vehicle to the outside through a cyclical thermodynamic process.

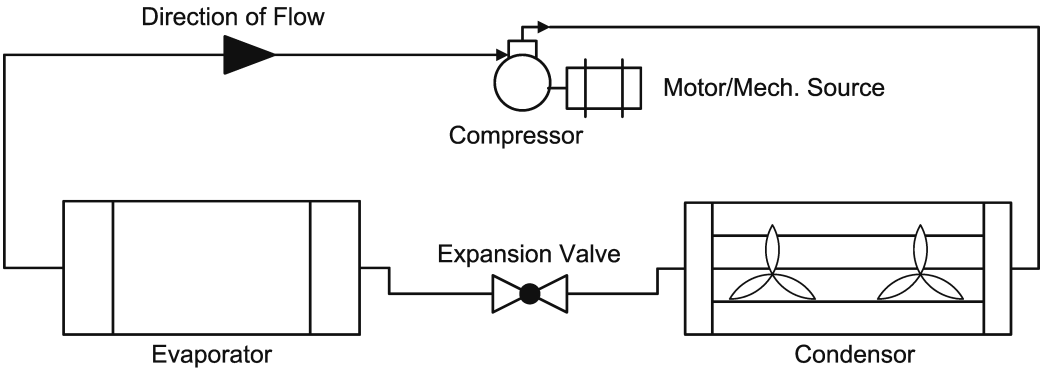

Figure 3.1: Refigeration System Outline

The compressor pumps the refrigerant (usually R-134a in modern vehicles) through the A/C plumbing circuit as shown. The restriction imposed

Table 3.1: UWAFT FCEV A/C Compressor Specifications

SANDEN SHS-33A4007 Specifications	
Type	Scroll Semi-Hermetic
Displacement	33.1cc per rev.
Speed Range	400-7812 rpm
Motor	DC Brushless
Motor Power	5 h.p. @ 7000 rpm
Refrigerant	HFC-134a
Power Source	320 VDC Nominal
Weight	10.4kg

[59]

by the expansion valve causes the pressure to build on the condenser side of the circuit relative to the evaporator side. This relative pressure difference causes the refrigerant to condense, rejecting heat in the condenser and in the evaporator it evaporates, absorbing heat. The refrigerant flows continuously around the circuit creating a constant flow of heat energy from the evaporator to the condenser [60]. The compressor is a Sanden SHS-33A4007 unit, designed specifically for EV applications, with operating specifications as shown in Table 3.1. As this compressor is capable of operating at any speed between 400 and 7812 rpm, the air-conditioning (A/C) system power and thus refrigeration capacity can be continuously adjusted. Fig. 3.2 is a graph of the compressor's input power plotted with compressor speed, refrigeration capacity and Coefficient of Performance (COP). COP is a metric used by refrigeration engineers to indicate system efficiency. It is defined as:

$$\text{C.O.P.} = \frac{Q_{In}}{W_{Cycle}} \tag{3.1}$$

where Q_{In} represents the heat energy absorbed by the system and W_{Cycle} represents the energy absorbed by the system to maintain the refrigeration cycle [60]. Dividing the numerator and denominator of 3.1 by seconds results in refrigeration capacity in Watts over the system input power in Watts.

Looking at the COP curve in Fig. 3.2, the variation in efficiency is approximately +/- 5% for the test system. As these results correspond to an experiment with constant temperatures and pressures, the real system will

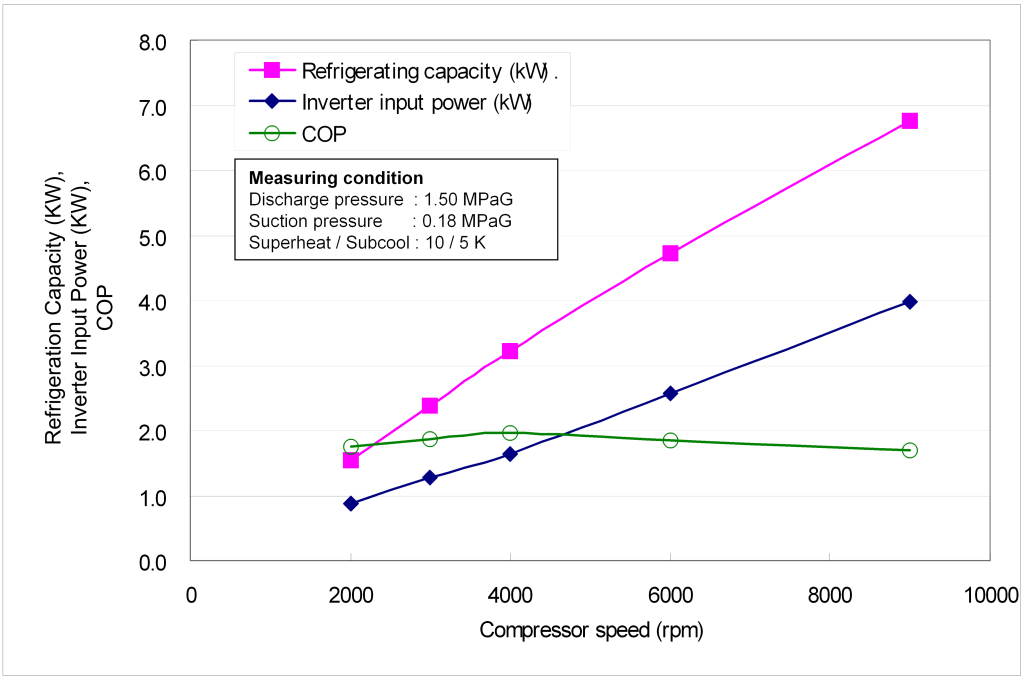

Figure 3.2: A/C Compressor Power Variation
Chart reproduced with permission from Sanden International Inc. [61]

perform slighly differently, however this data gives a good starting point.

As mentioned in section 1.1.5, typically, cars control the A/C system cooling by reheating the cabin air using engine waste heat. While there is an advantage to this in terms of reducing humidity in the vehicle interior, it is also very wasteful in terms of energy use [34]. With a variable speed compressor such as this unit, it is possible to directly control the refrigeration capacity, thereby a reduced passenger demand for cooling results in a reduced energy demand. A further benifit of this flexibility, is the removal of the need to cycle the compressor on and off for modulation of refrigeration capacity [35].

Boundaries of Operation

While having the flexibility to operate over a whole range of refrigeration capacities, the FCEV's A/C system must remain within certain operating parameters for proper operation. Firstly, the evaporator temperature must not be allowed to dip below 0°C, or ice buildup will impede airflow and dramatically reduce the system efficiency. Refrigerant pressure on the high-pressure side of the system cannot exceed the ratings for the piping or the system becomes unsafe. A pressure transnducer at the outlet of the compressor is used to monitor the system and turn off the compressor if the limit is reached. Lastly in an ideal refrigeration system the expansion valve is controlled to have a constant pressure differential. In practice, when using an orfice tube type expansion valve as installed in the FCEV, at very low flow rates this pressure differential is often unacheivable. Thus there is a minimum compressor speed that must be maintained to allow the system to transfer heat as designed [60].

3.1.3 Heat

As mentioned in section 3.1.1, the original heat exchanger used for heating the vehicle interior with powertrain waste heat was not usable with the low powertrain tempertures of the FCEV. It was replaced with a 300VDC 3kW resistive heater element in the dashboard climate control assembly. The heating power will be controlled with chopper circuitry, allowing the amount of heat produced to be adjusted precisely.

Requirements

As with the air conditioning system, there are few specific regulations for required heating capacity other than the industry rule of thumb of 22°C within 30 minutes after a cold soak. Heat, however, has a key role to play in defrosting the vehicle windshield, which is a definite safety factor and the defrost time should be minimized at all costs [29]. Therefore it is required that when in defrost mode, the heater should be running at it's max capacity, provided that it does not overheat.

3.2 Lights

A vehicle's lights, including headlamps, turning indicators, brake lamps and interior lighting consume a significant amount of energy. Headlamps are a critical safety system for vehicle operation at night and since 1989 also during the day under Canadian law. All exterior lighting is strictly regulated according to Transport Canada's technical standards document (TSD) No. 108, and FMVSS (Federal Motor Vehicle Safety Standard) 108 in U.S.A. [62, 63]. UW's FCEV uses the stock lighting systems from the 2005 Chevrolet Equinox that are compliant with both North American standards. These lighting systems operate with a nominal supply of 13.8V and comply with the standards when operating between 10V and 14.5V. This is to allow for fluctuations in the vehicle 12V bus without compromising safety. Table 3.2 outlines the minimum and maximum lighting power consumption figures when operating at the minimum and maximum compliant voltages.

Table 3.2: UWAFT FCEV Lighting Power Consumption

Light	**Min Power @ 10VDC** (W)	**Max Power @ 14.5VDC** (W)
Headlamps - Low-Beams	67.2	140.3
Headlamps - High-Beams	79.4	165.6
Brake Lights	31	63.6
Turn Signals	32	70.56
Interior Lights	41	85

The current lights use Incandescent lighting technology and can be replaced with higher efficiency systems as long as they meet the safety requirements outlined in the standards above. Interior cabin lighting is not subject to the same restrictive safety requirements as exterior lighting. The usage duty-cycle is also relatively low and thus does not contribute significantly to vehicle energy usage.

3.3 Power Steering

Power steering is an important component in today's front wheel drive, front engine vehicles. With so much weight over the front wheels, steering becomes very difficult to do at slow speeds without assistance. This is especially true in UW's FCPV, which weighs approximately 500kg more than the original vehicle. The steering system consists of a brushless DC machine, steering shaft torque sensors, and a complex control unit as seen in Fig. 3.3. This is quite obviously a safety critical system that directly affects how the driver interacts with the vehicle. Modification of the operation or failure of this system during driving can have an adverse affect on passenger safety.

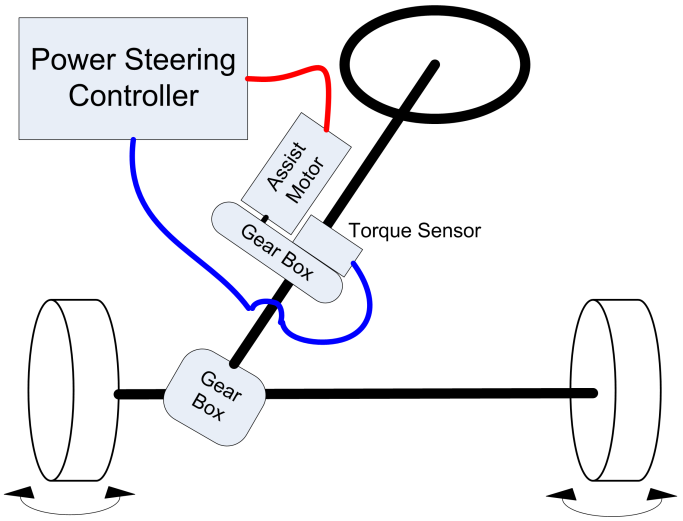

Figure 3.3: Power Steering System

This system consumes 300W with a duty cycle of approximately 30% depending on the driving situation. That is a significant energy usage, however, without entirely redesigning the complex control system, it is impossible to improve upon the efficiency of this sytem. The control is finely tuned to achieve a specific transient response, and restricting the power draw would hamper this. Further, any attempt to automatically restrict the power draw might hurt the stability of the system and lead to dangerous results. Considering the large efficiency gains acheived simply by using such electronic control over hydraulic power steering, further gains are not really waranted [64].

3.4 Power Brake Assist

Like power steering, stopping such a heavy vehicle becomes very difficult even with the help of hydraulic amplification. Therefore it is necessary to have braking assistance, which is provided by a vacuum operated brake booster in the stock Equinox. Without the vehicle's original ICE, however, there is no means of providing the vacuum required to operate the brake booster. In the FCEV, two Hella UP28 electric vacuum pumps are utilized to facilitate the operation of the brake booster. These pumps are powered by 12V and consume 200W when running.

Their operating duty cycle is 10–30% depending on the driving conditions and they are currently controlled in a bang-bang, on/off manner. A vacuum of approximately 0.65ATM is required for proper brake feel, and thus consumer acceptability. This must be maintained under all driving conditions with as few transients as possible. North American safety regulations dictate maximum stopping distances allowed when power brake assistance is not functioning, however, any loss or curbing of brake function is putting the vehicle occupants at a severely increased risk. Beyond simple safety, the brake feel must not change significantly during vehicle operation so that the driver is not confused from a customer acceptance point of view. What this essentially means, is that there is not any significant margin for energy savings in this application. Without a mechanical change in the brake actuation design, the 200W electrical power requirement of these pumps must be able to be satisfied at all times.

3.5 Windshield Wipers

Another safety critical system, windshield wipers directly affect driver visibility in adverse weather conditions. They consist of an uncontrolled DC Machine with multiple windings moving physical wiper arms across the glass of the windshield to wipe away water, snow, dirt etc. The multiple windings facilitate multiple speeds of operation for different severities of weather conditions. Although there are now technologies for automatically controlling wiper speed based on detected weather conditions, the system in the FCEV is completely manual, requiring the driver to select the operating speed. This system draws 64W at its highest speed of operation with a nominal voltage

of 13.8V. While 64W is not a very significant power draw, the wiper system is often left activated when not needed, leading to premmature wiper blade wear and excess energy usage. Using sensors to automatically control the speed and action of the wipers would reduce overuse and both of these consequences [65].

3.6 Rear Window Defog

The purpose of a defogging system is to evaporate condensation from the surface of vehicle windows. There are a couple of different ways in which this is achieved, complicating the energy usage calculations. For the front windshield of the vehicle, hot air from the cabin blower is directed up from the base of the glass to warm and thus evaporate the condensation. Modern vehicles including the 2005 Chevrolet Equinox, utilize the air-conditioner during defogging to de-humidify the air, improving defogging performance. The rear window is defogged by means of a resistive heater element coated in thin strips on the surface of the glass. As the air conditioning, heating and cabin blower systems were already discussed, this section will focus specifically on the rear window defogger.

Rear window defogging in the FCEV utilizes a resistive heater similar to the stock vehicle except on a polycarbonate window instead of glass. The heater element draws approximately 180W and this type of defogger is often left running un-wittingly by drivers. Therefore, despite the fact that the rear defog duty-cycle should be relatively low, it ends up being much larger because of driver error. An interesting feature would be to implement a fog sensing mechanism in order to automatically control the defog heater. In this manner it would only be on when and for as long as neccesary, reducing overall energy usage.

3.7 Momentary Auxiliaries

Momentary auxiliary loads encompasses the remaining components not already discussed above. These systems are characterized by extremely low

duty cycles, and thus negligible effect on vehicle energy consumption. These systems are:

- Power Windows
- Power Door Locks
- Power Seat Adjustments
- Power Mirror Adjustments
- Horn

Of all the systems listed here, the most energy consuming are the power windows. These consume approx. 100W each depending on various environmental factors that increase/decrease window friction. They also have the highest duty cycle of all the items in the list. As far as average energy consumption, these items are not significant, but if peak auxiliary load is ever an issue during vehicle operation, they are still significant. In order to help avoid worst-case peak loading, it may be beneficial to enable/disable some of these loads at different points in time. Of all of these, the Horn is the only load that is required to operate at all times for safety reasons. Door Locks should not need to be operated above a certain vehicle speed, and it might be argued that neither should the windows. Seat and mirror adjustments should be made when the vehicle is parked and therefore are not required while the vehicle is moving. It is yet to be seen, however, whether or not these concessions will yield any useful results.

3.8 Powertrain Cooling

Unlike the auxiliary loads discussed in the previous sections, powertrain cooling loads do not provide any immediate and therefore direct benifit to the vehicle occupants. Despite this, they are an essential part of the powertrain. None of the powertrain components are 100% efficient, they all create heat energy that must be removed to prevent excessive temperatures. Fig. 3.4 outlines the location and components comprising each of the powertrain cooling systems installed in the FCEV.

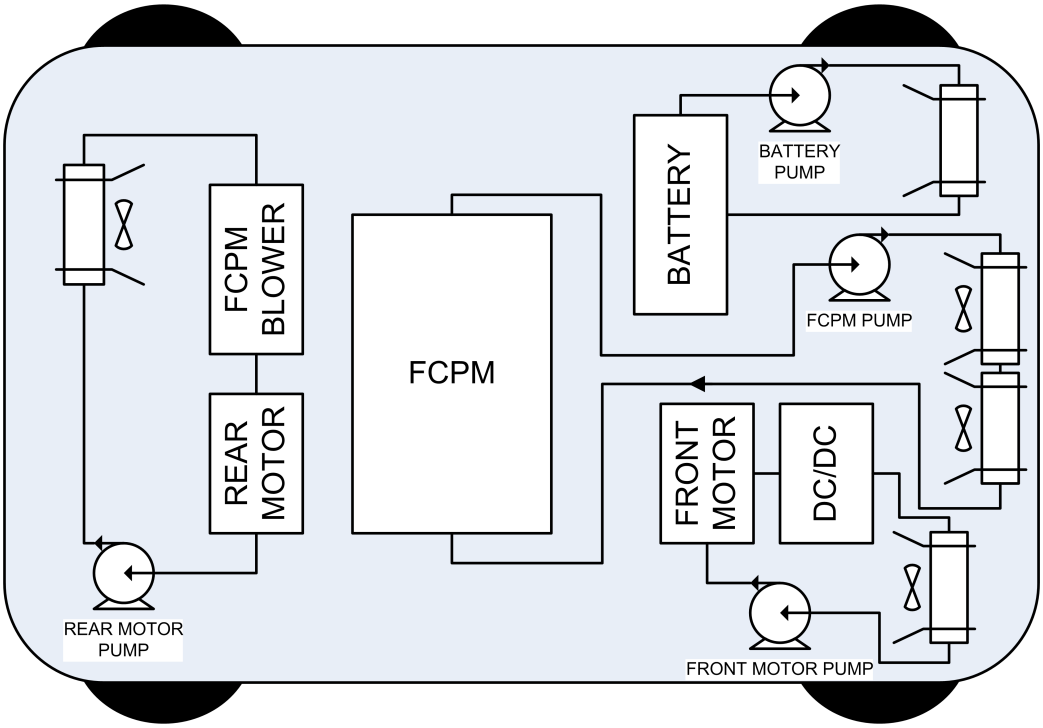

Figure 3.4: FCEV Powertrain Cooling Systems

3.8.1 FCPM Cooling

Although very efficient by automotive standards, PEM fuel cells are still only 50–60% efficient at the best of times. At the power levels required to facilitate reasonable vehicle performance, there is a significant amount of heat that must be rejected. For UofW's FCEV, the FCPM can produce upwards of 60kW of heat energy. Despite this large rate of heat generation, the FCPM must remain below its operating temperature limit of 80°C, requiring a powerful active cooling system. The two main energy consuming components of this cooling system are the 800W water pump and the two cooling fans at 130W each. These components, at present, are uncontrolled and operate continuously at maximum power.

Both of these parasitic loads have the capability to be modulated with an appropriate motor control technique. Beyond the 80°C maximum FCPM temperature limit, it also has a minimum coolant flow requirement. Coolant

flow is never allowed to cease or internal hotspots can occur within the FCPM leading to damage. Depending on whether or not there are multiple temperature sensors and/or hotspot detection, it may or may not be feasible to reduce the coolant flow very much. Rad fan speed on the other hand can be freely modulated between zero and max based on coolant and or FCPM temperature without worry of creating such hotspots.

3.8.2 Motor, DC/DC and Battery Cooling

Apart from the liquid cooling of the FCPM, there are 3 other liquid cooling systems in UofW's FCEV. These three cooling systems all operate via their own 24V water pump whose specifications are outlined below:

Table 3.3: Motor, Battery and DC/DC Cooling Pumps

Manufacturer — Model:	Iwaki — RD-20-CV-24-05
Pump Type:	Centrifugal
Motor Type:	Brushless DC
Power Input:	60 W
Max Flow Rate:	24 L/Min
Max Head:	10 m

[66]

The two 3-phase propulsion motors have an efficiency that ranges from 50–95% and have the potential to produce heat at a rate of up to 12kW each [67]. Along with these there are also the 65kW DC/DC converter, NiMH battery pack, and FCPM blower inverter that all produce heat at the rates listed below.

Table 3.4: Component Cooling Loads

Component	**Max Heat Production Rate (kW)**
Ballard/312V67	12
65kW DC/DC	5
Cobasys/NiMHax3 366-70	18
FCPM Blower	1.2

[68, 67]

Apart from the cooling pumps for these systems, the front and rear motor cooling loops also have fans for increasing radiator air flow as seen in Fig. 3.4. The front motor fan is a 12V motorcycle radiator fan which uses 60W, and the rear motor radiator fans are two 30W 12V fans. Currently the vehicle is designed to run all 3 cooling pumps continuously at full power while switching the fans on/off at set component temperature thresholds. There is currently no provision for scaling pump and/or fan speed which might prove a useful method for reducing the parasitic load of these components.

The last item in the powertrain cooling systems is the DC/DC air-cooling blower. Due to the design of the inductors used in this converter, air cooling is required in addition to the water-cooling provided by the front motor cooling system of Fig. 3.4. This blower is a 62W centrifugal type blower capable of delivering over 150 Cubic Feet per Minute (CFM) of air flow. It is also set to run continuously at full power and might benifit from speed control. One consideration for this particular component, however, is that in order to guarantee that water does not creep into the converter housing, it should be maintained at a positive pressure relative to its surroundings. This requires at least some blower operation at all times.

3.9 FCPM Air Delivery System

The fuel cell power module requires two main reactants to operate: hydrogen and oxygen. Hydrogen is supplied by an on-board storage tank in the trunk of the vehicle and oxygen is supplied from ambient air via a blower. The blower is powered by a controlled 3-phase AC motor which only delivers the amount of air required by the chemical reaction. The blower-motor controller is powered via the high voltage output from the FCPM itself and can consume over 3kW continuously. During startup, however, there is no high voltage yet available, so in the interm, 24V is stepped up to 150V via DC/DC converters to power the blower until the FCPM is producing power. This preliminary step-up conversion adds complexity and incurs losses which may be avoided by utilizing the FCEV's HV Bus and battery pack.

3.10 FCPM Recirculation Pumps

The other major parasitic load that the FCPM has is the hydrogen recirculation system. This system is required to maintain a steady concentration of humidified gaseous hydrogen available at the reaction site. These pumps use 300W each or 600W in total, and run constantly when the FCPM is in run mode. It has not been determined whether or not it will be possible to modulate the capacity/load of this system. At this point it is assumed that this system represents a static parasitic load. This does not mean that there is no possibility of improving the energy demands of this system. Rather, energy usage reduction for this system will have to be done indirectly, via the methods outlined in the following chapter.

3.11 Ballard Motor Oil Pumps

The vehicle propulsion motors have the further requirement of continuous lubricant flow within the gearcase. This is accomplished with the electric oil pump specified below.

Table 3.5: Oil Pump Specifications

Manufacturer — Model:	Walbro — F8Y8-7A103-AA
Oil Pressure:	6 psi
Motor Type:	12V DC Motor
Power Input:	55 W

This is a critical system that is controlled by the motor controller itself. Thus, only indirect power saving techniques can be applied as in the case of the FCPM hydrogen recirculation pumps.

3.12 12V NiMH Auxiliary Battery

While off, the FCEV's main power sources are disconnected from the high voltage bus via electronically activated contactors. In order to reconnect them on vehicle startup, a low-power auxiliary electrical source is required. This requirement is fulfilled by a small 13Ah 12V NiMH battery pack. Other than startup, it's other purpose is to provide power for the critical auxiliaries

such as the brake assist pumps in the event of a powertrain failure. Should such a failure occur, the battery is sized to allow for at least 10 minutes of 12V auxiliary system operation. With a charging current of 10A, this battery presents a 120W load to the vehicle while charging. In order to be available for an emergency situation, the battery should always be kept at a very high state of charge. Currently, the vehicle startup sequence involves turning on all the cooling fans, pumps etc. In the period before the powertrain begins supplying power, these auxiliary loads can drain a significant amount of energy out of this auxiliary battery. It would be benificial to reduce the power used by the vehicle before the powertrain is available.

3.13 Chapter Summary

Although there are many auxiliary systems constrained in various ways by safety and customer acceptance concerns, there is still enough flexibility to allow for some effective energy usage optimization. The more flexible systems that can have a significant impact on vehicle performance are air-conditioning and heating with power consumptions in the multiple kilowatt range. The other systems consume less power and/or are less flexible, however, savings in these systems combined should be significant. Now that the purpose of each component and its constraints is clearly understood, we can move on to an analysis of optimization strategies and algorithms in the following chapter.

Chapter 4

Auxiliary Control Strategies

With the background provided in the previous chapters, it is now possible to discuss methods of reducing the energy demands of the vehicle auxiliaries and parasitics. One thing to keep in mind, is that all of the energy consumed by the vehicle comes, initially, from the stored chemical hydrogen. As a result, all energy usage can be traced back to a usage of a fixed quantity of hydrogen fuel. This quantity is determined by the amount of energy used as well as the conversion efficiency of the devices in the power path. This leads us to two main methods of energy conservation:

1. Direct Method: Directly reducing the energy consumption of an auxiliary or parasitic component.

2. Indirect Method: Integrating powertrain control and auxiliary control in order to reduce parasitic losses within the energy path for both the powertrain and the auxiliaries.

These two methods are not mutually exclusive and are combined in various forms within the auxiliary control algorithm outlined towards the end of this chapter.

4.1 Direct Method

There are a number of ways of directly reducing a component's energy consumption. The first and arguably most obvious is to replace the component

with a high-efficiency counter-part. An example would be to replace a vehicle's existing headlights with LED versions. Another example is to replace a mechanical/hydraulic power steering system with a high efficiency electric system as outlined in [64]. Since we are concerned mainly with UofW's FCEV prototype vehicle, the main goal of this research is not to replace components with high-efficiency counterparts but to find means of reducing energy consumption with existing components. These means should apply equally to high efficiency components therefore further improving upon vehicles that have these components installed.

4.1.1 Voltage Reduction

Voltage reduction is a method of load control that has applications from the power distribution industry to the semi-conductor industry. The classic example is the light bulb on a dimmer switch. As the voltage decreases so does the current and the power consumed by the bulb. When less light is required and/or energy is at a premium, then less voltage and in turn less power should be supplied. In the semi-conductor industry, voltage reduction is a means used often in portable battery-powered devices to reduce integrated circuit power consumption [69]. When considering this method for a vehicle application, one must investigate the voltage specifications of the components and the design tolerance for it's fluctuations.

In a conventional vehicle with a belt-driven alternator and lead-acid battery, the 12V system is designed to be very insensitive to voltage fluctuations. The alternator is usually a claw-pole induction generator with voltage regulation achieved by varying the field current. With such a wide range of alternator operating speed and auxiliary loading, the voltage can swing significantly between 10 and 15 Volts. Thus the auxiliary components are designed to operate reasonably well across this entire range. In order to maintain the charge of the lead-acid battery, the nominal operating voltage is specified as 13.8V by the automotive industry. This is significantly higher than the 10-12V required to ensure proper component operation, and potentially results in significant power waste [30]. Power is only wasted, however, if power usage increases with voltage. As many of a vehicle's auxiliary and parasitic loads are resistive or uncontrolled dc machines, this is certainly the case. The following equations outline the relationship between power and voltage for resistive loads (4.1), and uncontrolled dc machines (4.2). In the

case of the dc machines, the relationship is not precisely known as it depends on the mechanical load present on the shaft of the machine. Most of these mechanical loads take the form of pumps and fans in a vehicle application, which will use less power or do less work as the voltage to the machine is decreased.

$$P = \frac{V^2}{R} \tag{4.1}$$

$$P \propto f(V), s.t.\ the\ slope\ \dot{f}(V) > 0 \tag{4.2}$$

Where P = Electrical Power

V = Voltage

R = Resistance

and $\dot{f}()$ = derivative of $f()$

In the case of UofW's FCEV, the 12V components are supplied by voltage controlled dc/dc buck converters as outlined in section 2.3.5. These have the capability of absorbing large load transients while maintaining a fixed output voltage. Further, the output voltage is externally controllable and can be monitored/controlled by the on-board vehicle controller. This means that there is the capability to set the 12V bus voltage arbitrarily anywhere between 5 and 16.5 volts. Also a specific voltage target can be maintained more precisely, reducing concern over transients. The battery charging complication still remains, however, this can be taken care of by either separating the 12V bus into independent segments as in Fig. 4.1, or charging the battery via a small buck converter from the 24V supply. With the equipment available, there is the possibility of having 3 or 4 independent 600W power dc/dc converters for the 12V bus. The problem then becomes a question of determining the grouping of the components by voltage requirements such that they can all be managed by 3 or 4 supplies. Note that the 12V battery only provides a small amount of energy at startup or in the rare occurance of an emergency, the total energy flowing through this path will be small. Therfore, if using a 24V to 13.8V buck converter the added inefficiencies should not be significant.

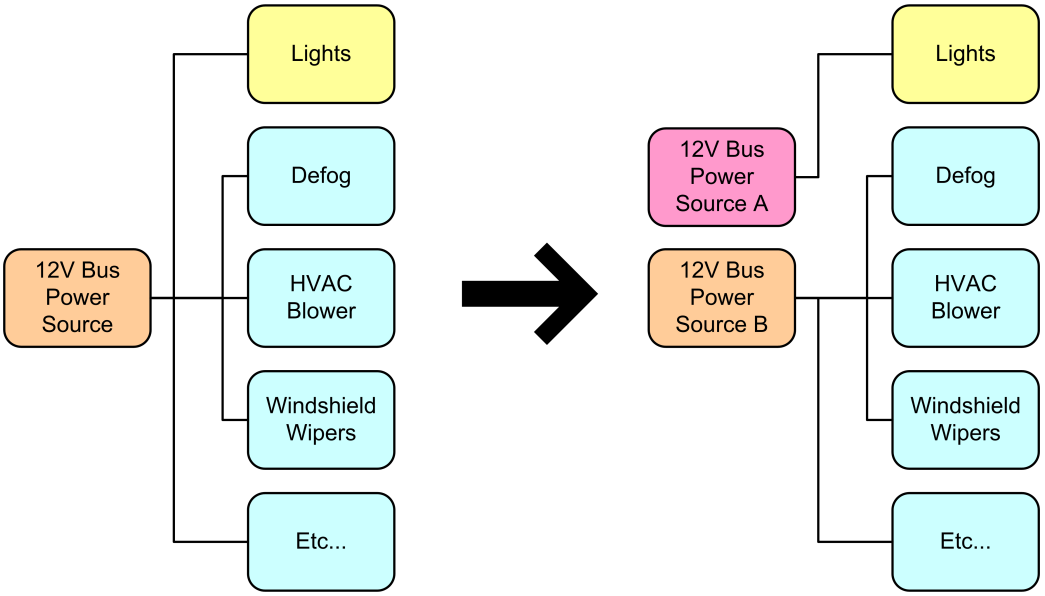

Figure 4.1: 12V Bus Separation

As seen in Chapter 3, Table 3.2, the power consumed by the lighting systems in the vehicle can be more than halved by reducing the voltage from 14.5V to 10V. This is the maximum allowable voltage swing for the light output to remain within industry and government specifications. For safety, the exterior lights must remain within these operational specifications but interior lights can be freely adjusted below the minimum specified voltage. Other resistive auxiliaries and parasitics can sustain voltage reductions within the bounds specified in Chapter 3.

4.1.2 Component Control

In addition to simple voltage reduction, another approach is to dynamically control each component independently or in small groups. Where voltage reduction reduces the engineered voltage transient margins to reduce power consumption in a fixed manner, dynamic control can modulate component power usage to correspond to occupant and vehicle requirements. For example, a cooling fan can be controlled to run only when a specific monitored temperature is greater than a fixed threshold. This type of simple on-off (or bang-bang) control, based on a single variable, is simple and easy to imple-

ment and can result in significant energy savings. With the use of a chopper circuit and slightly more complex logic, smooth power modulation is possible. Using the fan example again, instead of turning on the fan at a specified temperature, fan power can be made proportional to temperature. Then as the temperature increases so does the speed of the fan with a specified relationship. Further, every time a fan or pump is started from a stopped condition, there is a spike in power usage due to the low rotational speed and therefore low back EMF (Electro Motive Force). Using a current controlled start can further reduce motor energy consumption even with bang-bang control [70].

Control is not limited to a single variable, and the power used by a component can be modulated based on relationships with a number of variables. An example of this would be the A/C compressor, which might be controlled based on cabin temperature, refrigerant pressure, and condensor temperature. Once the hardware is in place to facilitate component control, the control variables become a question of software and algorithms alone. This allows for complex optimization calculations as long as they remain within the processing capabilities of the on-board vehicle controller.

Climate System Control

Previous research has shown that bang-bang control of compressor and fan systems leads to significant energy losses, particularly for the compressor in an air conditioning system. [35] has noted that compressor losses dominate in a refrigeration system utilizing bang-bang control. These losses can be almost halved if the compressor never completely turns off. As noted in Chapter 1, traditional automotive air conditioning systems also use series reheating of cooled cabin air to modulate the cooling capacity, further reducing climate system efficiency [34]. Finally, additional efficiency losses are incurred when using only fresh air for the climate control system, as in this way the system is effectively trying to cool the outdoors [29].

To solve these issues, an air conditioning control algorithm is proposed that utilizes closed loop control for targeting the temperature requested by the vehicle occupants, including system limits to ensure safe, effective operation and high efficiency. With this system, the air conditioning can be modulated to meet the cooling demands rather than adding heat to the overcooled cabin air.

Cabin Blower Control

Currently, blower speed control is acheived in steps utilizing resistors to reduce the voltage seen by the blower motor. These series resitors not only reduce control flexibility by limiting the choice of speeds to 4, they also decrease blower efficiency by converting some of the electrical energy to heat. Table 4.1 outlines the blower power consumption at various speeds of operation and the power consumed by the resistors.

Table 4.1: Blower Resistor and Total Power Usage

Selected Speed	**Resistor Power** (W)	**Total Power** (W)
High	N/A*	250
Med 2	30	153
Med 1	33	80
Low	27	45

*Resistor not used for high speed.

When using the three lower speeds, approximately 30 Watts is consumed to generate unwanted heat. Using a solid state switch such as an IRF2804 N-Channel Mosfet with a low on resistance of 2 mΩ and a pulse width modulated speed control signal, these losses would be reduced significantly [71]. This also has the added advantage of allowing any blower speed to be chosen without being restricted to 4 steps.

Air Conditioning Control Proposal

To implement closed loop control on the A/C system, the driver must have a temperature control inside the vehicle. This control would indicate to the vehicle controller what the desired temperature is. The driver would also select a desired blower speed, which will determine the system's cooling response time.

In a traditional automotive air conditioning system, as mentioned in [35], the compressor is cycled on when the driver requests cooling and off when any of the system boundaries are met. The system boundaries are evaporator temperature and compressor outlet pressure, as defined in Chapter 3.

Fig. 4.2 outlines the refrigeration system again, this time including the sensors locations for detecting system boundaries.

A control scheme following the traditional method is shown in Fig. 4.3 with hysteresis applied to the system boundaries to prevent unrealistic switching speeds. Using an air conditioning simulation in Matlab^{TM}, the curves shown in Fig. 4.4 show the compressor power, the evaporator temperature and the cabin temperature using this control scheme.

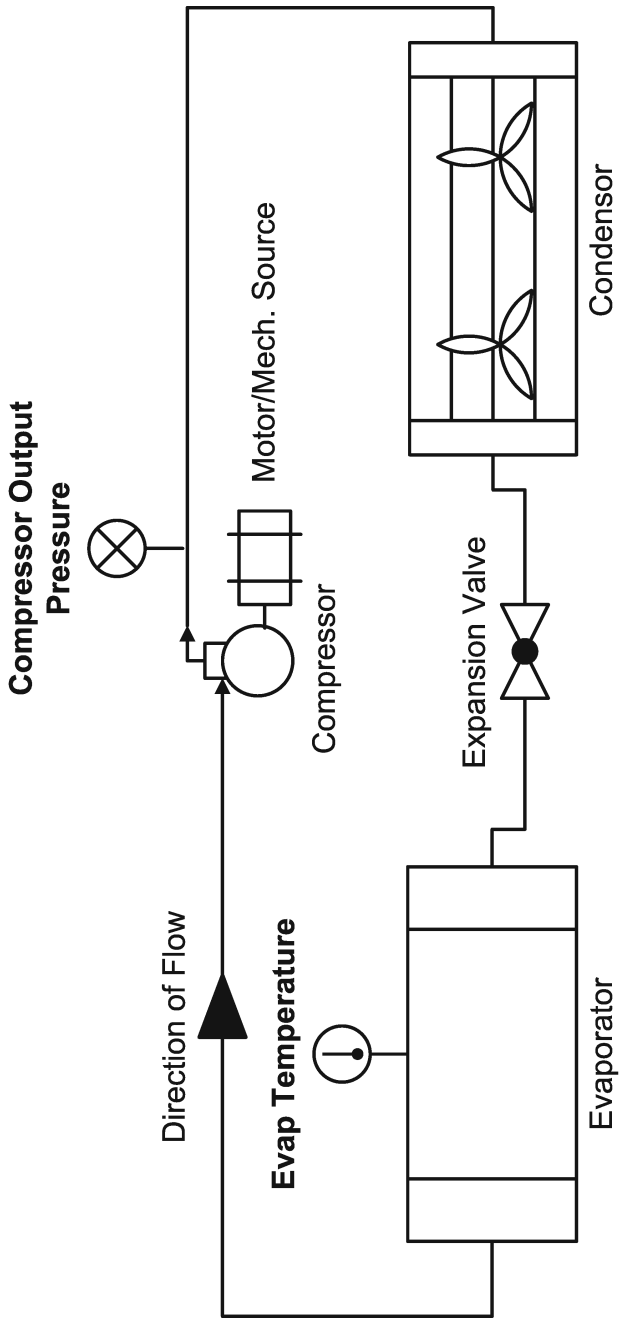

Figure 4.2: Refigeration System Outline with Boundary Measurements

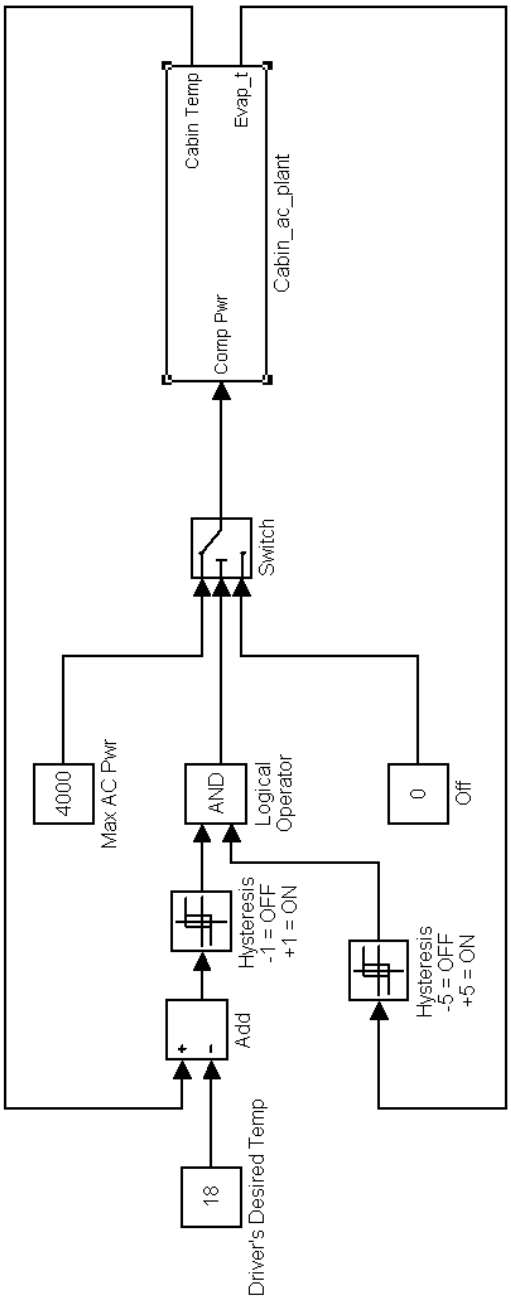

Figure 4.3: Traditional Automotive A/C Control Scheme

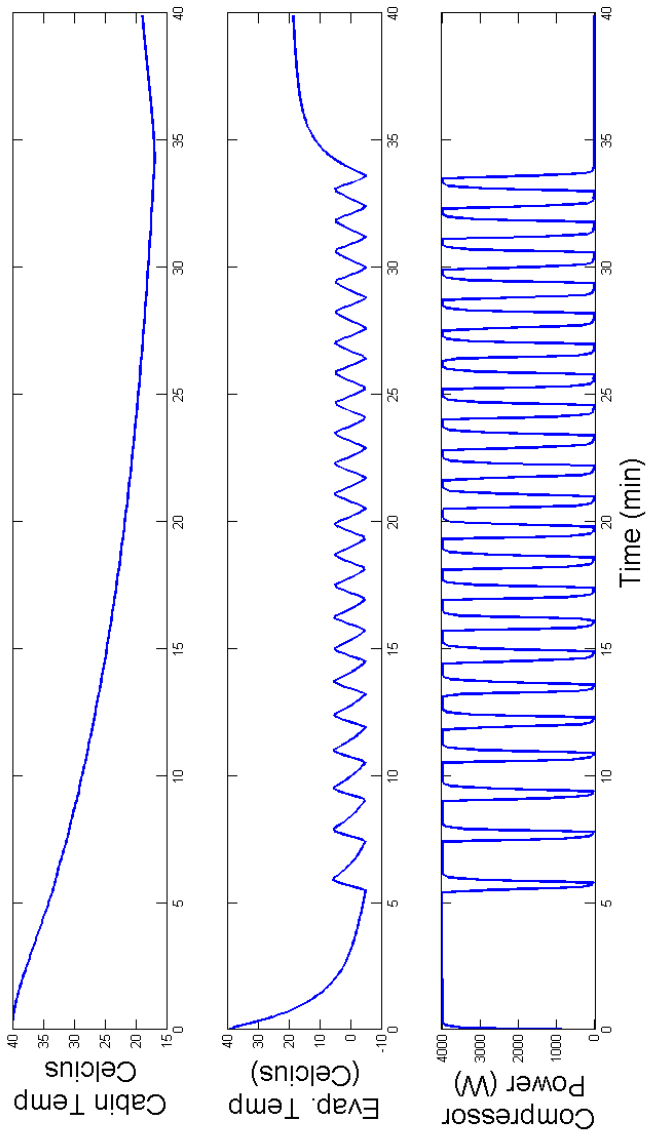

Figure 4.4: Simulation of Traditional Automotive A/C Control Scheme

Fig. 4.5 outlines the proposed control scheme utilizing closed loop proportional control. It was determined that proportional control is sufficient to meet the tracking requirements of this relatively slow system. Using the same Matlab^{TM} simulation, the results shown in Fig. 4.6 were achieved with this control scheme.

Looking at the simulation results, it is obvious that with proportional control it is possible to run the compressor at the required power level to achieve the desired cooling without cycling it on and off. It is the variable speed compressor that makes this possible as opposed to the fixed capacity belt-driven compressors typically used with ICE's. This will significantly improve the refrigeration system efficiency, ultimately using less power than the traditional method.

Using the traditional method, the evaporator temperature continually fluctuates between -5 and 5°C with the warm part of the cycle preventing any ice formation. Using proportional control, the evaporator is maintained precisely between 0 and 1°C. In both simulations, evaporator temperature is assumed to be the restrictive boundary and compressor output pressure is not controlled. This is for simplicity, and it could be controlled in the same manner. The saturator for evaporator temperature feedback in the proportional control scheme is designed such that this factor is zero until the evaporator temperature falls below the desired temperature.

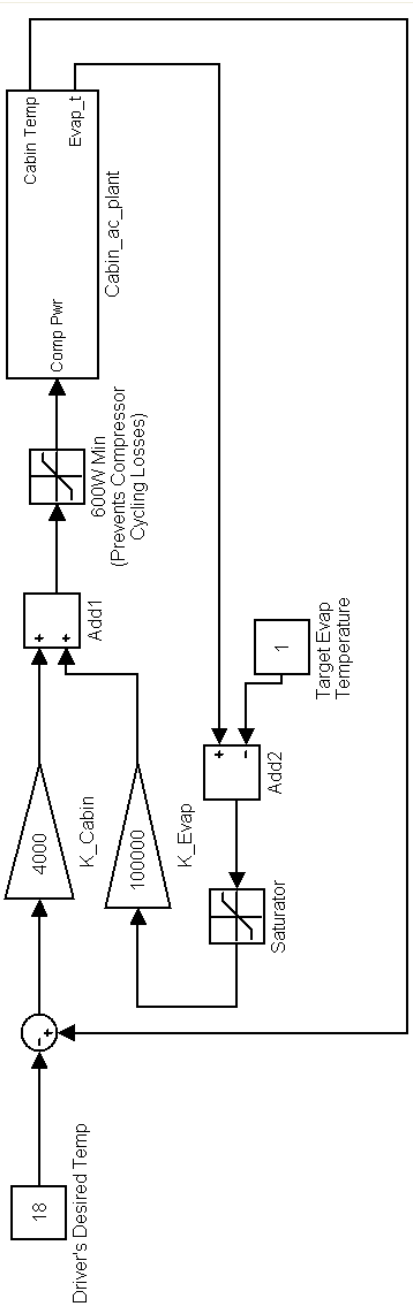

Figure 4.5: The Proposed Proportional Automotive A/C Control Scheme

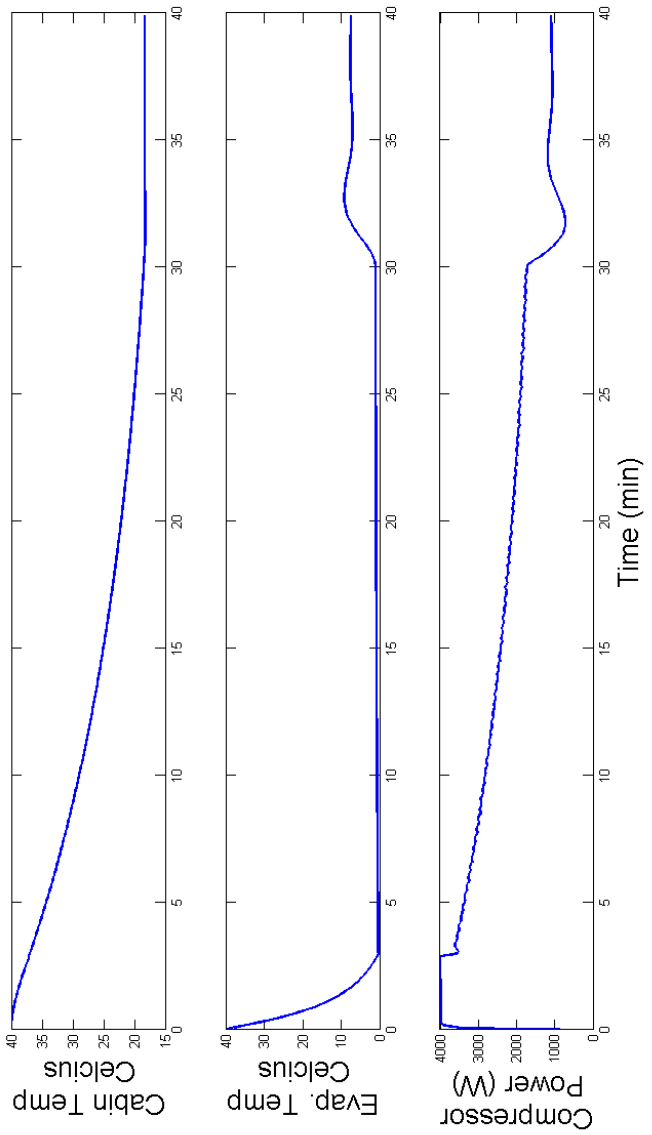

Figure 4.6: Simulation of the Proposed Proportional Automotive A/C Control Scheme

In both cases the response time is approximately the same, with the desired temperature being reached slightly faster using proportional control. At this point the compressor settles into steady state operation, balancing the vehicle's heat absorbtion rate, whereas with the traditional control scheme illustrated, it turns off entirely until the cabin temperature rises 1°C above the desired temperature. It is worth noting, that most vehicles do not turn off the compressor at this point yet continue to cool at the same capacity forcing the driver to add heat to the cabin air with the temperature selection control [35, 29].

Defog Control Proposal

The defogging system consists of the climate control system for the front windshield and side windows, whereas the rear window has a built-in heater element as described in Chapter 3. Defogging is an extremely energy intensive process as it neccesarily involves series reheating of the climate control air. The reason is that in this case the air conditioning system is utilized not as a cooling device but as a de-humidifier. The cold evaporator causes water to condense out of the air with the unwanted side-effect of cooling the air at the same time, requiring the air to be reheated by the resistive heater. The resulting hot, dry air is very effective at evaporating moisture from the surface of the windshield [29]. For the rear window, the resistive heater element is also energy hungry, consuming at a rate of 150W.

With both of these systems, the energy usage is neccesary, however the problem arrises when the windows have been succesfully defogged. At this point the rate of energy usage should drop to the levels required for climate control alone without the added burden of the defogging process. In conventional vehicles, this requires the driver to change the setting, a fact often overlooked by many drivers. The result is that the defog system typically operates for far longer than neccesary resulting in a large increase in auxiliary energy usage.

To correct this, the proposed control scheme requires a fog sensor such as the one outlined in [72] to be utilized. This device reports the level of moisture on the windshield surface electronically, allowing the controller to determine that the defog process is complete and the system can revert back

to climate control mode. For safety, it might also be benefical to allow the system to automatically enter defog mode when moisture is detected rather then waiting for a defog request from the driver.

Referring back to Fig. 4.6, the air conditioning load during defog mode would be the maximum load achievable without violating the system operating boundaries. At the same time, the heater would need to use enough energy to produce a net gain in air temperature. Thus, total defog system loads of 5400W are conceivable with air conditioning loads in excess of 2000W, heater loads of 3000W, and blower and rear window defog together using 400W.

Windshield Wiper Control Proposal

Windshield wipers present a similar problem as defogging although on a smaller energy usage scale. Driver's often leave the windsheild wipers on well after the weather has improved. This results in increased friction between the wiper blades and the window surface, not only wearing down the blades prematurely, but also causing increased and unneccesary power consumption. The solution, again, is an automatic shutoff, or speed control system using a sensor such as that outlined in [73].

Cooling pump and Fan Control Proposal

Again looking back at Chapter 3, the vehicle powertrain cooling is outlined and the individual cooling systems are shown in Fig. 3.4. Fig. 2.12 shows the vehicle communications network which allows the vehicle controller to receive temperature information from all powertrain components. With this temperature information, the controller can make intelligent decisions about whether or not to run individual cooling systems. The initial cooling strategy for UWAFT's FCEV involved turning on all of the cooling systems at full capacity 100% of the time. Realistically, these cooling systems do not need to be running 100% of time, as they are not always effective. When the vehicle first turns on for example, component temperatures are close to ambient and blowing ambient air over the radiators produces little effect. It is desirable then, to operate the cooling systems only when neccesary or when a useful effect is achieved. As heat transfer is most efficient at large temperature

gradients, bang-bang control would seem the most applicable form of control [60]. Using this type of control, the cooling systems would not turn on until component operating temperatures reach their upper range. The radiator fans have an extra characteristic to consider. They are only beneficial at low vehicle speeds when natural airflow from vehicle movement is limited. At higher speeds the cooling capacity is determined by air flow restrictions and paths through the radiator with the fan having little effect [74]. At high speeds, therefore, the fans can be turned off, saving vehicle energy.

To determine the optimal points of fan and pump operation requires an in-depth thermodynamic analysis of each cooling system, which is beyond the scope of this thesis. Despite this, it is important to understand that such optimization is possible before considering the indirect energy usage reduction techniques of the next section.

4.2 Indirect Method

Continuous component control such as illustrated in the previous section is not a new idea. There is existing research involving the control of these components based on varibles such as temperature. One thing that is rarely, if ever, discussed however is auxiliary component control based on powertrain operating point. The FCEV prototype's powertrain control strategy outlined in the previous chapter, calculates an optimal operating point for each of the major powertrain components. This calculation is constrained by the driver's torque demand which in turn dictates the powertrain output power in conjunction with the auxiliary loads. In the present vehicle, auxiliary loads have been assumed to be uncontrollable and determined only by the drivers choice of what to turn on or off. As has been outlined in the previous chapters on the auxiliary and parasitic loads, this is not entirely true. In fact, with a little logic, auxiliary loads can deliver the desired function while using less power and/or using power at more appropriate times. The intention is to define when those appropriate times might be and to propose an algorithm to implement such control on board the vehicle.

4.3 Optimal Auxiliary Power

With the implemented FCEV powertrain control, the only point of freedom is the fuel-cell output power. This is calculated via the determination of the optimal battery/fuel-cell power split factor α. Without the assumption that auxiliary power consumption is fixed, the optimization problem is slightly more complex. There is suddenly another degree of freedom; the total power demand P_{Out}. Fig. 4.7, illustrates this increase in complexity. Where the existing algorithm only has to calculate one of the columns in this cost table, an optimization including variations in P_{Out} must calculate an additional column for each step Δ.

P_{Out}, as defined by (4.3) is the sum of the power drawn by all the electrical loads in the vehicle. P_{Motors} is the propulsion power required by the motors, which is fixed by driver demand, and P_{Aux} is the total auxiliary power consumption. Therefore the columns in Fig. 4.7 are calculated for a range in P_{Out} determined by the allowable range in P_{Aux}.

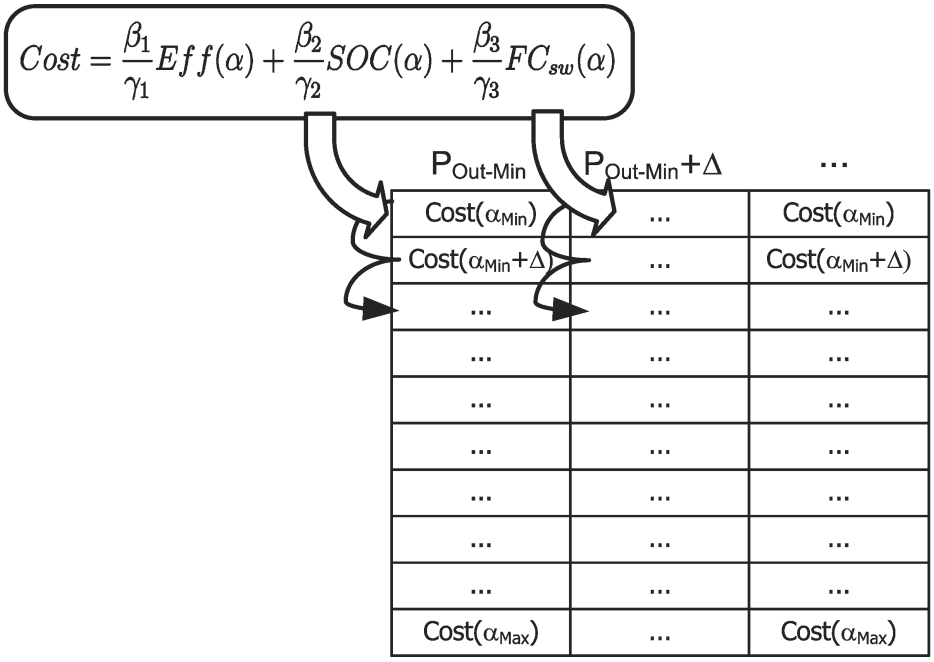

Figure 4.7: Optimization Cost Table

$$P_{Out} = P_{Motors} + P_{Aux} \tag{4.3}$$

4.3.1 Efficiency Curve Analysis

As stated when the powertrain optimization cost function was first introduced in Chapter 2, there are three terms which correspond to instantaneous powertrain efficiency, an SOC targeting factor and a FCPM cycle score. Of these, the key term is powertrain efficiency; the others serve to modify the efficiency factor to increase FCPM lifetime and future efficiency. Fig. 4.8 shows the instantaneous powertrain efficiency plotted with respect to α. Each curve in this figure represents a column in the cost table of Fig. 4.7 corresponding to a specific P_{Out}. The P_{Out} range shown, 1000W - 10000W, is an unrealistic variation in the auxiliary loads, however, it provides a good illustration of the cost-function response. The indicated shaded areas represent the locations of the optimal cost values for the curves shown. At low power the region on the right is optimal but as the power increases the leftward region is chosen more and more often. Above 10000W, the response settles down and shrinks into the right side of the graph, resulting in the leftward optimal zone stretching down to the right yet always above the rightward optimal zone.

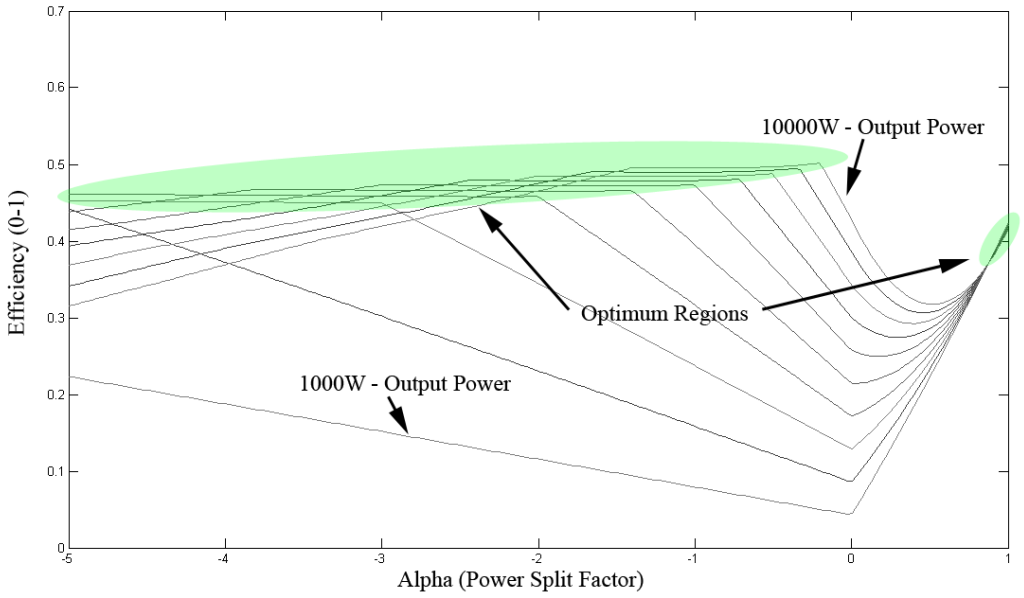

Figure 4.8: Efficiency vs. Alpha for 1000-10,000W

With this knowledge of the cost function response to variations in both

α and P_{Out}, lets look specifically at efficiency with respect to P_{Out} assuming the optimal α is always chosen. To start, let's assume a ficticious response as shown in Fig. 4.9(a). This ficticious example is interesting because as P_{Out} increases the input power or hydrogen usage actually decreases. It might seem that this violates the laws of thermodynamics, creating energy out of nothing, but it makes sense considering that the output power never exceeds the input power and towards the left side of the graph, all of the input energy is still being output except predominantly as heat rather than usable energy. To test whether or not an increase in output results in a decrease in input energy we refer to 4.4 which can be re-written as 4.5. Graphically this means that if one draws a line from the origin to a point on the curve and a vertical line through this same point, then any part of the curve in upper right hand quadrant made by these lines represents an operating point where output is increasing while input is decreasing. In Fig. 4.9(a) this quadrant is coloured green and no matter what point is chosen, the remaining part of the curve will be in this quadrant.

$$P_{In,new} > P_{In,old} \tag{4.4}$$

$$\frac{\mathrm{Ef}_{new}}{P_{Out,new}} > \frac{\mathrm{Ef}_{old}}{P_{Out,old}} \tag{4.5}$$

Attempting this test on the actual efficiency curve shown in Fig. 4.9(b), it can be easily seen that it will prove false for the majority of the curve except potentially the point where the two black lines intersect. At this point, there is a sharp increase in efficiency over a small increase in P_{Out}. Upon closer inspection, the test still fails, however this region is interesting as it shows an increase of 100W in P_{Out} without an appreciable increase in hydrogen usage. Therefore, it is beneficial to always run at the higher power as it has a negligible effect on fuel consumption.

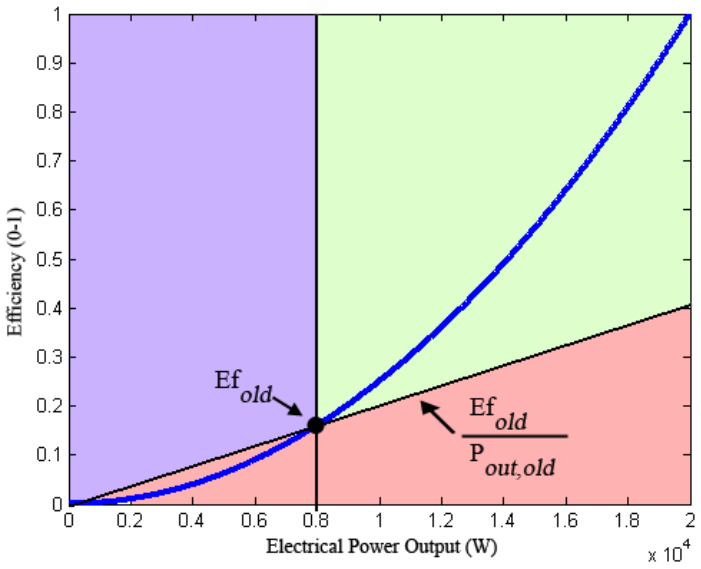

(a) example efficiency curve

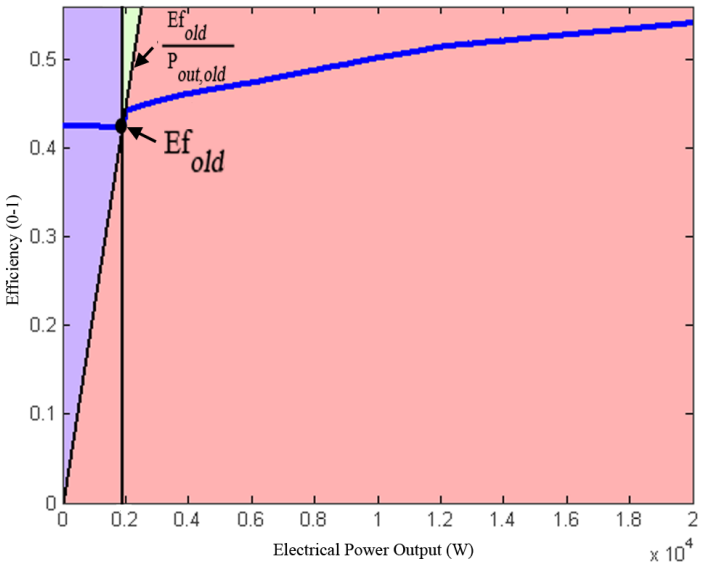

(b) actual efficiency curve

Figure 4.9: Efficiency vs. Output Power

The test of 4.4 and 4.5 does not determine the only circumstances where increased energy usage would be beneficial. It simply determines the best case in which, increasing auxiliary comforts directly improves the vehicle fuel-efficiency. For the actual efficiency curve as shown in Fig. 4.9, this is never the case, except for the noted point where it is close. The question then remains, why would it ever be benificial to increase the auxiliary load? To answer this, there are three main issues to consider:

1. Motor energy usage is required and dictated by the driver, where minimum auxiliary load is dictated by safety and comfort considerations.

2. Increases in energy usage beyond this minimum can be classified into useful and wasteful increases.

3. The actual efficiency shown in Fig. 4.9 is modified to correct for SOC and FCPM switching.

The first consideration reveals the fact that regardless of any auxiliary load adjustments, there is always a minimum output power. Any increase from this value can be considered usefull if it results in a corresponding future decrease in the minimum auxiliary load. Any increase that does not impact the future minimum auxiliary load is a wasteful increase. Therefore, even if the criteria of 4.5 is not met, it is beneficial to increase useful energy usage when it leads to a higher operating efficiency. The only time a wasteful increase can be justified, however, is when 4.5 is satisfied. Fig. 4.10 shows the SOC score adjusted efficiency curve vs. output power when the SOC is 70% or 10% above the target. With the SOC adjustment, the efficiency step that occurs at 6kW is sharp enough that a significant portion of the curve enters into the green quadrant. From this figure, it can be seen that a small increase in output energy will decrease fuel consumption and infact roughly an extra kilowatt of energy output can be obtained while maintaining fuel consumption at the same rate as at 6kW.

This leads to a discussion of the auxiliaries themselves and the reasoning behind the usuful and wasteful energy increase categories. The maximum bound on P_{Aux} must be less than or equal to the sum of the power consumed by all of the vehicle's auxiliary components operating at full power. Thus the feasible increase in output power is finite and determined by the auxiliary components with their corresponding operating conditions. The useful and

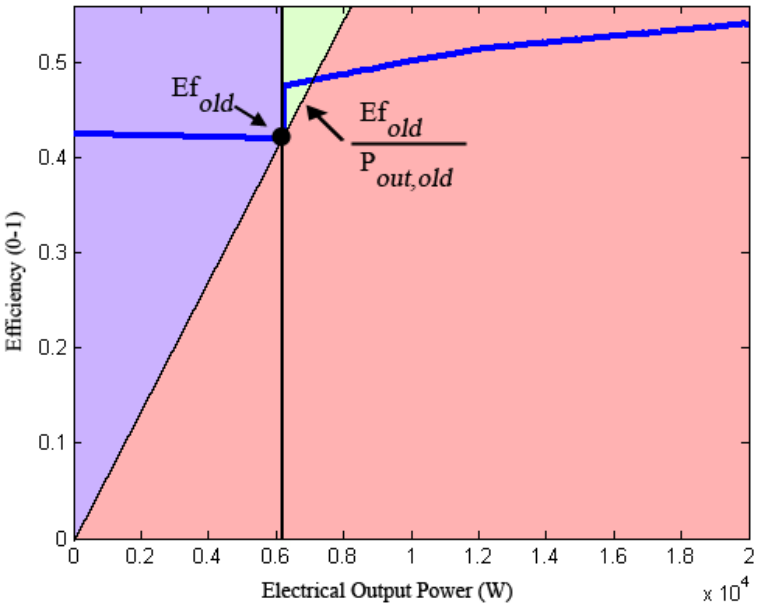

Figure 4.10: Efficiency vs. Output Power, SOC = 70%

wasteful categories of energy increase stem from the nature of the auxiliary load as will be described in the next section. A proposed auxiliary control algorithm based on this analysis is outlined in Fig. 4.11. In this algorithm, the allowable useful and wasteful variation in auxiliary power is determined by a power control module which sends this information to the powertrain controller. The powertrain controller chooses the best possible demand based on the cost and these two values and outputs it to the auxiliary controller.

The following section will look at the auxiliary loads and how to determine the allowable power flex in more detail. With the combination of the cost analysis from this section and proper auxiliary flex calculation with the information in the next section, a fully operable auxiliary control strategy can be implemented.

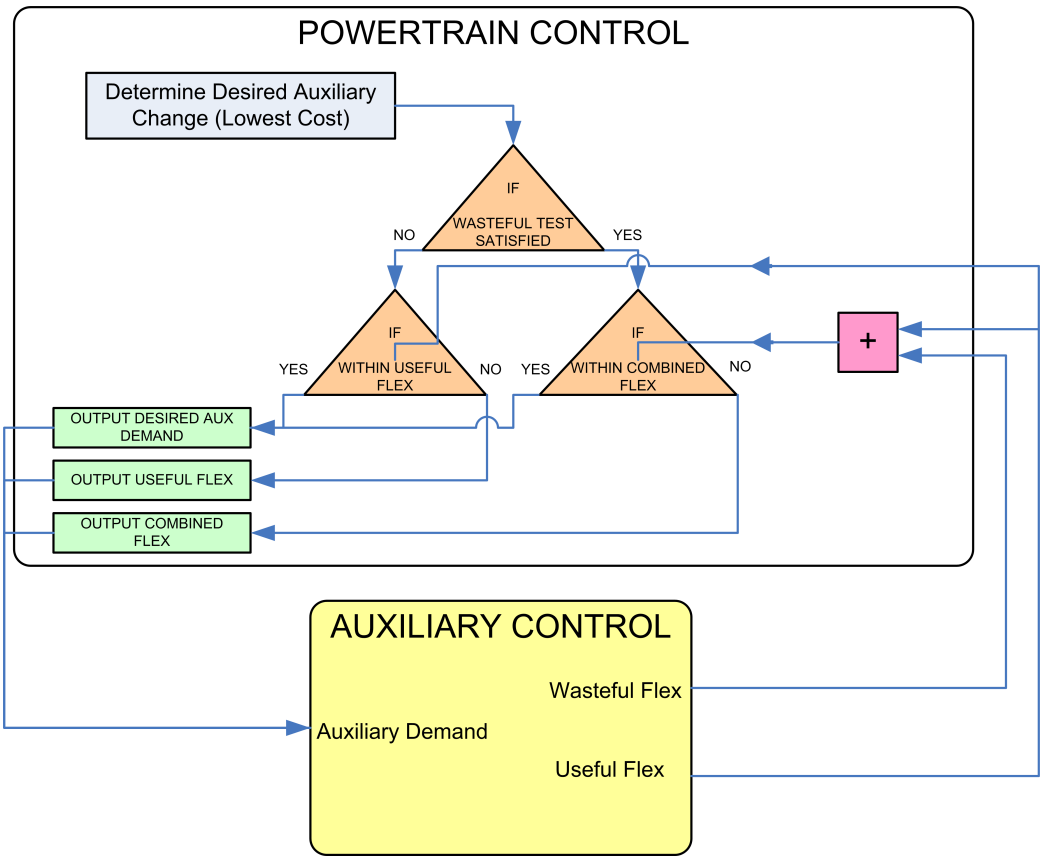

Figure 4.11: Auxiliary Control Algorithm

4.4 Determining Auxiliary Flexibility

This section discusses the power range restrictions imposed on the various loads as a result of safety, comfort and reliability requirements. Based on these requirements, the auxiliary and parasitic components can be grouped into four main areas: Flexible-Unbuffered, Flexible-Buffered, Rigid-Unvarying, and Rigid-Varying. Table 4.2 summarizes the auxiliary loads, their worst case power and category.

4.4.1 Flexible Loads

As the name implies, flexible loads are loads whose nature allows for a significant modification in their power consumption, while remaining within the

Table 4.2: Outline of Auxliary and Parasitic Loads

Component	**Load Category**	**Power (W)**
Exterior Lights	Flexible-UnBuffered	175
Headlights	Flexible-UnBuffered	125
Interior Lights	Flexible-UnBuffered	64
Windshield Wipers	Flexible-UnBuffered	64
Power Windows	Flexible-UnBuffered	180
A/C Compressor	Flexible-Buffered	4000
Cabin Heater	Flexible-Buffered	3000
Cooling Fans	Flexible-Buffered	400
Cabin Blower	Flexible-Buffered	250
Cooling Pumps	Flexible-Buffered	180
Rear Defog	Flexible-Buffered	150
12V Battery Charging	Flexible-Buffered	120
F/C Cooling Pump	Rigid Invarying	600
F/C Recirc Pumps	Rigid Invarying	400
Motor Lube Pumps	Rigid Invarying	120
F/C Blower	Rigid Varying	2000
Power Steering	Rigid Varying	800
Vacuum Pumps	Rigid Varying	200
Controllers, Relays and Contactors	Rigid Varying	100

safety, comfort and reliability requirements. This is further split into loads which contain or act on a naturally buffered system, or loads that do not. To give an example, a cooling fan acts on a radiator containing water with a finite heat capacity. This is a naturally buffered system, as the energy consumed by the fan to cool the water and ultimately some vehicle component is stored thermally. Lights, on the other hand, are an unbuffered system, as the light and heat energy is radiated immediately into the vehicle surroundings. This is where the idea of useful and wasteful energy increase comes from. A naturally buffered auxiliary system will tend to average the energy consumed over time, allowing brief deviations above and below the required power consumption. Un-buffered systems operating at the minimum required power will immediately breach their safety and comfort requirements with a momentary decrease in input power. Further, a momentary increase in power

will not allow for future decreases but will only serve to temporarily increase device output beyond the requirements without any lasting benifit.

4.4.2 Rigid Loads

Rigid loads, on the other hand, are loads whose nature does not allow for significant modification in their power consumption without resulting in safety violations or poor customer acceptance etc. These are also split into two categories: Varying and Invarying. The importance of this distinction is that invarying loads can be easily accounted for in the control algorithm. Varying loads, on the other hand, present a control problem; if the power consumption changes drastically, so does the powertrain operating point, and the control must be able to respond quickly to cope with the variations caused by these components.

4.4.3 Flex Categories

With the various flexible and rigid loads outlined in Table 4.2, this section will outline how these loads are typically used and a resulting method of calculating the available power flex.

Base Flex

This category includes the systems that are always or almost always running and have the capability of being varied at all times without affecting the vehicle occupants or vehicle driveability. This type of flex is always available to be requested by the powertrain controller and these components include the following (listed from largest to smallest power consumption):

- Cooling Fans (400 W)
- Lights (200-350W)
- Cooling Pumps (180W)
- Rear Defog (150W)
- 12V Battery Charging (120W)

With the climate control system off, there is little flexibility in the accessory load. The useful flex is comes from the buffered cooling system fans, pumps and the 12V battery charging system. This flex is, however, constrained by the direct control strategies outline previously.

The cooling pumps and fans must operate at specific temperature limits as defined by the direct control techniques, however, these temperature limits may be momentarily widened during auxiliary flex requests from the powertrain control strategy. By widening the temperature limits by a fixed percentage as safely determined by the thermodynamic analysis of the system, the auxiliary controller can determine exactly which fans and pumps will be able to turn on or off. Table 4.3 outlines an example of how this calculation would work.

Table 4.3: Cooling Flex Calculation Example

Component Temperature and Cooling Component	**Normal Limit**	**Flex Limits**	**Flex Power** (W)
FCPM Radiator: 65°C Cooling Fans	60°C	50°C – Lower 70°C – Upper	-180
Front Motor: 71°C Cooling Pump	80°C	70°C – Lower 90°C – Upper	+50
Front Motor Radiator: 55°C Cooling Fan	65°C	50°C – Lower 80°C – Upper	+80
Rear Motor: 85°C Cooling Pump	65°C	70°C – Lower 90°C – Upper	-50
Rear Motor Radiator: 78°C Cooling Fan	65°C	50°C – Lower 80°C – Upper	-80
DC/DC: 35°C Cooling Fans	40°C	30°C – Lower 50°C – Upper	+60

In this example, based on the current component temperatures, the normal on/off limit and the flex on/off limits, the useful flex allowed is +190W and -310W. This is to say that 190W worth of cooling pumps and fans are currently off but would be useful if turned on, and 310W worth of cooling pumps and fans are currently on but can be safely turned off for a short period.

12V battery charging flex will depend on it's current state of charge (SOC) in a similar manner to the temperature dependency of the cooling components. The main difference being that the control will be weighted towards keeping the battery completely full to maximize the emergency reserve power in the event of a loss of the high voltage powertrain systems.

The remaining components in this category contribute only to wasteful flex as extra energy use with these components does not achieve any useful goal. Wasteful flex constitutes only an increase in the current auxiliary power draw and not a decrease as these components are already operating at their minumum required levels. Any cooling components that are currently off and that would not turn on even with the expanded flex limits also contribute to the wasteful flex. The controller simply needs to add up the maximum power usage amount for each of these components and subtract the current power usage to arrive at this result.

Climate Control Flex

Components falling into the climate control category contribute a large amount of flexibility to the auxiliary system. As these components are only required when the vehicle occupants wish to cool or heat the vehicle interior, the powertrain controller is not always allowed to make use of this flexibility. Fortunately, however, the climate control system is often in use.

Looking back at Section 4.1.2 where air conditioning control was discussed, Fig.'s 4.4 and 4.6 illustrate the slow time constants for the cabin and system component temperatures. With such large thermal inertia's, it is possible to substatially vary the system power for short periods of time without violating the operating boundaries of the system or noticeably affecting vehicle cabin temperature. Therefore, when the air-conditioning is in use, the useful flex will simply be as defined by equation (4.6) and when using the heater, by (4.7). With the compressor often running at power consumption levels of 2000–3000W, useful flex values of 1000-2000W will often be the case.

$$\begin{aligned} Flex_{Positive} &= P_{Compressor-Max} - P_{Compressor-Actual} \\ Flex_{Negative} &= 0 - P_{Compressor-Actual} \end{aligned} \tag{4.6}$$

$$\begin{aligned} Flex_{Positive} &= P_{Heater-Max} - P_{Heater-Actual} \\ Flex_{Negative} &= 0 - P_{Heater-Actual} \end{aligned} \tag{4.7}$$

Wasteful flex in the climate control system is acheived by running both the air conditioner and the heater simultaneously. As this is the normal situation when using defrost, this is only a wasteful case when defrost is not enabled. This is calculated as shown in equation (4.8)

$$\begin{aligned} Flex_{Wasteful} = (P_{Heater-Max} + P_{Compressor-Max}) - \\ (P_{Heater-Actual} + P_{Compressor-Actual}) \end{aligned} \tag{4.8}$$

4.5 Chapter Summary

This chapter has proposed control strategies for the auxiliary components such that their energy consumption is directly minimized and the energy consumption of the overall vehicle is minimized. The direct control strategies are somewhat known and becoming more and more commonplace in vehicle design for various reasons including energy saving. The indirect strategy, however, is novel and needs to be to be analyzed further to determine it's validity and the potential energy savings. The following chapter presents simulations that aim to show this validation.

Chapter 5

Simulations and Analysis

With current computer processing technology it has become feasible to use numerical vehicle simulations in order to predict the performance and operating characteristics of a variety of vehicle designs. This is the key enabler that allowed the University of Waterloo's alternative fuels team to come to a decision on the type of powertrain to implement. It is also a powerful tool for the evaluation of the proposed control schemes set fourth in the previous chapters. This chapter will outline the simulation environment, methodology and final analysis of these schemes as they apply to the University's FCEV and to other vehicle's in general.

5.1 Simulation Environment

Argonne National Labs, a U.S. research body has developed a vehicle simulation toolbox on top of Mathwork's MATLAB/Simulink^{TM} mathematical software tools. This toolbox, called PSAT or Powertrain Systems Analysis Toolkit, includes mathematical models for accurately predicting vehicle energy usage and performance metrics over a number of standard drive cycles [39]. It is a very flexible and adaptable tool, allowing simulation of a variety of different powertrain configurations from the conventional single ICE power source to hybrid fuel-cell–battery configurations. Using a forward facing vehicle simulation technique, the data flow progresses in the manner outlined in Fig. 5.1.

Vehicle simulation software often utilizes a backward facing approach in which data flows backwards from the drive-cycle via the vehicle dynamics model to the powertrain model and through to energy consumption results. This approach allows for very quick, computationally simple simulations which can be very accurate. The main drawbacks to this approach are as follows:

1. Upstream powertrain limitations are ignored when the drive-cycle exceeds the modeled vehicle's capabilities.

2. Vehicle control algorithms must be implemented in reverse of reality and as a result have future information on which to base the calculations which is unrealistic.

Forward facing refers to the simulation model's evaluation of parameters in the same manner as occurs in an actual vehicle. A driver model outputs a torque (or throttle) command to the vehicle's powertrain model which, coupled with a vehicle dynamics model returns the actual vehicle speed. The vehicle speed and desired speed are compared within the driver model to compute the new torque command. This is an intuitive way of simulating a vehicle and it enables powertrain control algorithms to be implemented in the same way that they would be in an actual vehicle. The main drawback with this method is its computational demands due to the numerous integrations and states that must be calculated and stored throughout the model. [75] Despite this drawback, current computer technology can simulate a complex vehicle design using the forward-facing method quite quickly.

PSAT, designed as a tool for quickly prototyping and evaluating different powertrain designs, allows a significant amount of powertrain flexibility. The version used for this work, however, is restrictive in a couple of key areas. Each powertrain configuration is fixed and the data-flow cannot be customized, only the individual component models may be modified and/or replaced. This presented a problem when attempting to utilize an overall global braking and propelling powertrain control strategy. It also prevented the integration of auxiliary power controls into such a global control strategy. As a result, a PSAT generated Simulink^{TM} model was customized to allow for these capabilities and executed externally in MATLAB/Simulink^{TM}. The resulting simulation is as shown in Fig. 5.1, note that the red line indicated as "Auxiliary Command" does not exist in the original PSAT model.

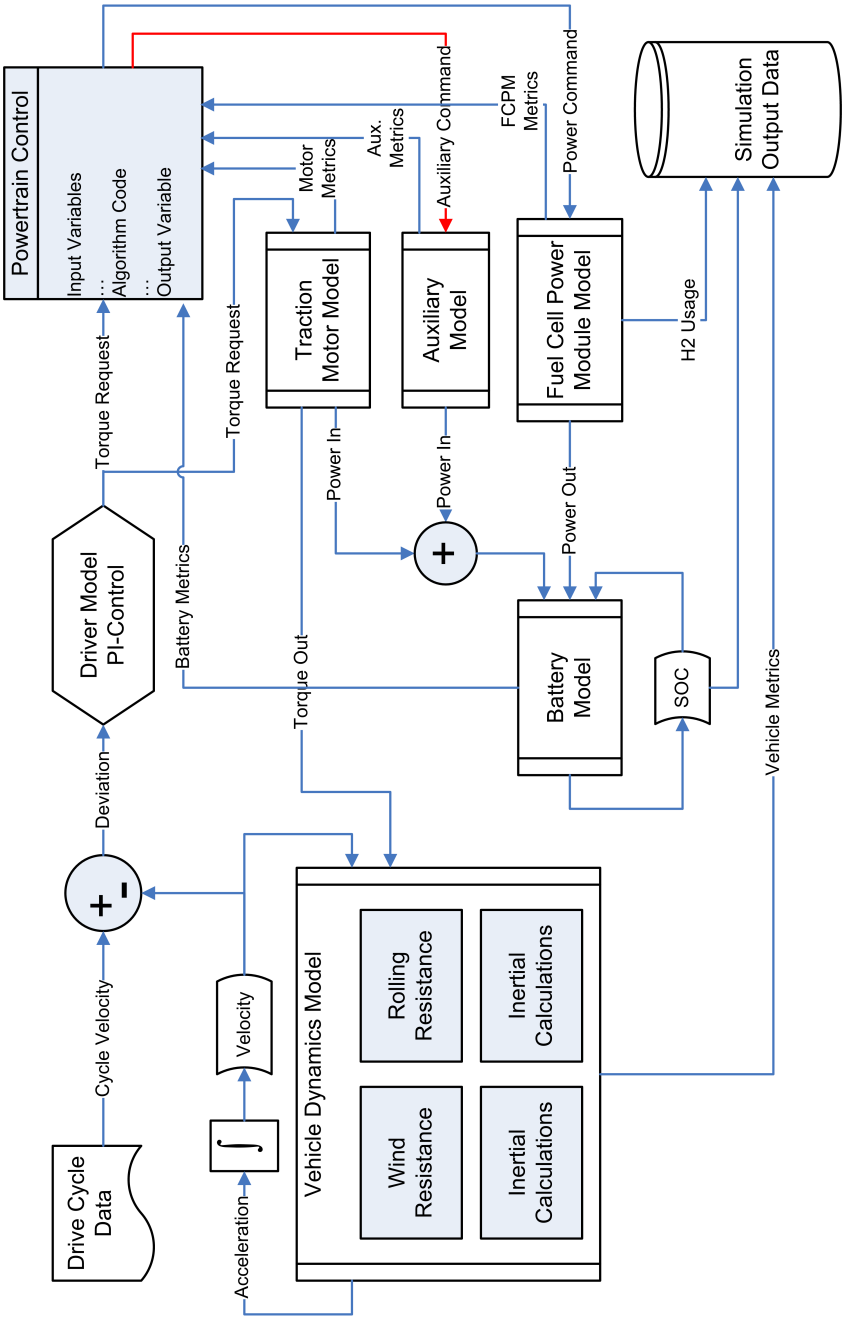

Figure 5.1: Simulation Data Flow

5.1.1 Powertrain Components

Many of the FCEV's powertrain component models were built using lookup tables and manufacturer provided performance data. These models existed from the previous powertrain analysis peformed by UWAFT during the initial design process as outlined in Chapter 2. The vehicle dynamics and tire models were provided in PSAT through ChallengeX for the 2005 Chevrolet Equinox. The powertrain models are geared towards energy usage calculations and therefore consist mainly of energy usage, conversion efficiency and fuel usage look up tables.

5.1.2 Auxiliary Modelling

Vehicle auxiliary loads are often modeled as a constant power consumption representing the average auxiliary load. In the vehicle simulation this is implemented as a controlled current source at constant power connected to the high-voltage DC output of the FCPM and battery pack. Although simplistic, this model is quite useful for characterizing the overall fuel usage penalty for various levels of auxiliary loading.

The key interest of this work is to determine whether or not transient changes in the auxiliary load have a significant effect on vehicle operation and fuel economy. In order to analyze this, the auxilary model must be externally controllable and not fixed to a constant power value. The model was changed to include an auxiliary command control input which may be connected to any external control including the vehicle controller model. Another external control source is the air conditioning model which was added to the vehicle simulation. The air conditioning models and control schemes outlined in Fig.'s 4.3 and 4.5 were both implemented and tested in seperate simulation runs to compare their effect. As air conditioning is the largest flexible and buffered auxiliary load, it's operation should dominate the results. Therefore it is a key element to examine through simulation analysis, and should act as an indication of the overall changes and gains that can be achieved.

5.1.3 Control Implementation

Powertrain Control

The powertrain controller is implemented in an embedded MATLAB^{TM} s-function block illustrated by the "Powertrain Control" block in 5.1. It has inputs and outputs corresponding to those in this figure and is executed on every iteration of the simulation. This block houses the powertrain optimization algorithm as outlined in Chapters 2 and 4.

As it is designed to be implemented onboard the actual vehicle controller for realtime optimization, the computational demands of this block must be kept at a minumum. To achieve this, the designer of the vehicle controller, Matthew Stevens of UWAFT, chose to implement the optimization using an piecewise evaluation of the cost function. This method still uses significant processor resources as compared to the other control code executing on the on-board vehicle controllers, however, total processor usage remains low at around 20%.

To implement the indirect auxiliary control method outlined in Chapter 4, this vehicle control block was re-written to run the powertrain optimization for 10 different auxiliary load values, spanning a range given by (5.1). In this equation, $P_{Pos-Flx}$ is the maximum allowable increase in auxiliary power, $P_{Neg-Flx}$ is the maximum allowable decrease (negative number), and finally $P_{Aux-Trgt}$ is the target or desired auxiliary power level.

$$P_{Aux-Range} = (P_{Aux-Trgt} + P_{Pos-Flx}) - (P_{Aux-Trgt} + P_{Neg-Flx}) \tag{5.1}$$

Auxiliary Control

To provide the values of $P_{Aux-Trgt}$, $P_{Pos-Flx}$ and $P_{Neg-Flx}$ to the vehicle controller, crisp rules are implemented as shown in Table 5.1. These rules allow the flexibility to be equal to the compressor power-consumption extremes or zero if an operating condition is violated.

If the flexibility is set to "Max", the compressor is free to operate at any level between the air conditioning controller's desired level and the maximum

Cabin Temp. - Desired Temp.	**Evaporator Temp.** ($^{\circ}C$)	**Positive Flex**	**Negative Flex**
> 1	> 5	Max	0
> 1	≤ 5	Max	Max
-1 $\leq$ error $\leq$ 1	< 12	0	Max
-1 $\leq$ error $\leq$ 1	> 18	Max	0
$<$ - 1	X	0	Max
X	< 0	0	Max

Table 5.1: Air Conditioning Power Flexibility Rules

swing (either positive or negative). When it is set to "0", the compressor must operate at the controller's desired level.

Drive Cycle

A drive cycle is a velocity vs. time graph representing the simulated vehicle speed over the duration of the simulation. There are two main categories of drive cycles representing Urban and Highway driving characteristics. It is expected that an urban drive cycle, with it's large transients in speed and low average propulsion power will show the largest impact of auxiliary load changes. Further, vehicles are generally considered to be driven predominantly in an urban environment. [6] Thus the industry standard UDDS or Urban Dynamometer Driving Schedule is used for the simulations performed here. Fig. 5.2 shows a graph of this drive cycle in km/h over it's full duration of almost 23 minutes.

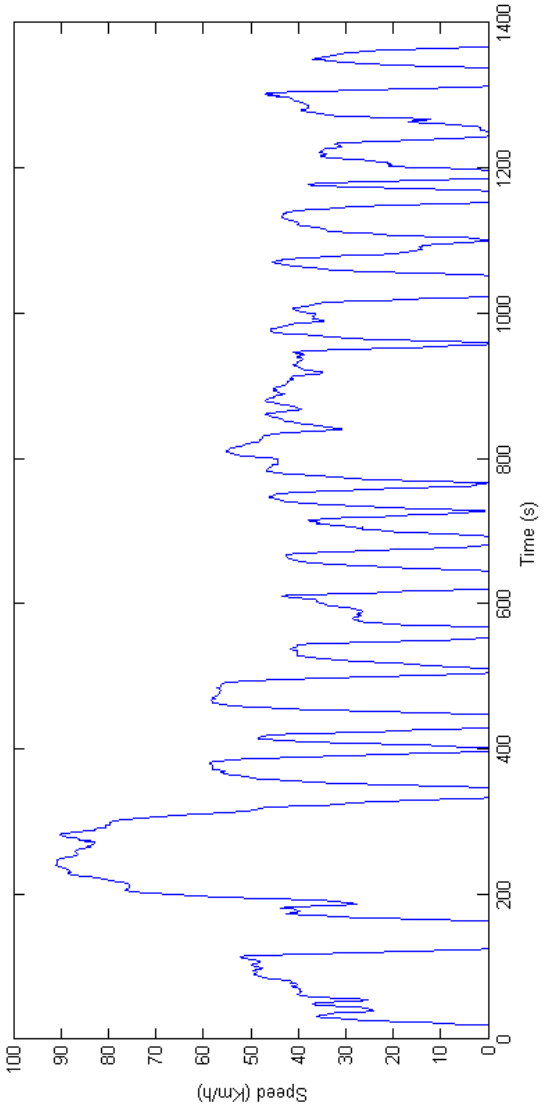

Figure 5.2: Urban Dynamometer Driving Schedule

5.2 Simulation Experiments

With the vehicle modelling environment set up, a number of seperate simulations were run in order to distil some useful information from the models. Firstly, to prove that the auxiliary loads are significant and to characterize their effect on the vehicle's fuel economy a batch of simulations each with increasing auxiliary loading were run. Using the air conditioning control models presented here, the next set of experiments show step-by step the gains achieved using each incremental change to the control strategy.

5.2.1 The Significance of Auxiliary Loading

To determine the effect of auxiliary loading on the FCEV's powertrain, simulations were run using the original control strategy and a constant auxiliary load. This load was varied from 500W in the first simulation to 8000W in the final simulation. Fig. 5.3 shows fuel economy results that were calculated and converted to Gasoline Equivalent units. These units, explained in Appendix B make it easy to compare with conventional gasoline powered vehicles. For each simulation, the propulsion and mechanical vehicle characteristics remain the same, resulting in an average propulsion energy usage rate of 4811W measured at the input of the motors.

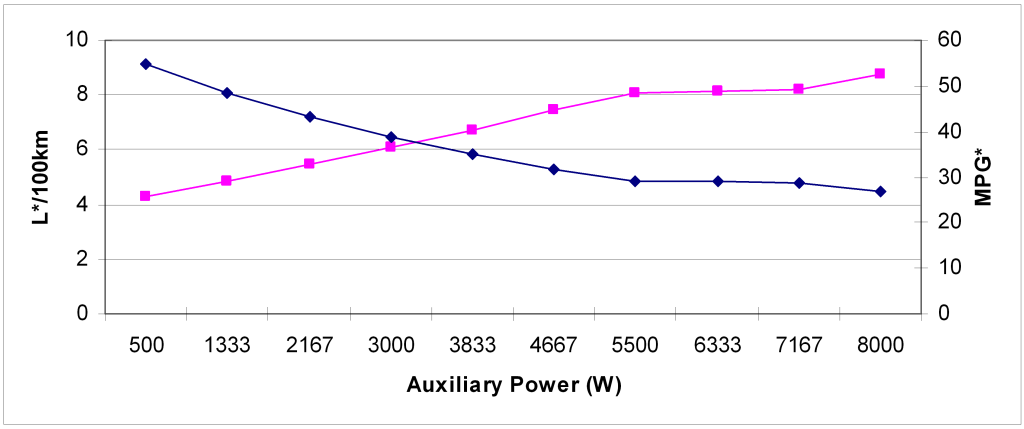

Figure 5.3: Fuel Economy vs. Auxiliary Loading
*Values are in Gasoline Equivalent Units. See Appendix B

Looking at these results, fuel economy is drastically affected by changes in auxiliary loading. On average from 500–8000W, the change in fuel economy is 0.594 L/100km per 1000W of auxiliary load, or 3.70 MPG per 1000W. Considering that the prototype vehicle has an average auxiliary load without air conditioning of $\approx 2500W$, an average air conditioning load of 1500W would reduce the fuel economy by $\approx 14\%$.

5.2.2 Air Conditioning with Conventional Control

In this experiment, the FCEV is simulated using air conditioning controlled in the conventional bang-bang manner. It is also assumed that temperature control at the vents is achieved using air mixing and therefore the refrigeration system is operating at maximum capacity on a continuous basis and the compressor does not shut off when the desired cabin temperature is reached. The results of this simulation are summarized in Table 5.2. A base vehicle auxiliary load of 2500W is applied as a constant to which the air conditioning adds when it is using energy.

Table 5.2: Simulation Results with Conventionally Controlled A/C

Factor	**Simulation Result**
Fuel Economy (L/100km)	6.767
Path Ratio	0.1498
Average Score (Unitless)	3.815
Average Instantaneous Eff.	0.4970
Hydrogen Usage (kg)	0.260
Final SOC	72.27%
Fuel Cell Startup Cycles	71
Average Auxiliary Load (W)	4332.8

The fuel economy results seem in line with the results from the constant load simulations run previously. Each time powertrain optimization occurs, the resulting overall cost function score (inverse of cost) and calculated instantaneous efficiencies are recorded. The average of these values is reported as the average score and average instantaneous efficiency. Final SOC is the resulting state of charge of the battery pack upon finishing the drive-cycle.

Any deviation from 60% is taken into account when calculating the fuel economy using the calculation specified in Appendix C. Fuel cell startup cycles reports the number of times the fuel cell had been turned of but then started up and is significant as the more cycles the shorter the FCPM lifetime and the increase in wasted hydrogen during the startup purge procedure. This purge quantity has not been quantified and is not included in the hydrogen usage numbers yet it is significant and must be minimized.

Fig. 5.4 shows the performance curves of the modeled air conditioning system for this simulation. It must be taken into consideration, however, that the thermodynamic efficiency losses incurred by stopping and starting the compressor are not modeled.

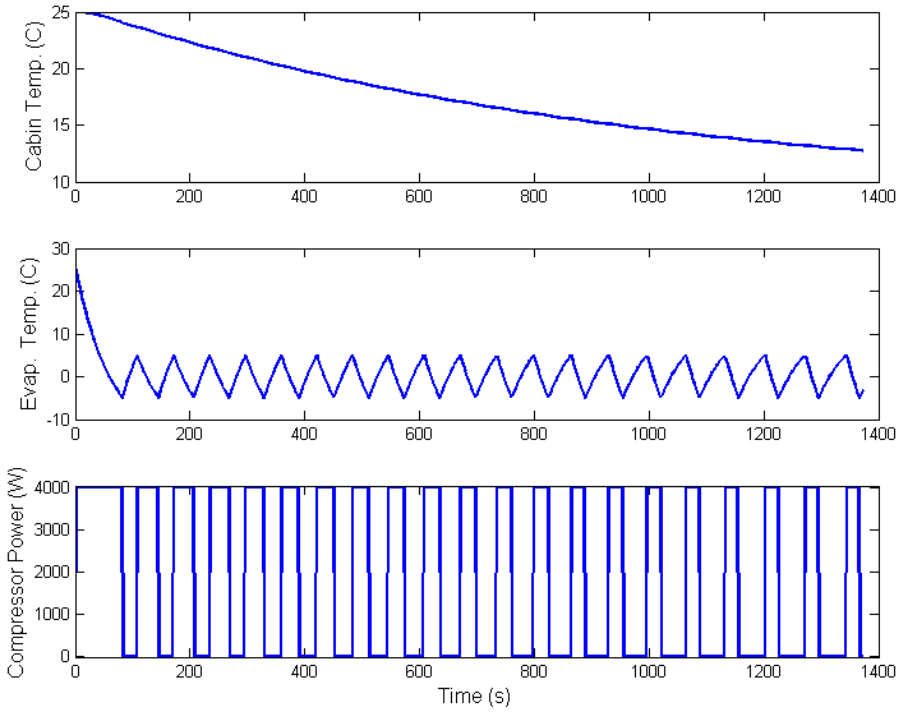

Figure 5.4: Air Conditioning Performance with Convential Control

NOTE: As the drive cycle is not long enough for a complete cool down from $40°C$, these experiments were run with an intial cabin temperature of $25°C$.

5.2.3 Air Conditioning with the Proposed Proportional Control

For this simulation, we compare the results of the traditional control scheme to the results of the proportional feedback control scheme for the A/C system. In this simulation it is still assumed that temperature is controlled via the method of air mixing inside the cabin, and the air conditioning is controlled to it's maximum operating point. Interestingly, although the average auxiliary power decreases by almost 60W and the fuel consumption in terms of Hydrogen usage also decreases, the fuel economy reported by this simulation is below that of the system with traditional A/C control. Table 5.3, displays the results for this simulation.

Table 5.3: Simulation Results with Proportionally Controlled A/C

Factor	**Simulation Result**
Fuel Economy (L/100km)	7.050
Path Ratio	0.1911
Average Score (Unitless)	3.899
Average Instantaneous Eff.	0.5163
Hydrogen Usage (kg)	0.236
Final SOC	63.29%
Fuel Cell Startup Cycles	57
Average Auxiliary Load (W)	4272.9

First of all, as mentioned earlier, the compressor cycling losses are not modeled and will hurt the performance of the previous simulation. Interestingly, though, without these losses it seems that a fluctuating auxiliary load allows for a better powertrain operating point on average. Looking at the path-ratio, we see that the percentage of the power that has travelled from the fuel-cell to the loads via the battery is significantly higher in this simulation than it was in the previous simulation with traditional a/c control. As the battery is a lossy sytem operating at $\approx 76\%$ turn-around efficiency in these simulations, this has a significant impact on fuel economy and explains the overall decrease. Another curiosity, however, is that the values reported by the real-time optimization do not reflect the decreased fuel economy in this simulation. In fact, these values indicate that the cost function was more

satisfied, producing a consistently higher score and the average instantaneous efficiency also improves. This phenomenon will be looked at in further detail in the analysis section of this Chapter. Fig. 5.5 shows the air conditioning performance curves seen using this control method.

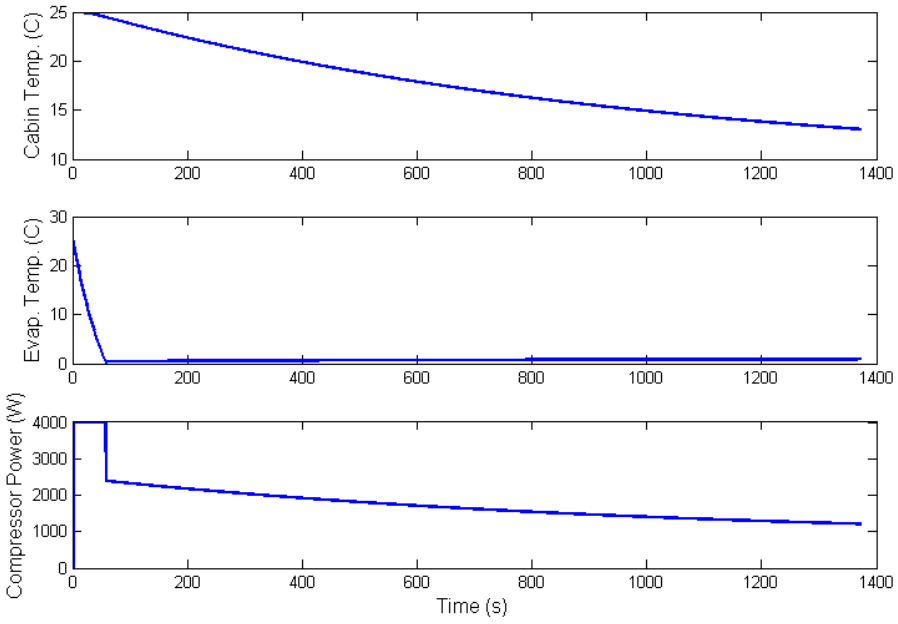

Figure 5.5: Air Conditioning Performance with Proportional Control

5.2.4 Air Conditioning with Proportional System and Temperature Control

The next step is to add the energy saving cabin temperature control to the simulation model. In this simulation, the desired cabin temperature is set to 18° with the intial and outdoor temperatures being 25°. The compressor power is controlled such that the interior cabin temperature remains at the desired temperature and the wasteful practice of temperature control via air mixing is avoided. As can be seen in Table 5.4, the average auxiliary load drops by $\approx 500W$ due to this change. The result is a dramatically improved fuel economy, further reduction in hydrogen usage and similar efficiency and path-ratio numbers to the last simulation without temperature control.

Table 5.4: Simulation Results with Proportionally Controlled Temp. and A/C System

Factor	**Simulation Result**
Fuel Economy (L/100km)	6.642
Path Ratio	0.1941
Average Score (Unitless)	3.895
Average Instantaneous Eff.	0.5151
Hydrogen Usage (kg)	0.227
Final SOC	64.59%
Fuel Cell Startup Cycles	59
Average Auxiliary Load (W)	3764.4

Looking at the curves in Fig. 5.6, it is apparent where the energy saving gains are made. When the cabin temperature reaches the desired temperature of 18°, the compressor power is scaled down significantly in order that the cabin temperature is not reduced beyond this setpoint. When this occurs, the evaporator temperature climbs as the heat transfer of the air conditioning system is reduced. Notice, however, the increase in fuel cell startup cycles compared to the previous simulation without temperature control. Notice, also, the continuing high path ratio as compared to the bang-bang control method. These results are significant and will be touched upon in the analysis section.

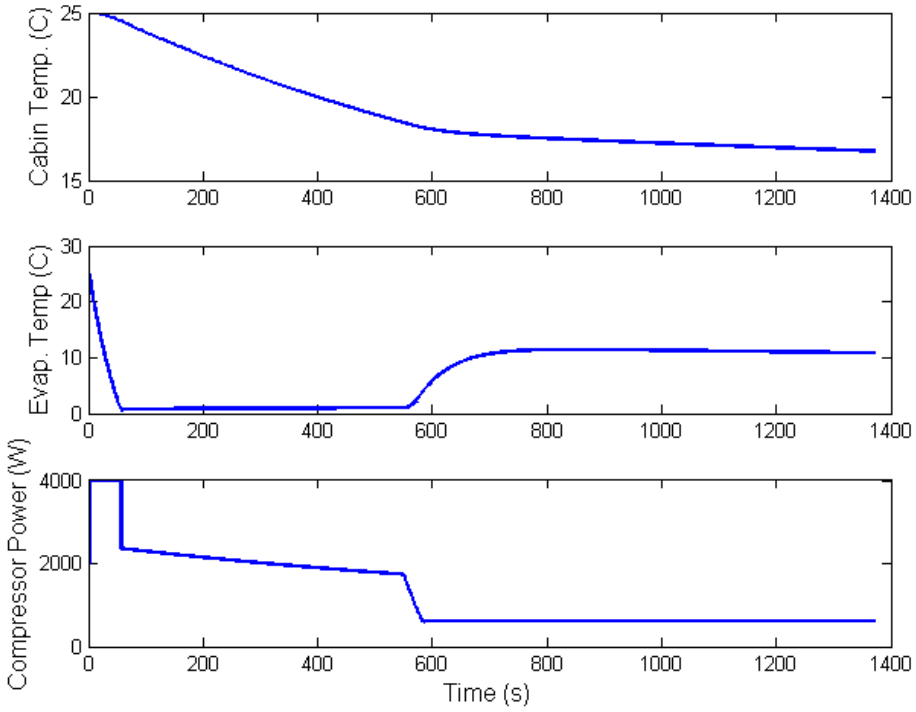

Figure 5.6: Air Conditioning Performance with Proportional System and Temp. Control

5.2.5 Integration with Powertrain Optimization

In this final simulation, the previous simulation is modified such that the air conditioning controller is integrated with the powertrain controller as shown in Fig. 4.11. The air conditioning controller is the same as shown in Fig. 4.6 with the addition of load flexibility outputs to the powertrain controller using the rules outlined in Table 5.1. Using these values, the powertrain controller populates the cost table as shown in Fig. 4.7 and chooses both the optimal powertrain operating point and the air conditioning operating point. The results of this simulation are encouraging and are shown in Table 5.5.

Ideally, the desired result of this simulation would be approximately the same air conditioning performance and auxiliary loading as the previous simulation with improved overall powertrain efficiency, and in general, better

Table 5.5: Simulation Results with Integrated A/C and Powertrain Control

Factor	**Simulation Result**
Fuel Economy (L/100km)	6.538
Path Ratio	0.1800
Average Score (Unitless)	3.908
Average Instantaneous Eff.	0.5231
Hydrogen Usage (kg)	0.229
Final SOC	66.10
Fuel Cell Startup Cycles	57
Average Auxiliary Load (W)	3718.54

cost function scores. The first point to note in the results is that the fuel economy has improved over the last simulation. Also note that the average cost function scores and instantaneous efficiencies are the highest when compared with the previous simulations. The path ratio has fallen to 18%, fuel cell startup cycles has fallen back to 57, in line with the simulation in Section 5.2.3, and the average auxiliary load was also reduced slightly. Interesting to note as well that although the hydrogen usage is marginally more than in the previous simulation, the remaining useable energy stored in the battery at the end of this drive cycle is significantly higher, offsetting that fact in terms of overall fuel economy. Fig. 5.7 illustrates what happens with the air conditioning system as a result of the integrated control strategy.

With this control implementation, the compressor power swings widely between the minimum and maximum flex values allowed by the air conditioning control algorithm. With the view compressed over the entire 23 minute drive cycle these variations seem quite violent, when in fact, they are relatively slow with durations of 1 to 40+ seconds. Another thing to keep in mind is that the bottom curve is not a disired speed nor refrigerant flow-rate curve and indicates instantaneous power delivered to the compressor motor which can be directly controlled via the compressor motor controller while the compressor speed and refrigerant flow rate float naturally to their corresponding levels.

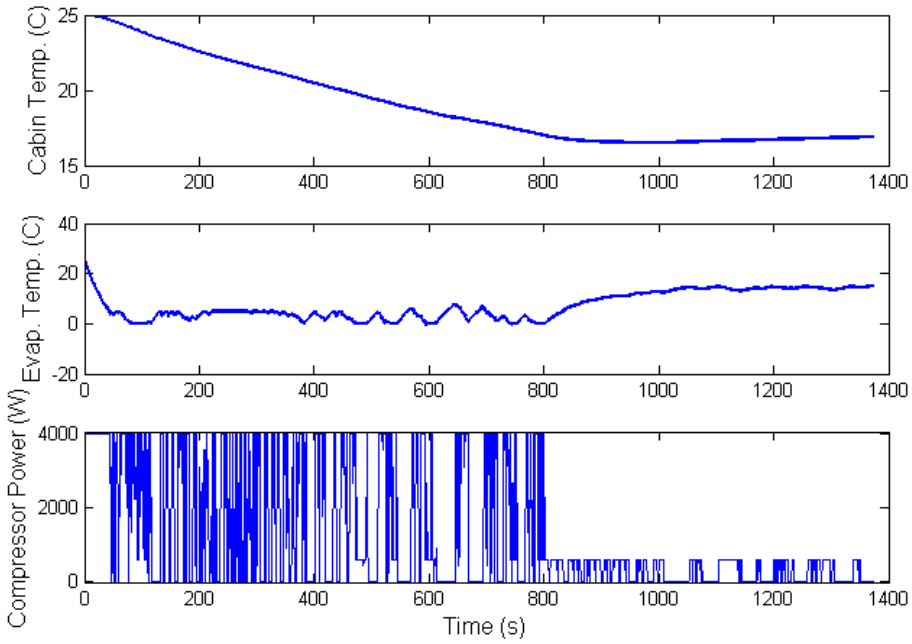

Figure 5.7: Air Conditioning Performance with Integrated A/C and Powertrain Control

5.3 Analysis

The simulations in the previous section show a number of useful results and also raise a number of questions. Firstly, it was shown that variations in auxiliary load have a dramatic effect on fuel economy, with air conditioning alone reducing the vehicle fuel economy in the neighbourhood of 14%. The prevelance of air conditioning in vehicles today makes this alone a worthwhile target of optimization [57]. These results are an indication of the potential gains to be achieved through the optimization and energy use reduction of all of the auxiliary systems in the vehicle. As noted for the first set of simulations, 1000W of auxiliary loading roughly corresponds to 0.594 L/100km or 8–9% of the fuel economy numbers produced by the FCEV simulations with typical auxiliary and air conditioning loads. That puts a 150W reduction in vehicle lighting power at $\approx 2\%$ increase in fuel economy. As seen in the later simulations, however, average magnitude of the auxiliary load is not the only consideration and the shape of the auxiliary power consumption curve throughout the drive cycle also plays a significant role.

Table 5.6 summarizes the key results of the air conditioning control simulations. When viewed together, there are a couple of interesting phenomena that are apparent. With the variable speed air conditioning compressor installed in the FCEV, it seems inefficient to implement a bang-bang control strategy such as the one used conventionally in vehicles. The simulation results show, however, that the overall vehicle fuel economy using this strategy is significantly better than that seen in the following proportional control simulation. This is curious as the average auxiliary load in the later simulation is actually lower than the former and points immediately to other factors involved in the determination of overall vehicle efficiency.

The path ratio indicates the reason for this discrepancy. In the conventional bang-bang control simulation, a smaller percentage of the electrical energy travelled through the battery on its way to the vehicle loads than when using the proportional control. With an average operating efficiency of $\approx 75\%$, 25% of the energy travelling through the battery is dissipated as heat and thus no longer useful. Interestingly, this difference in operation came about not because of the steady state or average auxiliary load but because of the transient nature of the auxiliary load using bang-bang control. This is a strong indication that variation of the auxiliary loads while

maintaining the same average auxiliary load can have a significant impact on fuel economy.

Table 5.6: Summary of A/C Control Simulation Results

Simulation Experiment	**5.2.2**	**5.2.3**	**5.2.4**	**5.2.5**
Fuel Economy (L/100km)	6.767	7.050	6.642	6.538
Path Ratio	0.1498	0.1911	0.1941	0.1800
Average Score (Unitless)	3.815	3.899	3.895	3.908
Average Instantaneous Eff.	0.4970	0.5163	0.5151	0.5231
Hydrogen Usage (kg)	0.260	0.236	0.227	0.229
Final SOC	72.27	63.29	64.59	66.10
Fuel Cell Startup Cycles	71	57	59	57
Average Auxiliary Load (W)	4332.8	4272.9	3764.4	3718.54

Despite it's superior fuel economy, the bang-bang control method is random with respect to powertrain optimization. This is to say that while fuel economy improvements are seen, there is no way to gaurantee these improvements as the transients are not engineered to create a fuel economy improvement, yet happen to have that effect.

The proportional control simulation 5.2.3, while having poorer fuel economy than simulation 5.2.2, represents the best performance case from a strictly auxiliary stand point, given the condition of air-mixing or series re-heating as a temperature control method. The addition of temperature control to the air conditioning system in simulation 5.2.4, and thus the elimination of the re-heating temperature control method, illustrates the potential for energy savings and fuel economy improvement from this auxiliary optimization alone. It is a good indication along with the simulations in 5.2.1 of the gains that can be achieved through auxiliary reduction alone.

Simulation 5.2.5 illustrates the fuel economy gains with respect to simulation 5.2.4 that can be achieved through deterministic addition of transients to the air conditioning power. The fuel economy gains of 1.8% are very significant in the automotive industry, especially when considering the number of vehicles in use today and the magnitude of energy that a 1.8% reduction represents. Therefore the algorithm proposed in Chapter 4 for indirect

auxiliary optimization has merit and can be applied not only to the air conditioning system, but to the auxiliary subsystems as a whole. To see where the efficiency gains are made, notice that the path ratio has decreased when compared to simulations 5.2.3 and 5.2.4. Thus, by choosing higher efficiency operating points, the proposed powertrain control algorithm has used the auxiliary flexibility to reduce the amount of power flowing through the battery over the drive cycle. With this implementation of the proposed control strategy the wasteful calculation is also performed as outlined in Chapter 4. Looking at the simulation results, however, only 0.003% of the auxiliary power is used in a wasteful manner as the calculation proves true only for an insignificant amount of time over the drive cycle.

Powertrain Optimization Accuracy

Due to the nature of the powertrain's real-time optimization algorithm, being a direct evaluation method, the chosen operating points are only an approximation of the actual optimal operating points. The discrepancies caused by this approximation directly result in a reduction in powertrain efficiency as well as a reduction in the accuracy of the auxiliary load operating point. One significant effect of this, as it applies to the algorithm implemented in simulation 5.2.5, is the inability of the algorithm to exactly match auxiliary power increases with fuel cell power increases, resulting in a higher than desired SOC at the end of the drive cycle. With the merits of auxiliary modulation shown for improving vehicle powertrain efficiency, further research needs to be performed to maximize the accuracy of the real-time optimization algorithm while remaining within the limits of vehicle on-board computing power.

5.4 Chapter Summary

This chapter looked at a number of different simulation experiments which illustrate the potential gains to be acheived through the proposed methods of auxiliary power reduction and modulation. The results are promising and indicate significant gains in fuel efficiency of around 2% for every 150W reduction in auxiliary load, and 1.8% through strategic modulation of that auxiliary load. There is, however, much room for improvement in the optimization techniques presently used in the vehicle, with the main challenge being to keep the processing requirements low.

Chapter 6

Conclusions and Recommendations

6.1 Conclusions

The automotive industry is changing, focusing more and more on vehicle efficiency and environmental friendliness. These two goals often go hand in hand, and with the usage of less fuel or energy, less environmental pollutants are released. This thesis focuses on vehicle auxiliary load research, which is often neglected and left as an afterthought to powertrain research and design. It looks specifically at the auxiliary systems as they exist in the University of Waterloo's prototype Fuel-Cell electric vehicle, while much of the analysis and research applies to more conventional vehicle architectures as well. The key areas that are addressed in this thesis are as follows:

1. Identification of auxiliary loads, their purpose and the constraints on energy conservation efforts.

2. Quantification of the effect of auxiliary loading on the University's FCEV prototype.

3. Outline of potential methods for conserving energy through modification and control of auxiliary systems.

4. Detailed analysis of air-conditioning auxiliary loading as a key area for energy conservation and as an example for the trial of several conservation techniques.

5. Quantification of the energy conservation results for the overall FCEV when the air conditioning system is modelled using various control methods.

By addressing each of these points, the importance of auxiliary system research and design is made clear as the potential for energy savings is significant. The energy saving methods presented consist of control methods of two types, direct and indirect.

The direct methods proposed include voltage reduction and direct auxiliary system control. These methods act to directly reduce the average energy consumed by individual auxiliary systems during the operation of the vehicle. **Voltage reduction, especially for resistive loads, can halve power consumption for certain auxiliaries.** This is acheived by reducing the voltage safety margin's within the system which comes at the cost of tighter voltage controls. With the FCEV's controlled buck converters supplying the power for the 12 and 24 Volt systems, the capability of maintaining strict voltage limits is already present. **Direct system control of the air conditioning system has the potential to save a large amount of energy**, as often this systems is designed to operate either on or off, i.e. maximum capacity or none. Temperature control is thus acheived in such a system through series re-heating of cooled air thereby counter-acting the energy expent to cool the air initially. Through direct control, temperature control can be achieved by throttling the energy input to the A/C compressor, removing the need for re-heating and avoiding the energy waste. **Increased control of other auxiliaries such as defog and windshield wipers such that they turn off automatically when not required also serves to save energy overall.** Finally, **control of the various cooling fans and pumps in the vehicle should also prove to conserve energy.** With control, these components will not consume energy when not required such that they operate more efficiently.

The indirect method, geared for the opportunistic usage of energy based on powertrain efficiency, stems from the FCEV powertrain efficiency analysis outlined in Chapter 4. As with the powertrain of any vehicle, the energy conversion efficiency from fuel to useful power available to the auxiliary systems varies with the propulsion load dictated by the driver. Taking these variations into account and increasing or decreasing the auxiliary load accordingly leads

to better overall vehicle efficiency. Auxiliary flex is introduced to represent the amount of flexibility in the power consumption of the vehicle auxiliaries. This is determined based on auxiliary specifications as well as passenger comfort and safety considerations. The proposed powertrain control algorithm calculates the ideal auxiliary power demand and the available auxiliary flex to produce reasonably optimal powertrain and auxiliary operating points.

The vehicle simulation environment in PSAT was modified to allow the validation of the proposed auxiliary control strategies. In Chapter 5, the simulation results are presented, which quantify the effects of these strategies on the fuel economy of the FCEV. **The first bank of simulations, summarized in Fig. 5.3, presents the effect of auxiliary load on fuel economy, which on average is 0.594 L/100km per 1000W of auxiliary load.** This is significant and it is determined that an A/C load of as little as 1500W continuously would reduce the vehicle's average running fuel economy by 14%. (Note: A reduction in fuel economy is an increase in fuel consumption per distance) The next four simulation runs determine FCEV fuel economy and operating parameters using an A/C model with three different types of control. The results are summarized in Table 5.6 and present a number of interesting phenomena:

1. PI control and temperature control via compressor throttling instead of series re-heating for the A/C system results in lower average auxiliary loads in the FCEV.

2. The shape of the auxiliary power curve over a drivecycle significantly affects fuel economy, with transient operation seemingly more favourable than steady operation. In this regard, however, it is clear that fuel economy is best when the transients are controlled to coincide with points of efficient powertrain operation.

3. Path ratio, or the percentage of energy travelling via the battery pack in a hybrid FCEV is a key metric for the indication of overall vehicle efficiency.

4. For an A/C system of the size simulated, control **using the presented indirect control algorithm alone can effect an increase in fuel economy in the neighbourhood of 1.8%.**

6.2 Recommendations

This thesis represents a first foray into the area of automotive auxiliary system optimization. It covers a range of systems in a prototype FCEV and explores the application of new control ideas and algorithms. It has shown that there are promising energy savings and fuel economy gains to be realized through these methods. Moving forward, however, there are many questions that need to be answered from an implementation standpoint.

Fields such as applied optimization and computer science can contribute to the further development of efficient code for the proposed control algorithms. As on-board vehicle computers become more and more powerful, more complex computational methods can be used. Reasearch should be performed to discover what methods these are and what they entail.

From a business standpoint, the cost effectiveness of such energy saving methods should be analyzed. Is there enough of a consumer demand for such energy savings to warrant the extra cost? This leads into a whole other field of research, which includes the discussion of government fuel economy and emissions regulations.

To summarize, there are many aspects of this research that could be further explored in detail. As mentioned previously, auxiliary research often goes unnoticed in the automotive world when compared to powertrain research. It is hoped that more attention will be paid to this area in future, so that we can all benefit from the results.

References

[1] J. Makower, R. Pernick, and C. Wilder, "Clean energy trends," Clean Energy Group, Montpelier, VT, 2006.

[2] (2007, Jan.) Earthtrends: The environmental information portal. World Resources Institute. Washington, DC. [Online]. Available: http://earthtrends.wri.org

[3] (2007, Jan.) Annual global diesel light-vehicle sales forecast. JD Power & Associates. Westlake Village, California. [Online]. Available: http://www.prnewswire.co.uk/cgi/news/release?id=109015

[4] (2007, Jan.) Canadian national population statistics. Statistics Canada. Ottawa, Ontario. [Online]. Available: http://www.statcan.ca/english/freepub/98-187-XIE/pop.htm

[5] M. G. Schultz, T. Diehl, G. P. Brasseur, and W. Zittel, "Air pollution and climate-forcing impacts of a global hydrogen economy," *SCIENCE*, vol. 302, Oct. 2003. [Online]. Available: www.sciencemag.org

[6] B. Oliver, "Greenhouse gas emissions and vehicle fuel efficiency standards for canada," *Pollution Probe*, Feb. 2005. [Online]. Available: http://www.pollutionprobe.org/

[7] R. W. Bentley, "Global oil & gas depletion: an overview," *Energy Policy*, vol. 30, no. 3, pp. 189–205, Feb. 2002.

[8] D. J. Holt, Ed., *100 Years of Engine Developments.* Warrendale, PA: Society of Automotive Engineers, 2005, pt-115.

[9] M. E. Kahn, "New evidence on trends in vehicle emissions," *The RAND Journal of Economics*, vol. 27, no. 1, pp. 183–196, Spring 1996.

[10] "Milestones in auto emissions control," U.S. Environmental Protection Agency, Ann Arbor, MI, Aug. 1994, 400-F-92-014.

[11] F. Zhao, M. C. Lai, and D. L. Harrington, "Automotive spark-ignited direct-injection gasoline engines," *Progress in Energy and Combustion Science*, vol. 25, no. 5, pp. 437–562, Oct. 1999.

[12] P. Zelenka, W. Cartellieri, and P. Herzog, "Worldwide diesel emission standards, current experiences and future needs," *Applied Catalysis B: Environmental*, vol. 10, no. 1–3, pp. 3–28, Sep. 1996, catalytic treatment of diesel emissions.

[13] R. B. Krieger, R. M. Siewert, J. A. Pinson, N. E. Gallopoulos, D. L. Hilden, D. R. Monroe, R. B. Rask, A. S. P. Solomon, and P. Zima, "Diesel engines: one option to power future personal transportation vehicles," *SAE International: Journal of Engines*, vol. 106, no. 97, Aug. 1997.

[14] M. R. Cuddy and K. B. Wipke, "Analysis of the fuel economy benefit of drivetrain hybridization," in *SAE International Congress & Exposition, Detroit, Michigan, February 24–27, 1997.* National Renewable Energy Laboratory, Feb. 1997.

[15] D. Hermance and S. Sasaki, "Hybrid electric vehicles take to the streets," *IEEE Spectrum*, vol. 35, no. 11, pp. 48–52, Nov. 1998.

[16] S. Dhameja, *Electric Vehicle Battery Systems.* Woburn, MA: Newnes Press, 2002.

[17] P. L. Spath and M. K. Mann, "Life cycle assessment of hydrogen production via natural gas steam reforming," National Renewable Energy Laboratory, Golden, CO, Feb. 2001, nrel/TP-570-27637.

[18] H. J. Herzog, "What future for carbon capture and sequestration?" *Environmental Science & Technology: American Chemical Society*, vol. 35, no. 7, pp. 148–153, Apr. 2001.

[19] J. Ivy, "Summary of electrolytic hydrogen production milestone completion report," National Renewable Energy Laboratory, Golden, CO, Sep. 2004, nrel/MP-560-36734.

[20] (2007, Mar.) Fuel cell: Wikipedia. Wikimedia Foundation, Inc. St. Petersburg, FL. [Online]. Available: http://en.wikipedia.org/wiki/Fuel_cell

[21] L. Carrette, K. A. Friedrich, and U. Stimming, "What future for carbon capture and sequestration?" *CHEMPHYSCHEM*, vol. 1, pp. 162–193, 2000, 1439-4235/00/01/04.

[22] C. E. Thomas, B. D. James, F. D. Lomax, and I. F. Kuhn, "Fuel options for the fuel cell vehicle: hydrogen, methanol or gasoline?" *International Journal of Hydrogen Energy*, vol. 25, no. 6, pp. 551–567, Jun. 2000.

[23] R. B. Moore and V. Raman, "Hydrogen infrastructure for fuel cell transportation," *Int. Journal of Hydrogen Energy*, vol. 23, no. 7, pp. 617–620, 1998.

[24] (2007, Feb.) Ford model T: Wikipedia. Wikimedia Foundation, Inc. St. Petersburg, FL. [Online]. Available: http://en.wikipedia.org/wiki/Ford_Model_T

[25] (2007, Feb.) The history of the automobile. About Inc., The New York Times Co. New York, NY. [Online]. Available: http://inventors.about.com/library/weekly/aacarsassemblya.htm

[26] J. G. West, "Powering up-a higher system voltage for cars," *IEE Review*, vol. 35, no. 1, pp. 29–32, Jan. 1989.

[27] G. Torrisi, J. Notaro, G. Burlak, and M. Mirowski, "Evolution and trends in automotive electrical distribution systems," in *Vehicle Power and Propulsion, 2005 IEEE Conference*, Sep. 2005.

[28] J.-H. Kim and J.-B. Song, "Control logic for an electric power steering system using assist motor," *Mechatronics*, vol. 12, pp. 447–459, 2002.

[29] D. Türler, D. Hopkins, and H. Goudey, "Reducing vehicle auxiliary loads using advanced thermal insulation and window technologies," in *SAE World Congress, Detriot, Michigan, March 3–6, 2003.* Lawrence Berkeley National Laboratory, Mar. 2003.

[30] J. G. Kassakian, H. C. Wolf, J. M. Miller, and C. J. Hurton, "The future of automotive electrical systems," in *Power Electronics in Transportation, 1996. IEEE*, Oct. 1996, pp. 3–12.

[31] S. M. Lukic and A. Emadi, "Performance analysis of automotive power systems: effects of power electronic intensive loads and electrically-assisted propulsion systems," *2002. Proceedings. VTC 2002-Fall. 2002 IEEE 56th Vehicular Technology Conference*, vol. 3, pp. 1835–1839, 2002.

[32] T. Hendricks and M. O'Keefe, "Heavy vehicle auxiliary load electrification for the essential power system program: Benefits, tradeoffs, and remaining challenges," in *International Truck and Bus Meeting and Exhibition, Detriot, Michigan, November 18–20, 2002.* National Renewable Energy Laboratory, Nov. 2002.

[33] P. J. McCleer, "Electric drives for pump, fan, and compressor loads in automotiveapplications," in *Industrial Electronics, 1995. ISIE '95., Proceedings of the IEEE International Symposium on*, vol. 1, Athens, Greece, Jul. 1995, pp. 80–85.

[34] W. O. Forrest and M. S. Bhatti, "Energy efficient automotive air conditioning system," in *SAE World Congress, Detriot, Michigan, March 4–7, 2002.* Delphi Harrison Thermal Systems, Mar. 2002.

[35] E. B. Ratts and J. S. Brown, "An experimental analysis of cycling in an automotive air conditioning system," *Applied Thermal Engineering*, vol. 20, pp. 1039–1058, 2000.

[36] D. Simic, H. Giuliani, C. Kral, and F. Pirker, "Simulation of conventional and hybrid vehicle including auxiliaries with respect to fuel consumption and exhaust emissions," in *SAE World Congress, Detriot, Michigan, April 3–6, 2006.* Arsenal Research, Apr. 2006.

[37] (2007, Aug.) University of waterloo alternative fuels team. University of Waterloo. Waterloo, Ontario. [Online]. Available: http://www.uwaft.com

[38] (2007, Aug.) Challengex: Crossover to sustainable mobility. Argonne National Laboratory. Argonne, IL. [Online]. Available: http://www.challengex.org

[39] (2007, Aug.) Powertrain system analysis toolkit. Argonne National Laboratory. Argonne, IL. [Online]. Available: http://www.transportation.anl.gov/software/PSAT/index.html

[40] T. J. Mali, J. Marshall, M. B. Stevens, C. Mendes, D. M. Shilling, K. Tong, E. Wilhelm, S. Beckermann, R. A. Fraser, and M. W. Fowler, "Fuel cell hybrid powertrain design approach for a 2005 chevrolet equinox," in *SAE World Congress, Detriot, Michigan, April 3–6, 2006.* University of Waterloo, Apr. 2006.

[41] (2007, Feb.) Emissions standards: U.s.a.: Cars and light-duty trucks — tier 2. EcoPoint Inc. Mississauga, ON. [Online]. Available: http://www.dieselnet.com/standards/us/ld_t2.php#bins

[42] A. Emadi, K. Rajashekara, S. S. Williamson, and S. M. Lukic, "Topological overview of hybrid electric and fuel cell vehicular power system architectures and configurations," *IEEE Transactions on Vehicular Technology*, vol. 54, no. 3, pp. 763–770, May 2005.

[43] M. Ahman, "Primary energy efficiency of alternative powertrains in vehicles," *Energy*, vol. 26, no. 11, pp. 973–989, Nov. 2001.

[44] T. J. Mali, "Automotive simulation, design and optimization — a capability review." *Pollution Probe*, Mar. 2006. [Online]. Available: http://www.pollutionprobe.org/

[45] A. Kulikovsky, "The voltage current curve of a pem fuel cell," *Nanotech*, vol. 3, pp. 467–470, 2003.

[46] (2007, Jul.) Cobasys: Transportation product information. Cobasys, Inc. Orion, MI. [Online]. Available: http://www.cobasys.com/products/transportation_product_info.shtml

[47] C. J. Mendes, "Torque control strategies for awd electric vehicles," *University of Waterloo – MASc Thesis*, 2006.

[48] (2007, Mar.) Data sheet: 375v input maxi family dc-dc converter module. Vicor Corp. Andover, MA. [Online]. Available: http://www.vicorpower.com/documents/datasheets/ds_375vin-maxi-family.pdf

[49] M. B. Stevens, C. Mendes, R. A. Fraser, and M. W. Fowler, "Fuel cell hybrid control strategy development," in *SAE World Congress, Detriot, Michigan, April 3–6, 2006.* University of Waterloo, Apr. 2006.

[50] M. Salman, N. J. Schouten, and N. A. Kheir, "Control strategies for parallel hybrid vehicles," in *American Control Conference, 2000. Proceedings of the 2000*, vol. 1, no. 6, Chicago, IL, USA, Sep. 2000, pp. 524–528.

[51] N. J. Schouten, M. A. Salman, and N. A. Kheir, "Fuzzy logic control for parallel hybrid vehicles," *IEEE Transactions on Control Systems Technology*, vol. 10, no. 3, pp. 460–468, May 2002.

[52] M. Koot, J. T. B. A. Kessels, B. de Jager, W. P. M. H. Heemels, P. P. J. van den Bosch, and M. Steinbuch, "Energy management strategies for vehicular electric power systems," *IEEE Transactions on Vehicular Technology*, vol. 54, no. 3, pp. 771–782, May 2005.

[53] N. Jalil, N. A. Kheir, and M. Salman, "A rule-based energy management strategy for a series hybrid vehicle," in *American Control Conference, 1997. Proceedings of the 1997*, vol. 1, Albuquerque, NM, USA, Jun. 1997, pp. 689–693.

[54] A. Brahma, Y. Guezennec, and G. Rizzoni, "Optimal energy management in series hybrid electric vehicles," in *American Control Conference, 2000. Proceedings of the 2000*, vol. 1, no. 6, Chicago, IL, USA, Sep. 2000, pp. 60–64.

[55] "Mototron documentation," Mototron Inc., Oshkosh, WI, 2007.

[56] M. Stevens and M. Wahlstrom, "Control strategy presentation: Fuel cell hybrid control," University of Waterloo, Waterloo, ON, Jun. 2007.

[57] D. M. Kyle and R. A. Sullivan, "Heating, ventilation and air-conditioning systems," Oak Ridge National Laboratory for the U.S. Department of Energy, Oak Ridge, TN, Feb. 1993.

[58] T. Q. Qureshi and S. A. Tassou, "Variable-speed capacity control in refridgeration systems," *Applied Thermal Engineering*, vol. 16, no. 2, pp. 103–113, 1996.

[59] (2007, Mar.) Electric compressor specifications. Sanden International Inc. Wylie, TX. [Online]. Available: http://www.sanden.com/products/ecspecs.html

[60] M. J. Moran and H. N. Shapiro, *Fundamentals of Engineering Thermodynamics: 4th Edition.* New York, NY: John Wiley & Sons, 2000.

[61] "Compressor performance documentation," Sanden International Inc., Wylie, TX, 060511Performance 33cc 27cc-1.ppt.

[62] *Lamps, Reflective Devices and Associated Equipment*, Transport Canada Safety and Security, Standards and Regulations Division TECHNICAL STANDARDS DOCUMENT 108, Rev. 3.

[63] *Lamps, reflective devices, and associated equipment*, National Highway Traffic Safety Administration Federal Motor Vehicle Safety Standard (FMVSS) 108.

[64] A. Badawy, J. Zuraski, F. Bolourchi, and A. Chandy, "Modeling and analysis of an electric power steering system," in *SAE International Congress, Detriot, Michigan, March 1–4, 1999.* Delphi Steering Systems, Mar. 1999.

[65] K. C. Cheok, K. Kobayashi, S. Scaccia, and G. Scaccia, "A fuzzy logic-based smart automatic windshield wiper," *IEEE Control Systems Magazine*, vol. 16, no. 6, pp. 28–34, Dec. 1996.

[66] (2007, Apr.) Rd series direct drive pump instruction manual. IWAKI America Inc. Holliston, MA. [Online]. Available: http://www.dieselnet.com/standards/us/ld_t2.php#bins

[67] "Ballard/312v67 documentation," Ballard Power Systems Inc., Burnaby, B.C., 2006.

[68] "Cobasys 366-70 applications manual," Cobasys Inc., Orion, MI, 2006.

[69] P. Macken, M. Degrauwe, M. Van Paemel, and H. Oguey, "A voltage reduction technique for digital systems," in *Solid-State Circuits Conference, 1990. Digest of Technical Papers. 37th ISSCC., 1990 IEEE International*, San Francisco, CA, USA, Feb. 1990, pp. 238–239.

[70] L. Armstrong, "Brushless dc fans need current control," Zetex Semiconductors Plc., Chadderton, Oldham, U.K., Jul. 2004. [Online]. Available: http://www.zetex.com/5.0/pdf/ZE0439.pdf

[71] (2007, May) Automotive mosfet: Irf2804. Datasheet. International Rectifier Inc. El Segundo, CA. [Online]. Available: http://www.irf.com/product-info/datasheets/data/irf2804.pdf

[72] (2007, May) Interior fog sensor. Datasheet. First Technology Innovative Solutions Inc. Southfield, MI. [Online]. Available: http://www.1firsttech.com/data_sheets_pdfs/fog_sensor.pdf

[73] (2007, Mar.) Trw body control systems europe & emerging markets: Rain sensor. Brochure. TRW Automotive Electronics Inc. Farmington Hills, MI. [Online]. Available: http://www.howstuffworks.com/pdf/rain-sensor.pdf

[74] W. Eichlseder, J. Hager, and M. Raup, "Designing vehicle cooling systems using simulation calculations," *STEYR-DAIMLER-PUCH Engineering Center*, vol. 99, no. 10, pp. 638–647, Oct. 1997.

[75] K. B. Wipke, M. R. Cuddy, and S. D. Burch, "ADVISOR 2.1: a user-friendly advanced powertrain simulation using acombined backward/forward approach," *IEEE Transactions on Vehicular Technology*, vol. 48, no. 6, pp. 1751–1761, Nov. 1999.

[76] "Transportation energy data book," Oak Ridge National Laboratory, Oak Ridge, TN, May 2007. [Online]. Available: http://cta.ornl.gov/data/Index.shtml

Appendix A

Transportation Energy Calculations

Canadian Detailed Calculation:

Total final energy consumption (Sums direct energy usage numbers from all sectors of society.)

$$= 186,134 \text{ ktoe (thousands of tons (metric) of oil eq.)}$$

Transportation Sector

$$= 54,093 \text{ ktoe} => 29\% \text{ of Final Energy}$$

Motor Gasoline Usage (All fuel for spark ignition engines excluding stationary applications)

$$= 6,451 \text{ mltr (millions of litres)}$$

Note: 1209 ltr/toe (Standard conversion used by World Resources Institute) [2]

$$\frac{36,451 \times 10^6}{1,209} = 30,531 \text{ ktoe} => 16\% \text{ of Final Energy}$$

U.S. Detailed Calculation:

Total final energy consumption (Sums direct energy usage numbers from all sectors of society.)

$$= 1,475,504 \text{ ktoe (thousands of tons (metric) of oil eq.)}$$

Transportation Sector

$$= 601,275 \text{ ktoe} => 29\% \text{ of Final Energy}$$

Motor Gasoline Usage (All fuel for spark ignition engines excluding stationary applications)

$$= 465,319 \text{ mltr (millions of litres)}$$

Note: 1209 ltr/toe (Standard conversion used by World Resources Institute) [2]

$$\frac{465,319 \times 10^6}{1,209} = 384,879 \text{ ktoe} => 26\% \text{ of Final Energy}$$

Appendix B

Gasoline Equivalent Units

With the prevalence of gasoline as a fuel in the automotive industry, it's often easier to think in terms of equivalent gasoline energy than units such as joules. The main reason for this is that conventional vehicles are rated for fuel economy in terms of L/100km (MPG in the U.S.A.) of gasoline and when looking for a new fuel efficient vehicle consumers need a common scale for comparison. Table B.1 below lists standard values for the energy content of various fuels. To convert a quantity of hydrogen to an equivalent quantity of gasoline, the net or lower heating values of the two fuels are equated to determine the quantity ratio required for the same amount of energy.

Table B.1: Upper and Lower Heating Values for Various Fuels

	Heating Content	
Fuel	**Gross (Upper Value)**	**Net (Lower Value)**
Gasoline	125,000 Btu/gal	115,400 Btu/gal
Hydrogen	134,200 Btu/kg	113,400 Btu/kg
Diesel	138,700 Btu/gal	128,700 Btu/gal
Methanol	64,600 Btu/gal	56,560 Btu/gal
Ethanol	84,600 Btu/gal	75,670 Btu/gal

[76]

For example, what is the equivalent amount of gasoline represented by 2kg of hydrogen?

$$2kg - H_2 \times \frac{113,400Btu}{1kg} \times \frac{1gal - Gasoline}{115,400Btu} = 1.9653gal - Gasoline$$

$$1.9653gal - Gasoline \times \frac{3.7854L}{1gal} = 7.4394L - Gasoline$$

Using the distance that the car travelled on this amount of fuel, L/100km or Miles-Per-Gallon (MPG) can now be calculated.

Appendix C

SOC Deviation Adjustments

When evaluating the fuel economy of a hybrid vehicle the energy consumed from or added to the potential energy stored in the battery pack must be accounted for. Vehicle fuel economy is typically evaluated over a fixed drive-cycle to maintain experimental accuracy and minimize error. Throughout such a drive-cycle the state of charge (SOC) of the battery in a hybrid vehicle will fluctate as this battery is charged and discharged. This means that the battery will most likely contain a different amount of energy or have a different SOC at the end of the drivecycle then it did at the beginning. Should it have a higher SOC at the end, then running the drive-cycle again would result in a different amount of fuel being consumed as some extra energy is already available in the battery. In order to remove the error caused by this fluctuation in SOC, calculations have been devised to approximate the "actual" fuel economy that would have been acheived had the battery SOC ended at exactly the same point as it started.

Throughout the simulations performed in this thesis, battery current (I_{Batt}) and voltage (V_{Batt}) are recorded for each timestep (ts - in seconds). Using this data, the energy going into or coming out of the battery can be calculated for each timestep aswell. Summing these values over the duration of the simulation results in the total energy added to or removed from the battery throughout the drive-cycle (ΔE) as shown in C.1.

$$\Delta E = \sum I_{Batt} \times V_{Batt} \times ts \tag{C.1}$$

There are two possible cases at the end of a drivecycle: (1) The battery contains extra energy beyond what it initially had, and (2) It contains less energy then it initially did. As fuel can only be consumed and not regenerated in the vehicle, it makes sense to consider that any extra energy as in case (1) would ultimately be removed through driving further and that any lack of energy as in case (2) would ultimately be replenished by consuming more fuel. Therefore, to adjust the fuel economy in case (1), the distance travelled by consuming the extra energy in the battery is added to the total distance actually covered throughout the drive-cycle. In case (2), the amount of fuel required to replenish the energy in the battery is added to the fuel actually consumed throughout the drive-cycle.

These two results are approximated using the average energy used per kilometer, the average fuel used per joule of electrical energy and the average component efficiencies which can be calculated from the simulation data.